

November 1987

LU TP 87-18

Status of Fragmentation Models*

Torbjörn Sjöstrand

Department of Theoretical Physics,
University of Lund, Sölvegatan 14A,
S-223 62 Lund, Sweden

Abstract:

Phenomenological models of multiparticle production have become increasingly important for the interpretation of experimental data in high energy physics. The evolution of these models fills a gap left open by the present limited theoretical understanding of the hadronization process, i.e. the transformation of outgoing coloured partons into colour singlet hadrons. The three main schools of thought, string fragmentation, cluster fragmentation and independent fragmentation, are presented in this paper. Included are discussions on similarities and differences, successes and failures, and recent developments. Also perturbative QCD aspects with strong ties to the multiparticle production picture are covered, in particular parton showers. An account is given of experience gained in the comparison between data and models. Since fragmentation studies are particularly well developed for e^+e^- annihilation events, this field is described in detail. A few comments are also presented for lepton production and hadron collisions.

*review article submitted to International Journal of Modern Physics A

1. Introduction

In current high energy accelerators a collision between two incoming particles may typically lead to the production of ten to a hundred particles. There is every reason to believe that this production process can be described by the standard model for strong and electroweak phenomena. Unfortunately, while the theory is there, no method of extracting detailed event information from this theory seems to be within reach. One major problem is the sheer number of particles involved: even in the best of possible worlds, with an explicitly solvable theory, it is a fair conjecture that matrix elements for $2 \rightarrow 100$ processes would be impossibly complex. Another problem is our limited understanding of nonperturbative QCD: the only promising approach known is that of lattice calculations, calculations which so far mainly cover static properties in simple systems. It is in the light of these problems that one should see the development of phenomenological models, as an attempt to bridge the gap between the gross features that can be predicted theoretically and the detailed event structures that are observed experimentally.

The general situation is illustrated in Fig. 1, for an $e^+ e^-$ annihilation event. At small time scales, perturbation theory can be used to describe the annihilation of the incoming $e^+ e^-$ pair into a virtual γZ^0 , and the creation of an outgoing $q\bar{q}$ pair. QCD perturbation theory may even be used to describe the subsequent emission of extra partons. At a somewhat larger time scale ($c\tau \approx 1 - 5$ fm), the outgoing coloured partons are transformed into colour singlet hadrons – the fragmentation or hadronization process. This transformation reflects the nonperturbative confinement property of QCD. Many of the hadrons produced in the fragmentation process are unstable. These may in their turn decay further, so that decay chains of varying complexity appear. The theoretical understanding of these decays is again (with a few exceptions) scanty, but branching ratios are often well determined experimentally [1]. It is therefore more straightforward to model this phase than the preceding perturbative and fragmentation ones. Finally, the end products of the decay chains are observed in detectors. These are placed far away, in terms of the typical decay length scales. And yet, it is from the particles observed here that experimentalists try to study the physics of the initial perturbative stage!

Since the hadronization mechanism is not understood from first principles, it is not possible to formulate one single unique phenomenological model of fragmentation. Rather, different concepts and ideas can be taken as ideological starting points for the development of realistic models. Many constraints on possible model assumptions come from the requirement that these models should not disagree with existing data. As time goes by, and more experimental information is accumulated (often prompted by the predictions of the models), this leads to an almost Darwinian scenario, where the unsuccessful models are eliminated, and the successful ones continuously evolve. The models that attract most attention today therefore look rather different from the ones that were popular five years ago, say. As we will see, this evolution has also led to some convergence of opinion between the successful models. Today there therefore exists the beginning of a "standard" ideological framework for the hadronization process.

Fragmentation models can be formulated and studied in purely analytical terms, but this paper will deal almost exclusively with those models that have been implemented in terms of computer programs. Monte Carlo techniques are then used to generate complete events, from the perturbative partonic state to the observable particles. There are several good reasons for a bias towards numerical methods. Firstly, Monte Carlo programs can be made rather elaborate and sophisticated, while any number of approximations and simplifications may be necessary to make analytical methods work. Secondly, the presence of a well documented, publicly available program pins down all the detailed assumptions and properties of a model, in a form that can be checked and reproduced by anybody so inclined. Thirdly, many variables of interest are of a collective character, and can only be defined if all particles in an event are known. Finally, experimentalists can interface an existing program to detector simulation and event reconstruction routines, and thereby make more accurate comparisons between models and data than would otherwise have been possible.

The outline of the paper is as follows. In section 2 the different fragmentation models are introduced in their historical context. The modelling of QCD aspect is summarized in section 3. Sections 4 – 6 cover the three main frameworks, string fragmentation (SF), independent fragmentation (IF) and cluster fragmentation (CF). The experience accumulated with these models in $e^+ e^-$ annihilation is described in section 7. It is here that the models are confronted with each other. Other physics areas are considered in section 8. A summary and outlook is given in section 9.

2. Historical Overview of Models

The study of multiparticle production has a long history, and various models have been used to describe the main features: phase space, longitudinal phase space, thermodynamic models, multiperipheral models, gas analogies, etc. [2]. Most early models dealt with the distribution of particles in momentum space, without any predictive power for flavour properties or correlations. In particular, there was no strong underlying picture of hadron physics in terms of quarks and gluons. It is only during the early seventies that studies were initiated with iterative and other cascade models [3], which pointed in the direction of the models in use today.

The idea of an iterative ansatz is the following. Assume that a quark is kicked out by some hard interaction, carrying a well-defined amount of energy and momentum. This quark jet q is split into a hadron $q\bar{q}_1$ and a remainder-jet q_1' , essentially collinear with each other. The sharing of energy and momentum is given by some probability distribution $f(z)$, where z is the fraction taken by the hadron, leaving $1-z$ for the remainder-jet. The remainder-jet is assumed to be just a scaled-down version of the original jet, in an average sense. The process of splitting off a hadron can therefore be iterated, to yield a sequence of hadrons, Fig. 2. In particular, the function $f(z)$ is assumed to be the same at each step, i.e. independent of the remaining energy. If z is interpreted as the fraction of the jet $E_{\text{jet}}^{\text{jet}}$, i.e. energy plus longitudinal momentum w.r.t. the jet axis, this leads to a flat central rapidity plateau dN/dy for a large initial energy.

The simple iterative approach was made increasingly more sophisticated by the inclusion of resonance production and decay, strangeness production, baryon production, and transverse momentum properties. Most of those threads were collected in the Field-Feynman model (1978) [4], which rapidly became the standard in the field. In particular, the possibility to obtain significant results by the use of Monte Carlo techniques was made amply clear.

While the iterative approach, as outlined above, is very convenient for the simulation of one jet, the colour neutrality of matter requires that jets always appear at least in pairs. This is obvious in an $e^+e^- \rightarrow q\bar{q}$ event, where the two quarks emerge back-to-back, but is equally true in leptoproduction, where the kicked-out quark is balanced by a target remnant. The two-jet structure is readily visible, also in leptoproduction, if events are boosted to the hadronic CM frame. Furthermore, it is easy to see that a single jet by

itself can not conserve flavour or (all components of) energy and momentum of the original parton. Two jets, on the other hand, can be balanced so as to achieve overall conservation.

An early successful solution to the conservation problem was presented in the Artru-Mennessier model (1974) [5]. In this model it is assumed that a string is spanned between the two emerging partons. This string has a uniform probability PdA to break within a given space-time area dA , Fig. 3. The probability that the string has not already broken introduces an extra factor $\exp(-PA)$, where A is the string area within the backward light cone (in analogy, for $A + t$, with radioactive decay). Each string break corresponds to the production of a new $q\bar{q}$ pair. A large initial mass colour singlet system is thus successively broken into smaller and smaller colour singlet subsystems, "clusters". If the process is allowed to continue unchecked, the cluster masses will go to zero. With some procedure for stopping the breaking, a cluster mass spectrum is generated. These clusters may then be associated with higher resonances and allowed to decay into the more long-lived hadrons.

The Artru-Mennessier model was probably the first fragmentation model implemented in a Monte Carlo form. Its original appearance seems to have passed unnoticed. For the later development of cluster fragmentation, it has become a major source of inspiration, however.

Instead the Field-Feynman model came to be the starting point in the development of the Hoyer et al. [6] and Ali et al. [7] Monte Carlo programs for e^+e^- events (1979-1981). Two-jet events are in this scenario considered as two back-to-back independently fragmenting jets, patched up so as to conserve flavour, energy and momentum. A similar approach is used for three-jet ($q\bar{q}g$) events and, in the Ali program, four-jet ($q\bar{q}gq$ and $q\bar{q}q'\bar{q}'$) ones; the jets in an event are first generated independently of each other in the hadronic CM frame, and afterwards particles are slightly adjusted for overall conservation of flavour, energy and momentum. This is the independent fragmentation (IF) framework, which enjoyed considerable success in the description of e^+e^- data.

The IF models are not "just" straightforward applications of the Field-Feynman algorithm to e^+e^- events, but introduce a large number of new aspects, like gluon and heavy flavour fragmentation, matching decay routines, the abovementioned conservation algorithms, and a generation of multijet events according to perturbative QCD matrix elements. In addition to the Ali and Hoyer programs, a large number of IF based programs have been developed. The

most well-known of these is ISAJET by Paige and Protopopescu [8], which provides a description of the physics of hadron-hadron collisions.

A different approach was, at about the same time, developed by the Lund group [9]. At the core of this string fragmentation (SF) model is a space-time picture of a string being spanned between the q and \bar{q} of a simple two-jet event. The string is assumed to fragment into hadrons with well-defined masses, Fig. 4. The slow particles in the central region are the first to be produced, and the fragmentation process thereafter spreads outwards. Since the breakup points are causally disconnected, it is still possible to use an iterative algorithm from either end inwards. For two-jet events, the resulting picture is akin to the IF one, except that flavour, energy and momentum are now conserved at each step of the fragmentation. In the generation of transverse momenta and flavour composition at the string breaks, a tunnelling suppression mechanism is invoked [10-12]. Again, this is not in contradiction to the IF procedure, but is more cogently introduced here.

For three-jet events, the SF and IF approaches part company, however [13,14]. In string language, the natural way to introduce a gluon is as an energy and momentum carrying kink on a string stretched between a q and a \bar{q} end, Fig. 5. Thus the double colour charge of the gluon corresponds to having two string pieces attached to it, whereas a q or \bar{q} only has one. In particular, there is no string directly between the q and \bar{q} . When the string pieces between q (or \bar{q}) and g fragment, the transverse motion of these strings tends to boost the particles produced away from the central region, i.e. to deplete the region between q and \bar{q} of particles, Fig. 6. No corresponding effect is expected in IF.

Immediately after this prediction, the JADE group did indeed observe the expected string effect (1980) [15]. The early reports were met with scepticism, however, and it took several years of further JADE studies [16,17] before the phenomenon came to be more generally accepted [18,19]. Eventually (~1984) SF supplanted IF as the "standard" fragmentation framework. Today IF is on the verge of extinction in e^+e^- analyses. IF is still going strong in hadron physics, where the complicated event structure has precluded any decisive confrontation between fragmentation models.

In the original e^+e^- studies, the perturbative QCD description was in terms of first [20] or second [21-24] order matrix elements, i.e. with events containing at most four partons. This is as far as it has been proven possible

to carry out the required calculations. An alternative picture is that of successive parton branchings, Fig. 7, obtained by some leading log approximation [25] to the full QCD structure. This branching process may be described in probabilistic terms by the Altarelli-Parisi evolution equations [26], in a "jet calculus" [27]. Here events with a larger number of partons may be included. The average number of partons per event depends sensitively on which cutoffs are used to avoid the collinear and soft emission divergences in the branching probability distributions.

Nothing forbids a parton shower picture from being combined with either IF or SF and, in fact, this was done fairly early on [28]. However, a tempting idea would be to assign more importance to the parton branching stage, and less to the fragmentation one, than is done in either IF or SF, as follows. If the branching process is used to produce many partons, and if all gluons are forced to branch into $q\bar{q}$ pairs, the quarks and antiquarks of an event may be combined into disjoint colour singlet subsystems, Fig. 8. Each such subsystem could be represented by a string stretched between q and \bar{q} endpoints. In the cluster fragmentation (CF) ansatz, this internal structure of a subsystem is deemed irrelevant (unmeasurable); what matters is only the overall mass and the flavour quantum numbers. Each subsystem, "cluster", should therefore be allowed to decay isotropically in its rest frame, e.g. according to some simple phase space model. In particular, the CF approach ascribes the overall event shape, with jet properties etc., mainly to the distribution of partons generated by the shower, i.e. to calculable perturbative QCD aspects. This is in contrast to the SF and IF schools, where a detailed physical picture is required for the uncalculable, nonperturbative fragmentation aspects.

The first cluster fragmentation models were developed at Caltech [29,30], but were never successfully applied to e^+e^- phenomenology. This task instead fell on the program developed by Webber (1984) [31], based on a new parton shower picture implemented by Marchesini and Webber [32]. In this "coherent" parton shower approach, proper account is taken of a number of interference effects previously neglected [33,34]. Subsequently, coherence has become a standard feature of all shower models on the market. In addition to the Webber model, the Caltech-II (Gottschalk and Morris) cluster model [35,36] will be covered in the detailed descriptions. The Webber model is the more successful one, phenomenologically, and has found widespread use in recent years.

Additions have been made to the original cluster concept [37]. In order to describe the decay of massive clusters, where isotropy is not a good approximation, a splitting into smaller clusters along the "string direction" is implemented. The collapse of low-mass clusters into one single particle is also allowed for. In the Caltech-II model, even forced $g \rightarrow q\bar{q}$ branchings have been abolished, so that gluons are given the Lund interpretation as kinks on strings.

If thus cluster models have shown a tendency to evolve in the SF direction, the use of parton showers has come to be deemed more and more important for a successful application of SF ideas: there are aspects of the event structure, mainly related to the emission of fairly soft gluons, that are not well described by a combination of matrix elements and SF [38].

The examples above do not exhaust the possibilities of mixing different approaches. In fact, no really new ideas have been introduced into fragmentation models for the last three to five years. What progress has been made has either been in refining an already existing description, and/or in the synthesis of models. This may be seen either as a sign that the field is beginning to mature, or that a radically new departure is needed if further progress is to be made.

In addition to the major fragmentation schools mentioned above, several alternative formulations have indeed been proposed [39], but none so far with comparable success. The best worked-out alternative probably is the fire-string model by Preparata and co-workers [40]. The model involves a suggested reformulation of QCD, in which gluons do not play any rôle as dynamical degrees of freedom. The assumed hadronization process has some similarities with SF and CF, but is formulated in rather different terms.

3. Perturbative QCD Aspects in $e^+ e^-$ Annihilation Events

The normal starting point for a fragmentation model is a set of partons, given by a perturbative treatment of the standard model. For the QCD piece, two main approaches are possible, matrix elements and parton showers.

3.1. Matrix Elements

If the lowest order process $e^+ e^- \rightarrow q\bar{q}$ is in first order QCD modified by the probability for the q or \bar{q} to radiate a gluon, i.e. by the process $e^+ e^- \rightarrow q\bar{q}g$. The matrix element for this is conveniently given in terms of scaled energy variables in the CM frame of the event, $x_1 = 2E_q/W$, $x_2 = 2E_{\bar{q}}/W$ and $x_3 = 2E_g/W$, where W is the total energy in the CM frame, i.e. $x_1 + x_2 + x_3 = 2$. For massless quarks the matrix element reads [20]

$$\frac{d\sigma}{dx_1 dx_2} = \sigma_0 \frac{\alpha_s}{\pi} \frac{2}{3} \frac{x_1^2 + x_2^2}{(1-x_1)(1-x_2)}, \quad (1)$$

where σ_0 is the lowest order cross-section and the kinematically allowed region is $0 < x_i < 1$, $i = 1, 2, 3$. The strong coupling constant α_s is not known a priori. In fact, α_s determinations is one of the major applications of fragmentation models.

The cross-section in eq. (1) diverges for x_1 or $x_2 \rightarrow 1$ but, when first order propagator and vertex corrections also are included, a corresponding singularity with opposite sign appears in the $q\bar{q}$ cross-section, so that the total cross-section is finite. In a Monte Carlo program, the problem of divergences may be solved by imposing cuts, so that events with a hard gluon is generated according to the matrix element in eq. (1), but three-jet events with a soft or collinear gluon are lumped together with the two-jet ones. The cuts may e.g. be given in terms of the parameter y_{\min} , corresponding to the requirement that the invariant mass-square between any two partons in an event be larger than a fraction y_{\min} of the total mass-square, $m_{ij}^2 > y_{\min} W^2$.

Two new event types are added in second order QCD, $e^+ e^- \rightarrow q\bar{q}gg$ and $e^+ e^- \rightarrow q\bar{q}q'\bar{q}'$. The four-jet cross section has been calculated by several groups [21,22], which agree on the result. These results can be applied directly for IF models, but for SF models (and CF ones, were they to be used with matrix elements) a special problem arises: there are two possibilities to stretch the string between the partons in a $q\bar{q}gg$ event, Fig. 9. A knowledge of quark and gluon colours, obtained by perturbation theory, will uniquely specify the stretching of the string [41], so long as the two gluons do not have the same colour. The probability for the latter is down in magnitude by a factor $1/N_C^2$, where $N_C = 3$ is the number of colours. One may then either choose to neglect these terms entirely, or to keep them for the choice of kinematical setup but then drop them at the choice of string drawing. Comparing the two possibilities, differences are typically 10-20% for a given kinematical

configuration, and less for the total four-jet cross-section, so from a practical point of view this is not a major problem.

In second order, the three-jet rate is affected both by virtual corrections and by four-jet events which fail the y_{\min} requirement above, and therefore should be classified either as three- or as two-jet events. This has been a subject of long-standing controversy: whereas everybody agrees on the virtual corrections, the question of how to project the kinematics of a "failed" four-jet event onto that of ordinary three-jet ones is not unambiguous [22-24]. Today agreement seems to exist that, whereas large parts of these corrections can be written in closed analytical terms, pieces remain that have to be integrated numerically.

3.2. Parton Showers

Parton showers are based on an iterative use of the basic $q \rightarrow qg$, $q \rightarrow gg$ and $q \rightarrow q\bar{q}$ branchings, as given by the Altarelli-Parisi equations [26]

$$\frac{dp_{a \rightarrow bc}}{dt} = \int dz \frac{\alpha_s(Q^2)}{2\pi} p_{a \rightarrow bc}(z) \quad (2)$$

for the probability that a branching $a \rightarrow bc$ will take place during a small change dt . Here the $p_{a \rightarrow bc}(z)$ are the Altarelli-Parisi splitting kernels, z gives the sharing of energy and momentum between the daughters b and c , and t is some evolution parameter like $t = \ln(m_a^2/\Lambda^2)$. The running coupling constant α_s is, in first order, given by

$$\alpha_s(Q^2) = \frac{12\pi}{(33 - 2n_f) \ln(Q^2/\Lambda^2)}, \quad (3)$$

with n_f the effective number of flavours and Λ an unknown parameter. Starting at the maximum allowed mass for a , t may be successively degraded until a branching occurs. The probability that no branching occurs between t and some t_{\min} is given by the Sudakov form factor

$$S_a(t, t_{\min}) = \exp \left\{ - \int_{t_{\min}}^t dt \int_{z_{\min}}^{z_{\max}} dz \frac{\alpha_s(Q^2)}{2\pi} p_{a \rightarrow bc}(z) \right\}. \quad (4)$$

The products b and c may be allowed to branch in their turn, and so on, Fig. 7. The parton branching process is stopped whenever a parton mass is evolved below some minimum value, m_{\min} .

A wide selection of algorithms have been developed [28,29,32,35,38], which mainly differ in the interpretation of the variables t , Q^2 and z . Many of the variations are formally of a subleading character, and therefore are not constrained by theoretical leading log analyses. The splitting variable z may be applied to E , or to $E+p_z$, or to $|E+p|$, or some other energy-momentum combination. Very valuable input for model builders is provided by the theoretical studies of higher order corrections, like coherence effects [33,34]. In particular, it has been shown that an ordering in terms of a decreasing emission angle correctly takes into account soft gluon interference effects. The traditional Q^2 scale in α_s is m_a^2 , but studies of loop corrections indicate that $Q^2 = z(1-z)m_a^2 \approx p_T^2$ is better. (The parton shower cutoff then also has to be modified so that $p_T > m_{\min}/2$.)

Angular ordering is explicitly obtained in the Marchesini-Webber program [31,32], as follows. The evolution parameter is chosen to be $t = \ln(E\xi/\Lambda^2)$, $\xi \approx 1 - \cos\theta$. Here E is the energy of a parton and θ the opening angle between its decay products. The z variable refers to sharing of energy. Events are not studied in the CM frame, but rather in a boosted frame where the two initial partons form an opening angle of 90° , i.e. $\xi_0 = 1$. With the energy E_a of one of these partons a given, $(E\xi)_{\max} = E_a^2$ provides the starting value for the t evolution. From the selected t value ξ_a may be found. The simultaneously selected z value gives the sharing of energy, $E_b = zE_a$ and $E_c = (1-z)E_a$ (where energy dependent z_{\min} and z_{\max} values guarantee that $E_b > m_b$ etc.). Because of the requirement of ordering in angle, the maximum virtualities of the daughters are $E_b^2\xi_a$ and $E_c^2\xi_a$, respectively. These may now be degraded in virtuality to find $\xi_b < \xi$ and $\xi_c < \xi_a$, etc. When all branchings have been found, the actual invariant masses of the intermediate partons may be reconstructed, by moving backwards from the daughters to the mothers, using the relationship

$$m_a^2 = m_b^2 + m_c^2 + 2E_b E_c \xi_a. \quad (5)$$

Obviously the equality $\xi = 1 - \cos\theta$ is only correct for $m_b = m_c = 0$; eq. (5) is taken to be the exact definition of ξ . With all parton energies and invariant masses known, the reconstruction of the full kinematics is now straightforward. The azimuthal angle at each branching is chosen at random; azimuthal correlations are available as an option [42,43]. In the end, the event may be boosted to the CM frame, where the two initial partons are back-to-back.

A few minor modifications have successively been introduced to the original model. In particular, it was found that the number of hard three-jet events was underestimated (relative to other jet production) with a 90° initial opening angle θ_0 [44]. The discrepancy is related to the choice of relative energy sharing between the two initial partons: the probability distribution for $z = E_q/E_\gamma$ in $\gamma + q\bar{q}$ is normally given by $z^2 + (1-z)^2$, but this expression is actually valid only in the collinear limit (i.e. with an infinite boost). It is therefore necessary, either to add an extra term to the z distribution used for this branching, or to use a smaller θ_0 , say $\theta_0 \approx 30^\circ$ [44, 45].

While angular ordering enters very naturally in the Marchesini–Webber approach, there are a few unusual features, like the choice of frame to do the showering in and the related explicit breaking of Lorentz invariance (which is still approximately preserved in the final result), the choice of evolution variable, and the fact that parton masses can only be reconstructed after the evolution has been terminated. In particular, the invariant mass of the system is not known beforehand. It is therefore necessary, either to accept masses within a certain range, or to rescale all parton momenta at the end. In an upcoming version of the Marchesini–Webber program [45], this problem is solved by evolving each of the two partons independently in a back-to-back configuration, with $E_a = W/2^{1/2}$ and $\xi_{\max} = 1$. Since the evolution only depends on $E_a^2 \xi$, this is equivalent to $E_a = W/2$, $\xi_{\max} = 2 (\theta_{\max} = 180^\circ)$, but the kinematically and conceptually difficult region $\xi > 1$ is avoided. It is afterwards possible to define separate longitudinal boosts for the two parton systems, such that overall conservation of energy and momentum is achieved.

In the showering algorithm developed by Bengtsson and Sjöstrand for the Lund Monte Carlo [38, 46], events are considered in the CM frame, with z defined as energy fraction in this frame. Evolution is carried out in terms of $t = \ln(m^2/N^2)$. Angular ordering is therefore not automatically guaranteed, but rather imposed as an extra constraint on the mass and z values of one branching, in relation to m and z in the previous step. For the very first branching of the initial q and \bar{q} , angular ordering provides no constraint. Correction factors are instead introduced to match on to the first order matrix element for $q\bar{q}$ production, eq. (1). One should note that some implicit differences do remain. In a parton shower the probability for a first branching at a given mass m is reduced by the probability that no branching has taken place at a larger virtuality, i.e. by a Sudakov form factor, an effect with no correspondence in lowest order matrix elements. Further, a_s is allowed to run during the evolution of the parton shower, as given by the

argument $Q^2 = z(1-z)m^2$, but is kept fixed in matrix element based studies. (Implicitly the effects of a running a_s are contained in higher order corrections, however.) The combination of parton showers and Lund string fragmentation will, in the following, be denoted Lund+PS, to distinguish it from the older matrix element option, Lund+ME.

The algorithm included in the Caltech-II program [35, 36] is closer in spirit to the Lund than to the Marchesini–Webber algorithm, but has its own special features. The z variable for the process $p + a (+ ..) \rightarrow b + c$ is defined by

$$z = \frac{1}{2} \left(1 - \frac{m_a^2}{m_p^2} \right) (1 + \cos\theta_b^*), \quad (6)$$

where θ_b^* is the angle of the daughter b in the rest frame of a , with respect to the motion of a in the overall CM frame of the event. For the first branchings of the initial q and \bar{q} this is equivalent to fraction of $E + |\mathbf{p}|$. Again the correct first order matrix element is imposed in the first branchings, and angular ordering in the subsequent ones. A major difference, compared to the other two algorithms presented above, is that the argument in a_s is $Q^2 = m^2$ and not $Q^2 \approx z(1-z)m^2 \approx p_T^2$. This is motivated by a study of the z choice in eq. (6).

An alternative to parton shower algorithms is the dipole formulation, suggested by the Leningrad group [47] and studied in detail by Gustafson and Pettersson [48]. The picture is based on identifying the string pieces between partons with colour dipoles or colour antennae, so that the emission of a gluon corresponds to the breaking of a dipole into two. This breaking is simple and well-defined in the rest frame of a dipole, and yet it automatically includes angular ordering and nontrivial azimuthal effects when the boost back to the overall CM frame is taken into account.

All the algorithms presented above keep track of the colour flow at each parton branching, as a prerequisite to the subsequent fragmentation description. Since only leading order branchings of the type $a \rightarrow bc$ are included, this is straightforward. In proposed next-to-leading order algorithms [49], branchings of the type $a \rightarrow bcd$ would give similar problems as discussed above for four-jet matrix elements.

3.3. QCD Parameters

As we have seen, both matrix element and parton shower descriptions have two main parameters. One of these is Λ , which for matrix elements may be replaced by α_s . The larger Λ or α_s is, the larger is the multijet production rate. Whereas α_s in matrix elements has a well-defined meaning, order by order, in terms of a $\overline{\text{MS}}$ renormalization scheme, the Λ value of a shower is very strongly coupled to the choice of kinematics definition for non-collinear emission, and to the choice of Q^2 scale in α_s . The Λ values obtained with different shower programs are therefore not directly comparable with each other.

The other main parameter is a cutoff, Y_{\min} or m_{\min} . (In practice, a flavour dependence may have to be introduced in the cutoff procedure, with further complications.) The two are related by $Y_{\min} = m_{\min}/w^2$. Physically, it makes sense to keep m_{\min} fix when w is varied, so that the same soft gluon emission region is always neglected in the perturbative treatment. The effective fragmentation parameters should then be energy-independent. For a fixed Y_{\min} cut, it would be necessary to include more and more soft gluon effects in the fragmentation description as w is increased. This is not a desirable state of affairs, but is forced on us in the matrix element approach, since a decreasing Y_{\min} would give a three-jet probability larger than unity.

4. String Fragmentation

String fragmentation (SF) has, from the start, been almost synonymous with the Lund model. It is therefore the Lund framework that will be discussed in this section. Basic information may be found in [50]. Later additions to the Lund model include symmetric fragmentation [51], fragmentation of arbitrary multiparton states [52] and the "popcorn" baryon production model [53]. A detailed description of the Lund Monte Carlo for jet fragmentation and e^-e^+ physics, JETSET version 6.3, is given in [54]. Examples of possible extensions will be found in section 7.

4.1. The Conceptual Picture

In QCD, a linear confinement is expected at large distances. This provides the starting point for the string model, most easily illustrated for the production of a back-to-back $q\bar{q}$ jet pair. As the partons move apart, the

physical picture is that of a colour flux tube being stretched between the q and the \bar{q} , Fig. 10. The transverse dimensions of the tube are of typical hadronic sizes, roughly 1 fm. If the tube is assumed to be uniform along its length, this automatically leads to a confinement picture with a linearly rising potential. In order to obtain a Lorentz covariant and causal description of the energy flow due to this linear confinement, the most straightforward way is to use the dynamics of the massless relativistic string with no transverse degrees of freedom [55]. The mathematical, one-dimensional string can be thought of as parametrizing the position of the axis of a cylindrically symmetric flux tube. From hadron mass spectroscopy the string constant, i.e. the amount of energy per unit length, is known to be $\kappa \approx 1$ GeV/fm ≈ 0.2 GeV 2 . The expression "massless" relativistic string is somewhat of a misnomer: κ effectively corresponds to a "mass density" along the string.

If several partons are moving apart from a common origin, the details of the string drawing become more complicated. For a $q\bar{q}g$ event, a string is stretched from the q end via the g to the \bar{q} end, Fig. 5, i.e. the gluon is an energy and momentum carrying kink on the string. As a consequence of the gluon having two string pieces attached, the ratio of gluon/quark string force becomes 2, a number that can be compared with the ratio of colour charge Casimir operators, $N_C/C_F = 2/(1-1/N_C^2) = 9/4$. In this, as in several other respects, the string model can therefore be viewed as a variant of QCD where the number of colours N_C is not 3 but infinite ("the large N_C limit" [56]). Note that the factor 2 above does not depend on the kinematical configuration: a smaller opening angle between two partons corresponds to a smaller string length drawn out per unit time, but also to an increased transverse velocity of the string pieces, which gives an exactly compensating boost factor in the energy density per unit string length. In an event with several gluons, these will still appear as kinks on the string between the q and \bar{q} ends. It is also possible to have a closed gluon string, e.g. in $T \rightarrow ggg$ decays, Fig. 11.

4.2. Flavour Properties

Now again consider a simple $q\bar{q}$ two-jet event. As the q and \bar{q} move apart, the potential energy stored in the string increases, and the string may break by the production of a new $q'\bar{q}'$ pair, so that the system splits into two colour singlet systems $q\bar{q}'$ and $q'\bar{q}$. If the invariant mass of either of these systems is large enough, further breaks may occur, and so on until only ordinary hadrons remain. Typically, a break occurs when the q and the \bar{q} ends of a

colour singlet system are 1 - 5 fm apart in the $q\bar{q}$ rest frame. Each hadron is formed by the quark from one break and the antiquark from an adjacent break. The hadrons can therefore be arranged in a flavour chain, and numbered consecutively from one end of the jet system, Fig. 12. This ordering is called rank [4]. Two nearest neighbours in rank thus have one quark-antiquark pair in common (this statement is modified somewhat by baryon production).

In a colour field a 'q' pair, where the 'q' and ' \bar{q} ' have no mass or transverse momentum, can classically be created in one point and then be pulled apart by the field. If the quarks have mass and/or transverse momentum, however, they must classically be produced at a certain distance so that the field energy between them can be transformed into the transverse mass m_T^2 . Quantum mechanically, the quarks may be created in one point and then tunnel out to the classically allowed region. The production probability for this tunneling process is proportional to [10-12]

$$\exp(-\pi m_T^2/\kappa) = \exp(-\pi m^2/\kappa) \exp(-\pi p_T^2/\kappa). \quad (7)$$

The factorization of the transverse momentum and the mass terms leads to a flavour-independent Gaussian spectrum for the p_T of 'q' pairs. Since the string is assumed to have no transverse excitations, this p_T is locally compensated between the quark and the antiquark of the pair. In a perturbative QCD framework, a hard scattering is associated with gluon radiation, and further contributions to what is naively called fragmentation p_T comes from unresolved radiation. Therefore the mean p_T observed experimentally is somewhat higher than obtained with the formula above, $\langle p_T^2 \rangle = \sigma^2 \approx (350 \text{ MeV})^2$ rather than $\kappa/\pi \approx (250 \text{ MeV})^2$. Effectively the radiation has a non-Gaussian shape but, when combined with the ordinary fragmentation p_T , the overall shape is very close to Gaussian, and is parametrized correspondingly in the program. Hadrons receive p_T contributions from two 'q' pairs and have $\langle p_T^2 \rangle = 2\sigma^2$.

The formula also implies a suppression of heavy quark production $u : d : s : c \approx 1 : 1 : 0.3 : 10^{-11}$. Charm and heavier quarks are hence not expected to be produced in the soft fragmentation. The suppression of $s\bar{s}$ production is left as a free parameter in the program, but the experimental value agrees qualitatively with theoretical prejudice.

The simplest scheme for baryon production is that, in addition to quark-antiquark pairs, also antidiquark-diquark (colour triplet-triplet) pairs occasionally are produced in the field [57]. Such an assumption does not imply

that a diquark should be considered as a single excitation of an elementary field, only that the soft chromoelectric field effectively acts on a diquark as were it a unit. Due to the large uncertainty in the definition of diquark masses, the tunneling formula can not be used directly to predict the expected rate of diquark production. Rather, from data a relative probability for diquark to quark production is determined to $q\bar{q} : q : 0.09 : 1$, corresponding to a typical nonstrange diquark mass around 420 MeV. Using this in combination with expected mass differences between diquarks, the relative probability for the production of the various diquarks is determined by the tunneling formula and the number of spin states available.

A more general framework for baryon production is the so-called popcorn one [53], in which diquarks as such are never produced, but rather baryons appear from the successive production of several 'q' \bar{q} ' pairs. Part of the time, the end result will be exactly the same BB situation as above, i.e. with an adjacent baryon and antibaryon sharing a diquark-antidiquark pair. However, further possibilities of the type BMB, B \bar{B} , etc., here are possible, i.e. where a varying number of mesons are produced in between the baryon and antibaryon, Fig. 13. The B and \bar{B} then have just one 'd' \bar{q} ' pair in common, rather than two. In its present form, the program generates BMB and B \bar{B} configurations with equal probability, while BMM \bar{B} and even longer meson chains are neglected.

The resulting baryon production model has a fair number of parameters, which would be uniquely predicted by the model only if quark and diquark masses were known unambiguously. Already mentioned are the $s : u$ ratio and the $q\bar{q} : q$ one; the latter has to be increased from 0.09 to 0.10 for the Popcorn model, since the total number of possible baryon production configurations is lower in this case (the particle sitting between the B and \bar{B} is constrained to be a meson). Further parameters in the simple diquark model include the suppression of spin 1 diquarks relative to spin 0 ones and the extra suppression of strange diquarks compared to nonstrange ones, over and above the ordinary $s : u$ ratio (this is because what appears in the exponent of the tunneling formula is m^2 and not m , so that the diquark and the strange quark suppressions do not factorize for a strange diquark). For the popcorn model, exactly the same parameters are needed to describe the B \bar{B} configurations. For BMB configurations, the square root of a suppression factor should be applied if the factor is relevant only for one of the B and \bar{B} , e.g. if the B is formed with a spin 1 effective diquark but the \bar{B} with a spin 0 one. Additional parameters include the relative probability for BMB configurations, a

suppression factor for having a strange meson M between the B and \bar{B} (as opposed to having a lighter nonstrange one) and a suppression factor for having a $s\bar{s}$ pair (rather than a $u\bar{u}$ one) shared between the B and \bar{B} of a $B\bar{B}$ configuration.

A quark and an antiquark may combine to produce either a pseudoscalar or a vector meson. The production of higher resonances is neglected, from orbital angular momentum arguments this rate is anyhow assumed to be low in a string framework. From counting the number of spin states one would expect the relative probability for pseudoscalar : vector to be 1 : 3. This should be modified by wave function effects, as manifested e.g. in the mass splitting between pseudoscalar and vector mesons [58], and further parameters are here required. A given quark-diquark pair may combine either to produce a spin 1/2 ("octet") or a spin 3/2 ("decuplet") baryon. Again higher resonances are neglected. A very important constraint is the fact that a baryon is a symmetric state of three quarks (neglecting the colour degree of freedom). When a diquark and a quark are joined to form a baryon, it is therefore necessary to weight the different flavour and spin states by the probability that they form a symmetric three-quark system.

4.3. Longitudinal Fragmentation

In an iterative framework, the fraction z of remaining $E+P_L$ (energy plus longitudinal momentum) taken by a hadron can be given by some probability distribution $f(z)$. In principle, $f(z)$ could be any sensible function, but an arbitrarily chosen $f(z)$ would suffer from the disease of not being "left-right symmetric". Left-right symmetry means the following. It is possible to treat the fragmentation of a $q\bar{q}$ jet system by starting at the q end of the system and iterating "left" towards the \bar{q} end. Alternatively, one could have started at the \bar{q} end and iterated the other way, towards "right", instead. Since iteration schemes are derived under the assumption that there is much energy left, an iteration from the q end can not trivially be taken all the way to the \bar{q} and vice versa. In the central rapidity plateau of a reasonably large jet system, however, there should be no artefact left to tell the direction of iteration [4, 50].

The most general left-right symmetric answer is given in [51]. When the invariant mass of the system is large, this answer can be implemented in an iterative scheme. For the production of a hadron with a known transverse mass

m_T , the shape of $f(z)$ is then

$$f(z) \sim \frac{1}{z} z^\alpha \left[\frac{1-z}{z} \right]^\beta \exp\left\{-\frac{bm^2}{T}\right\}, \quad (8)$$

where the indices α and β corresponds to the flavours produced at the "old" and "new" $q'\bar{q}'$ vertices that together define the hadron. There is in principle one free parameter α_q for each flavour and a common β parameter. It is normally assumed that all α_q :s are the same, so that the formula collapses to

$$f(z) \sim z^{-1} (1-z)^\alpha \exp\left(-\frac{bm^2}{T}/z\right). \quad (9)$$

For $\alpha = 0$ this gives an exponential decay area law of exactly the same type as in the Artru-Mennessier model [5], but for arbitrary discrete masses rather than a specific continuous mass spectrum. The similarity in final result is all the more surprising, since a discrete mass spectrum implies that string breaks are only allowed along one-dimensional hyperbolae rather than inside two-dimensional areas. A good fit to experimental data can be obtained with the parameter values $\alpha = 1$, $b = 0.7 \text{ GeV}^{-2}$ for Lund+ME, and $\alpha = 0.5$, $b = 0.9 \text{ GeV}^{-2}$ for Lund+PS.

As a by-product, the derivation of $f(z)$ also gives the probability distribution in invariant time τ of $q'\bar{q}'$ breakup vertices. In terms of $\Gamma = (\kappa\tau)^2$, this distribution is

$$P(\Gamma) d\Gamma \sim \Gamma^\alpha \exp(-b\Gamma) d\Gamma, \quad (10)$$

with the same α and b as above. In a given event, the connection between adjacent Γ values is given by the formula

$$\Gamma_i = (1-z_i) (\Gamma_{i-1} + \frac{m_i^2}{T_i}/z_i), \quad (11)$$

where Γ_{i-1} is the "old" and Γ_i is the "new" value obtained after taking a step z_i for the production of a hadron with transverse mass m_{Ti} . The initial values at the q and \bar{q} ends of the system are $\Gamma_0 = 0$.

The $f(z)$ formulae above, for the breakup of a system into a hadron and a remainder-system, strictly speaking only apply when the mass of the remainder-system is large. In a Monte Carlo program, it is therefore necessary to introduce a special procedure to cover the production of the last two particles. This contains no new physics, but has just to be constructed so that the place where one selects to "patch up" the fragmentation from the q end with that from the \bar{q} one looks as closely like any other as is possible.

4.4. String Fragmentation of Jet Systems

A three-jet $q\bar{q}g$ event initially corresponds to having a string stretched from the q via the g to the \bar{q} , i.e. two string pieces. In the string piece between the g and the q (\bar{q}), g four-momentum is flowing towards the q (\bar{q}) end and q (\bar{q}) four-momentum towards the g end. When the gluon has lost all its energy, the g four-momentum continues moving away from the middle (i.e. where the gluon used to be), and instead a third string region is formed there, consisting of inflowing q and \bar{q} four-momentum, Fig. 14a. If this third region would only appear at a time later than the typical time scale for fragmentation, it could not affect the sharing of energy between different particles. This is true in the limit of high energy, well separated partons.

For a small gluon energy, on the other hand, the third string region appears early, and the overall drawing of the string becomes fairly two-jetlike, Fig. 14b. In the limit of vanishing gluon energy, the two initial string regions collapse to naught, and the ordinary two-jet event is recovered. Also for a collinear gluon, i.e. θ_{qg} (or $\theta_{\bar{q}g}$) small, the stretching becomes two-jetlike, Fig. 14c. In particular, the q string endpoint first moves out a distance \bar{p}_q/κ , and then a further distance \bar{p}_g/κ , a first half accreting gluon four-momentum and a second half reemitting it. The end result is, approximately, that a string is drawn out as if there had only been a single parton with energy $|\bar{p}_q + \bar{p}_g|$, such that the simple two-jet event again is recovered in the limit $\theta_{qg} \rightarrow 0$. These properties of the string motion are the reason why the string fragmentation scheme is "infrared safe" with respect to soft or collinear gluon emission.

The discussions for the three-jet case can be generalized to the motion of a string with q and \bar{q} endpoints and an arbitrary number of intermediate gluons [52]. Anytime one of the original gluons has lost its energy, a new string region is formed. As the extra "corners" on the string, created in pairs each time a gluon lost its energy, meet each other, old string regions vanish and new are created. Each of these regions can be understood simply as built up from the overlap of (opposite-moving) four-momentum from two of the initial partons, according to well specified rules. The stability noted above carries over, and makes it possible to use the Lund model both with matrix elements and with parton showers, without any significant break in continuity: soft and collinear gluon emission just add "wrinkles" on the basic event shape given by the hard radiation.

The generalization of the left-right symmetry requirement to the fragmentation of multiparton configurations is not unique. In the program, the physical assumption is that the fragmentation should still be characterized by eq. (10), i.e. that the distribution in invariant time of breakup vertices does not depend on the exact shape of the string. The z variable no longer has any simple physical interpretation, but eq. (9) and eq. (11) taken together still provide a valid recipe for the relationship between adjacent Γ values. These Γ values themselves are always well defined and, if taken together with the constraint of hadrons on mass shell, uniquely defines the position of each vertex.

5. Independent Fragmentation

In independent fragmentation (IF) models, the fragmentation of the different partons is assumed to take place independently of each other in the CM frame of the event. This rather innocent-looking formulation hides a lot of possible ambiguity. The two most well-known IF e^+e^- Monte Carlos are Hoyer et al. [6] and Ali et al. (QCJET) [7]. In an attempt to provide a more controlled environment for the comparison between IF and SF, without any bias from differences in matrix elements or particle composition and decay, IF options are also available in the Lund Monte Carlo [54].

5.1. Fragmentation of an Independent Jet

The fragmentation of each individual jet in a system can be described in iterative terms, as outlined in sections 2 and 4. With the longitudinal direction defined by the parton, the z variable of the fragmentation function is chosen as the fraction of remaining $W_+ = E + p_L$ that is taken by a hadron. Note, however, that a choice of a z value close to 0 corresponds to a particle moving backwards, i.e. with $p_L < 0$. It makes sense to allow only the production of particles with $p_L > 0$, but to explicitly forbid z values that give particles with $p_L < 0$ would destroy the invariance under longitudinal boosts inherent in the basic one-jet scheme. The most straightforward way out [4] is to allow all z values but then discard hadrons with $p_L < 0$. Note that flavour, transverse momentum and W_+ carried by these hadrons are "lost" for the forward jet. The average energy of the final jet comes out roughly right this way, with a spread of 1 - 2 GeV around the mean. The jet longitudinal momentum is decreased, however, since the jet acquires an effective mass

during the fragmentation procedure. For a two-jet event this is as it should, at least on the average, because also the momentum of the compensating opposite-side parton is decreased.

A number of different fragmentation functions $f(z)$ have been proposed. The Field-Feynman [4] parametrization

$$f(z) = 1 - a + 3a(1-z)^2, \quad (12)$$

with default value $a = 0.77$, is frequently used for ordinary hadrons. There are indications that this shape is too strongly peaked at $z=0$ [55]; instead a shape like

$$f(z) = (1+c)(1-z)^c \quad (13)$$

may be used. Charm and bottom data [60] clearly indicate the need of a harder fragmentation function for heavy flavours. Among the many possible parametrizations, the "SLAC" or "Peterson" formula [61]

$$f(z) = \frac{1}{z\left\{1 - \frac{1}{z} - \frac{\epsilon}{1-z}\right\}^2} \quad (14)$$

has acquired the status of a standard. Here one expects $\epsilon = (m_0/m_Q)^2$, with m_0 some reference scale and m_Q the heavy quark mass.

The iterative ansatz provides a well-defined flavour correlation scheme, of exactly the same character as in string fragmentation. Each quark-antiquark pair created during the fragmentation is assumed to have opposite and compensating transverse momenta given by a Gaussian distribution, with width to be determined from data. The s/u quark ratio is another parameter of the model. The original Field-Feynman model does not address the question of baryon production, and neither do the Hoyer or Ali programs. Since IF has no strong ties to any physical production mechanism, many different possibilities could be imagined [62]. One approach is to use then same diquark or popcorn type scenario as in the Lund model. Meyer [63] has introduced baryon production by a minimal scheme of the generic diquark type, but with the two quark flavours of the diquark generated independently of each other, according to ordinary $u : d : s$ probabilities.

Within the IF framework, there is no unique recipe for how gluon jet fragmentation should be handled. One possibility is to treat it exactly like a quark jet [6], with the initial quark flavour chosen at random among $u, \bar{u}, d, \bar{d}, s$ and \bar{s} , including the ordinary s quark suppression factor. Since the gluon

is supposed to fragment softer than a quark jet, the fragmentation function may be chosen independently. Another main option is to split the g jet into a quark and an antiquark one, again $u\bar{u}$, $d\bar{d}$ or $s\bar{s}$ according to ordinary fragmentation probabilities, and allow the two jets to share the total energy, e.g. according to the Altarelli-Parisi splitting function [7]. The fragmentation function could still be chosen independently, if so desired. Further, in either case the fragmentation P_T could be chosen to have a different mean.

5.2. Conservation Issues

The concept of IF inevitably leads to the total flavour, energy and momentum not being exactly conserved. For a long time it was thought that this could be corrected for trivially, so that the subject was normally not mentioned in model descriptions. When different q_s values were obtained with different conservation schemes the problem was noted [64,65].

Little attention is usually given to flavour conservation. Typically, that aspect is solved by reassigning the flavour content of centrally produced particles, without changing their three-momenta, so that the net number of each flavour is vanishing.

Several different schemes for energy and momentum conservation have been devised. All of them assume that the event is given in its CM frame. The Hoyer approach [6] is to conserve transverse momentum locally within each jet, so that the final momentum vector of a jet is always parallel with that of the corresponding parton. Then longitudinal momenta may be rescaled separately for particles within each jet, such that the ratio of rescaled jet momentum to initial parton momentum is the same in all jets. Since the initial partons had net vanishing three-momentum, so do now the hadrons. The rescaling factors may be chosen such that also energy comes out right. A different procedure is used in the Ali program [7]. Given the momentum imbalance \vec{P}_{imbal} and the total energy E_{tot} of the event after fragmentation, a boost vector $\hat{B} = -\vec{P}_{imbal}/E_{tot}$ is defined, such that the Lorentz boosted event has vanishing total momentum. Energy conservation can now be obtained by rescaling all particle three-momenta by a common factor.

The reason that the choice of conservation scheme matters for a s determinations is that one has to correct, not only for a random momentum imbalance, but also for a systematic component [65]. To see this, consider a three-jet event. If the total momentum before fragmentation is vanishing, and if the final jet momenta are parallel with the initial parton momenta, then all initial momenta would have to be scaled down by the same factor to keep total momentum conserved. In the IF framework, however, a parton energy independent amount of momentum, 1 - 2 GeV, is subtracted from each jet on the average, such that the relative change is largest for a low-energy parton. Thus, the final state net momentum imbalance vector \vec{P}_{imb} is typically pointing oppositely to the direction of the lowest-energy jet. According to the QCD three-jet matrix element this is the gluon one most of the time, Fig. 15a. In the Hoyer program, the average effect of momentum conservation is then to significantly scale up longitudinal momenta within the gluon jet, and slightly scale them down for the q and \bar{q} ones, Fig. 15b. This scheme thus tends to make the events more three-jetlike as far as energy sharing between jets go, whereas angular correlations are kept fixed. In the Ali program, the boost tends to be along the gluon jet direction, such that the q and \bar{q} jets become more back-to-back, Fig. 15c. The main effect is therefore a shift towards more two-jetlike events in angular correlations, whereas the shuffling of energy into the gluon jet is rather insignificant.

No post facto conservation scheme need be imposed in SF (or CF), since energy and momentum are conserved at each step of the fragmentation procedure. The following deliberation may still be helpful. Assume that an IF event were to be "patched up" to resemble an SF one. To describe the effect that particles are distributed along hyperbolae in momentum space, low-momentum particles in the q and \bar{q} jets would then have to be shifted in the g jet direction, Fig. 15d. It is precisely this shift that also would compensate for the momentum imbalance along the gluon direction. Note that the Hoyer and Ali methods mainly affect high-momentum particles, whereas the Lund string effects are felt predominantly by low-momentum ones.

5.3. Further Aspects of IF

The most serious conceptual weakness of the IF framework is the issue of Lorentz invariance. In a limited sense IF can be said to be Lorentz invariant, in that the fragmentation is explicitly defined to be carried out in the hadronic CM frame. This is just a technical excuse, however: for a system more

complicated than a pair of back-to-back jets there is no natural way to describe a scaling procedure, with z of the fragmentation function giving fraction of $E + P_L$, in terms of Lorentz invariants. Furthermore, there is no good underlying physical reason why the fragmentation must be carried out in the hadronic CM frame. The lack of underlying physical picture is also illustrated by the issue of jet masses: how does a massless parton turn into a massive jet, if each parton is supposed to fragment independently of other partons in the event?

It should be noted, however, that a Lorentz covariant generalization of the string model exists, in which separate "gluon-type" and "quark-type" strings are used, the Montvay scheme [66]. The quark string is characterized by the ordinary string constant κ , whereas a gluon string is taken to have a string constant κ_g . If $\kappa_g > \kappa$ it is always energetically favourable to split a gluon string into two quark ones, and the ordinary Lund string model is recovered. Otherwise, for a three-jet $q\bar{q}g$ event, the three string pieces are joined at a junction, Fig. 16. The motion of this junction is given by the compositant of the string tensions acting on it. In particular, it is always possible to boost an event to a frame where this junction is at rest. In this frame, much of the standard naive IF picture holds for the fragmentation of the three jets; additionally, a correct treatment would automatically give flavour, energy and momentum conservation. Unfortunately, the simplicity is lost when events with several gluon jets are considered. In general, each event will contain a number of junctions, resulting in a polyopod shape with a number of quark and gluon strings sticking out from a skeleton of gluon strings, a situation which would be exceedingly difficult to model correctly. A simplified treatment of the Montvay scheme is available as an option in the Lund Monte Carlo. Studies with this option has shown that the experimental observation of string effects puts a constraint that $\kappa_g/\kappa > 1.5$.

A second problem with IF is the issue of collinear divergences. The very word independent implies that jets are assumed to fragment independently of each other, however close they happen to be. In a parton shower picture, where a quark or gluon is expected to branch into several essentially collinear partons, the independent fragmentation of one single parton or a bunch of collinear ones will give quite different outcomes, however. As a simple example, start out with a jet of energy E . When this jet fragments, the expected multiplicity is $c \cdot \ln(E/\langle m_{\text{hadron}} \rangle)$, with some constant c , whereas two collinear jets with half the energy each would give something more like $2c \cdot \ln(E/(2\langle m_{\text{hadron}} \rangle))$, i.e. a larger number. As more and more emission is

allowed, the average multiplicity will therefore increase, whereas the probability for finding one single hadron carrying a significant fraction of the original jet momentum will decrease. As the parton shower cutoff is changed (or, for that matter, the matrix element one), it is therefore necessary to perform a significant retuning of fragmentation parameters, and too small cutoffs in the shower may lead to a complete breakdown of a fragmentation description. There is no corresponding sensitivity to soft gluon emission: a very low energy parton gives no particles whatsoever, and thus the event shape is not changed by such additions. Also the collinear sensitivity problem would disappear in the Montvay approach: two almost collinear partons, coming from the branching of a mother parton (and thus sharing colours), would pull with them a junction and only be connected to the rest of the system by a single string.

6. Cluster Fragmentation

The concept of cluster fragmentation (CF) offers the great promise of a simple, local and universal description of hadronization. A generic cluster scheme contains three components:

- (i) generation of clusters by parton shower evolution, usually supplemented by forced $g \rightarrow q\bar{q}$ breakups;
- (ii) fragmentation of large (i.e. heavy) clusters into smaller ones; and
- (iii) decay of clusters into hadrons.

None are the long, ordered decay chains present both in SF and IF. In their place appear simple clusters, which are assumed to be the basic units from which the hadrons are produced. If the procedures in steps (i) and (ii) are chosen such that most clusters have masses of a few GeV, the cluster mass spectrum may be thought of as a superposition of fairly broad (i.e. short-lived) resonances. Phase space aspects may then be expected to dominate the decay properties, so that e.g. the decay is assumed to be isotropic in the rest frame of the cluster. This gives a compact description with few parameters. In particular, the separate longitudinal and transverse momentum fragmentation descriptions in SF and IF are here replaced by a unified framework, wherein parton showers and cluster phase space decays give the full momentum distribution.

Ideally, the component (ii) should not be needed at all. Indeed, that was the hope in the early days of CF. This hope was based on the concept of "preconfinement" [67]: the colour-anticolour charges created at parton branchings tend to end up in partons which are nearby, both in coordinate and momentum space. By enforced $g \rightarrow q\bar{q}$ branchings, the partons generated can be arranged in low-mass colour singlet clusters, Fig. 8. Unfortunately, despite the preconfinement property, there is no known way of avoiding a rather large spread of cluster masses. The introduction of step (ii) is one way of controlling the high-mass tail of the spectrum.

The details of how clusters are arrived at may vary, as may the rules according to which they subsequently decay. Here the Webber program may be considered one extreme, and the Caltech-II another.

6.1. The Webber Model

In the (Marchesini-)Webber program [31,32], EAWIG version 4.1, the shower model outlined in section 3.2 is used. The cutoff of the parton shower is given by $Q_0 = m_g \approx 0.7 \text{ GeV}$, i.e. a fictitious gluon mass is used to prohibit $g \rightarrow gg$ branchings at invariant masses below $2Q_0$ ($\approx m_{\min}$ in the terminology of section 3.3). On the other hand, light quark masses are chosen to be $m_u = m_d = 0.3 \text{ GeV}$, $m_s = 0.5 \text{ GeV}$. The branching $g \rightarrow u\bar{u}$ or $d\bar{d}$ is therefore always kinematically allowed. So long as the gluon virtuality is much above threshold, the $g \rightarrow gg$ branching clearly dominates over the $g \rightarrow q\bar{q}$ one but, as threshold is approached, the gluons predominantly branch into $q\bar{q}$ pairs. If some gluons should remain when the cutoff mass Q_0 is reached, they are then explicitly forced to branch. The final state of the parton shower thus consists of disjoint $q\bar{q}$ systems, Fig. 8, with no gluons present.

In the original model, only quark-antiquark pairs were created at branchings. This leads to problems in the description of baryon production (section 7.1). The present model therefore also includes, as an option, the possibility that a gluon may branch into a diquark-antidiquark pair [45]. This process is turned on below some scale Q_d in the shower evolution, with an arbitrary strength relative to ordinary $q\bar{q}$ production, and a constant probability per unit in $\ln Q^2$. The light diquarks $u\bar{u}$, $u\bar{d}$ and $d\bar{d}$ are produced with equal probability. All diquarks are too heavy to be produced in the forced $g \rightarrow q\bar{q}$ branchings. If baryon data are to be understood, the required relative diquark production rate is roughly 5%.

An example of the resulting cluster mass spectrum is given in Fig. 17. The preconfinement picture is here visible: the cluster mass distribution is peaked at low values, and falls off rapidly for higher ones. It is also essentially energy independent. If the high-mass tail is neglected for the moment, this mass spectrum may be thought of as a smeared out version of the "primordial resonance" mixture formed in the early stages of confinement in real jets. In an average sense, these resonances may be expected to decay isotropically into quasi-two-body channels, with branching ratios determined by density of states, i.e. phase space times spin factors.

The decay procedure is the following. For each $q_1\bar{q}_2$ cluster, a new flavour q_3 is chosen at random, such that the flavours of the decay products are given by $q_1\bar{q}_3$ and $q_3\bar{q}_2$. Here the symbol q may either represent a quark or an antiquark (in a colour triplet state), and \bar{q} either an antiquark or a diquark. The flavour q_3 is chosen among the possibilities $u, d, s, c, \bar{u}, \bar{d}, \bar{s}, \bar{c}, \bar{d}\bar{d}, \bar{d}\bar{s}$ and $\bar{s}\bar{s}$. Choices which would give a diquark-antidiquark particle are dismissed outright. The flavour combinations $q_1\bar{q}_3$ and $q_3\bar{q}_2$ are associated with admissible hadrons. For mesons this means a choice between the 0^- (pseudoscalar), 1^+ (vector), 1^- (pseudovector) and 2^+ (tensor) multiplets, for baryons between the $1/2^+$ ("octet") and $3/2^+$ ("decuplet") ones. A chosen combination is associated with a weight equal to the density of states, $(2s_1 + 1)(2s_2 + 1)(2p^*/m)$, where s_1 and s_2 are the spins of the two particles produced, and p^* the common momentum of the products in the rest frame of the cluster with mass m . The weight gives the relative probability that the choice be retained; in case of rejection a new q_3 is selected and the procedure repeated.

It should be noted that the new q_3 quark flavour is not associated with any dynamical properties, such as a mass or, for diquarks, a total spin. It is only the properties of the final, "observable" particles that can influence the relative production rate. Further, the "fragmentation" transverse momentum is determined by the average energy release in cluster decay, and in subsequent resonance decays.

For large cluster masses it would be unrealistic to assume that isotropic two-body decays still dominate. Instead an algorithm is then used to break a cluster anisotropically into two smaller ones, as follows [45]. With even probability, a $u\bar{u}$, $d\bar{d}$ or $s\bar{s}$ pair is produced and paired off with the original flavours. No diquark-antidiquark production is allowed here. For each of the

two subclusters, a mass is chosen uniformly in m^2 , between a minimum value given by the sum of subcluster quark masses and the mass of the whole cluster. Kinematically impossible solutions, with subcluster masses $m_1 + m_2 > m$, are rejected. In the rest frame of the cluster, the directions of motion of the two subclusters are given by the directions of the original cluster endpoint partons, i.e. strictly "along the string direction". If a subcluster obtained this way still has a large mass, the breaking procedure above is repeated.

If all clusters are to decay into at least two particles, the probability of producing a single particle carrying a large fraction of the total jet energy is severely underestimated (section 7.5). In an option, all quarks may be given their "current quark masses" ($m_{u,d} \approx 10$ MeV, $m_s \approx 150$ MeV) after perturbative branchings have stopped. Then the cluster mass spectrum extends almost all the way down to zero. If a cluster mass is below threshold for the lightest two-body state with matching flavours, the cluster is allowed to collapse into the lightest possible single particle. Four-momentum is shuffled to or from nearby clusters, so as to achieve overall energy and momentum conservation.

The Webber program has not been optimized for heavy flavour decays. Specifically, the b or t quark in a cluster is allowed to undergo a weak decay before cluster decay is considered. If the virtual W decays into a $q\bar{q}'$ pair, the result is the formation of two clusters, else one cluster is accompanied by a charged lepton and a neutrino. For a $t \rightarrow b$ decay, the process is repeated for the resulting bottom cluster. In several experimental studies clusters are instead allowed to decay into the ordinary bottom hadrons, with subsequent decays handled e.g. by the Lund routines.

The fragmentation procedure outlined above is explicitly Lorentz covariant. A potential problem is related to the emission of soft gluons, as follows. When an event contains no gluons, the cluster mass is the full mass of the system, W . If a gluon is emitted at roughly 90° to the jet axis, with an energy E_g , and is subsequently split into a $q\bar{q}$ pair with $E_g/2$ each, the system is subdivided into two clusters of mass-square approximately $W \cdot E_g/4$ each. In particular, in the limit of vanishing E the two cluster masses also collapse to naught. The addition of one very soft gluon is therefore enough to change completely the nature of the event, from one large cluster that is likely to decay (via the production of subclusters) into many hadrons, to a situation with two very small clusters of maybe one particle each. The same kind of phenomenon, on a more modest scale, may happen any time a soft gluon is

emitted, however many partons the event as a whole already contains. If the emission of a soft gluon is rare enough, this need not be a serious practical problem: even events containing only two particles are acceptable, so long as they are reasonably rare. It is a peculiarity of cluster fragmentation, however. It may also give visible effects in the Monte Carlo implementations. Thus a reduction of the cutoff scale for parton shower evolution in the Webber program, i.e. an increase of the amount of parton shower evolution, gives a reduction of the average charged multiplicity, contrary to naive expectations. The issue is not clear-cut however: a more sophisticated choice of subcluster masses in large cluster breakups might also remove this anomalous behaviour.

6.2. The Caltech-II Model

The Caltech-II model by Gottschalk and Morris [35,36] is the latest step in an evolutionary process, which has its origin in models along the general lines of the present-day Webber program [29,30]. Compared to the earlier Caltech programs, there are two important differences. Firstly, the forced $g \rightarrow q\bar{q}$ branchings at the end of the parton shower evolution are rejected, in favour of a scenario where longer strings fragment into clusters, Fig. 18. In this respect, Caltech-II is then intermediate to classical SF and CF programs. Secondly, rather than assuming cluster decays to be given by two-body phase space, a parametrized description of cluster decays into a variable number of particles is used.

Once a parton configuration has been evolved according to the Caltech-II coherent parton shower model, the definition of string drawing and the rules for the subsequent string motion are the same as used in the Lund program. Whereas the Lund requirement that produced hadrons end up on mass shell introduces nontrivial rules for the positioning of adjacent breakup vertices, a simple area law decay rule can be used in Caltech-II: the probability for the string to break at a given point is $dP_{\text{break}} = P_0 dA$. Here P_0 is a parameter of the model and dA the invariant string area element, which contains a factor $1-v^2$ for a string piece with (transverse) velocity v . If the area is expressed in a momentum space picture, P_0 is to be replaced by $\rho_c = P_0/\kappa^2$, where κ is the ordinary string tension. As in the Artru-Mennissier model, the breaking probability in a given point is reduced by the probability that the string has already broken, resulting in an exponential decay law. Whereas the Artru-Mennissier model only (explicitly) describes the breaking of a simple $q\bar{q}$ string piece, however, the Caltech-II formalism covers the breaking of a

string consisting of several straight pieces, i.e. a string stretched from a quark end via a number of intermediate gluons to a \bar{q} end.

The area decay law leads to an uninterrupted fragmentation into smaller and smaller string pieces. It therefore becomes necessary to stop this process at some point, i.e. to introduce a rule that a sufficiently small string piece should be identified with a cluster, with subsequent history to be described by the cluster decay parametrization. The probability that an object of invariant mass W is to be treated as a string, i.e. allowed to fragment further, is parametrized as

$$P_{\text{String}}(W) = [1 - \exp(-\frac{1}{2}\rho_c(W-W_{\text{2pth}})^2)] \theta(W-W_{\text{2pth}})^2. \quad (15)$$

Here W_{2pth} is the two particle threshold, which depends on the string endpoint flavours, whereas W_{max} is assumed to be an energy-independent parameter, $W_{\text{max}} \approx 2.2$ GeV. Assumed endpoint quark masses are given by the masses of the lightest particles that can be produced out of them, i.e. $m_u = m_d = m_s = m_K$. Occasionally, a cluster formed during the fragmentation may have a very small mass, so that it is more logical to associate it with a single particle than with a collection of particles. This collapse to a single particle is assumed to take place for masses smaller than $W_{\text{2pth}} + W_{\text{min}}$, where $W_{\text{min}} \approx 0.25$ GeV. The position of the latest breakup vertex is then adjusted slightly, so that the particle ends up on mass shell.

In summary, the parameters not directly related to flavour properties are the Λ and cutoff of the parton shower, ρ_c , W_{max} and W_{min} . The shower cutoff normally used is $t_0 = m_{\text{min}}^2 = 2 \text{ GeV}^2$, i.e. a fairly low value, comparable to what is used in Webber and Lund+PS. The string breakup probability parameter $\rho_c \approx 1.6 \text{ GeV}^{-2}$ is closely related to the b parameter of the Lund symmetric fragmentation function, eq. (9). A large ρ_c value gives a string that breaks rapidly, into a few low-mass clusters, whereas a small ρ_c delays the breakup, leading to more clusters and a larger average cluster mass.

In the decay of a cluster into observable hadrons, the Caltech-II creators take a philosophical attitude different from that of other model builders: since the physics of hadron production at small mass scales is very complicated and is (at present) incalculable from QCD, one should not try to give a model for this process. If instead it is assumed that hadronization is a local, universal process, it is only necessary to introduce a parametrized description of cluster decays. Why this parametrization works could then be left for later generations (of, e.g., lattice QCD people) to find out.

A cluster is assumed to decay, isotropically, into one hadron plus a remainder, which may be a hadron or a new cluster at a reduced mass. As in the Webber model, this requires the selection of a new flavour q_3 which splits the original $q_1\bar{q}_2$ cluster into a $q_1\bar{q}_3$ hadron and a $q_3\bar{q}_2$ remainder. The relative probability for a particular decay mode is taken to be the product of a flavour factor, a spin factor and a kinematic factor. The flavour factor is related to the choice of q_3 among the same quark and antiquark possibilities as in the Webber program. Here the strange quark is suppressed relative to u and d quarks by a factor $\kappa_s \approx 0.60$, diquarks are suppressed relative to quarks by a factor $\kappa_B \approx 0.60$, diquarks containing an s quark relative to nonstrange diquarks by a factor $\xi \approx 0.10$ and ss diquarks relative to nonstrange diquarks by a factor $\xi' \approx 0.08$. (Exactly the same flavour parameters appear in the breakup of a string into clusters.) For $q\bar{q}$ pairs assumed to form hadrons, a particle is selected among the possible alternatives. The spin factor counts the number of states, $(2s_1 + 1) \cdot (2s_2 + 1)$. A meson subcluster is here assumed to have spin 0 and a baryon subcluster spin 1/2. The kinematic factor is $2p^*/m$, where p^* is the momentum of the two decay products in the rest frame of the decaying cluster with mass m . In the alternative where one of the products is a cluster, this is replaced by an integral over $2p^*/m$ values as a function of cluster mass, weighted by a parametrized cluster mass spectrum of the form $(m-M_0)^{1/2}$. Here M_0 is a flavour dependent parameter approximately equal to W_{2ph} . An additional factor is also included in the relative weight for a hadron plus a cluster rather than two hadrons. With the parameter values properly tuned, low energy data can be reproduced to within 10 – 15%.

7. Comparison with e^+e^- Data

A vast amount of information has been collected by the PETRA/PEP experiments [68–73], and what is discussed below is just a selection of some of the more interesting studies, from the point of view of testing fragmentation models.

7.1. Flavour Properties

There is perhaps no area where fragmentation models diverge as much as when it comes to modelling and predicting the particle content of events. The IF concept as such offers no guidance: a parametrization of different baryon production probabilities could be made arbitrarily complicated. In SF schemes,

the tunneling mechanism is invoked but, since quark and diquark masses are unknown, the predictive power is limited. Instead a number of adjustable parameters is introduced, with some suggestions as to most reasonable values. The Caltech-II cluster model is based on parametrizations of low energy data, supplemented by data at higher energies where necessary. The number of parameters involved is almost as large as in the Lund program, and the parameter values are not constrained by any physical principles. A special place is taken by CF models, like the Webber one, where two body phase space times spin factors are allowed to determine the relative probability of all possible channels. Here the number of free parameters is at a minimum: in addition to the ones coming from the parton showers, only those that describe the splitting of a large cluster into smaller and the collapse of a small cluster into one particle. In the end, what matters is the cluster mass spectrum: large cluster masses means an excess of baryons and tensor mesons, small cluster masses a dearth.

A summary of particle production rates in models is given in Table 1. For mesons, the agreement between the simple phase space ansatz of Webber and the more complicated tuning procedure in the Lund program is surprisingly good. In particular, the rate of tensor meson production [70] represents a true prediction of the Webber model, and here data agree well. Tensor mesons are not included in the Lund Monte Carlo, but could very well be, with the introduction of additional parameters. Meson data can therefore not easily be used to distinguish between the models. The larger number of baryon states allows a much more detailed study to be made, in particular since the cluster mass spectrum is already more or less fixed by the meson results. Here the cluster models seem to have problems in predicting ratios correctly, Fig. 19.

For the Webber model the suppression of the heavier baryon species is underestimated, i.e. the penalty factor for having a higher spin or more quarks in a baryon does not seem to be obtained from simple phase space considerations alone. The lack of significant suppression in the Webber model is easily understood: whereas all baryons are heavy (on the scale of typical mesons), the relative mass differences between baryons are not that large. For those clusters that are heavy enough to give a significant contribution to baryon production in the first place, the extra price to be paid for producing heavier baryons is not that large. A cluster mass spectrum with a stronger falloff above 2.5 GeV might improve the baryon situation, at the danger of having problems crop up elsewhere.

In Caltech-II the opposite trend seems to hold true, i.e. heavier baryons are too much suppressed. This most likely shows that the particle composition observed at very low energies can not be used as a reliable guide for the composition in a jet system with a larger mass, at least not in the sense of the flavour content of a large cluster being obtained just as an incoherent sum of contents in separate small clusters. At the expense of losing its soul, the Caltech-II program could certainly be made to agree much better if the parameters were fitted to PETRA/PEP data rather than to data at low energies.

The Lund type parametrization seems to provide the best description of baryon production. No detailed study has been made whether the same parameters would also work at lower energies, i.e. below the 10 GeV region. Compared to the Caltech-II type of parametrization, there is a significant difference, however. Heavy particles are suppressed by the reduced rapidity range available for their production. For a hadron h this introduces a factor roughly $\langle(y_h)_{\max}\rangle/\langle(y_h)_{\max}\rangle \approx \ln(W/\langle m_{\text{Th}} \rangle)/\ln(W/\langle m_{\text{Th}} \rangle)$, which approaches unity when the invariant mass W of the system becomes large. The flavour composition is therefore expected to be different at lower energies, with fewer heavy particles. In the Caltech-II approach, on the other hand, such a suppression would go into the low energy parametrization, and then be propagated to higher energies by the subdivision of a large invariant mass into low-mass clusters. The Lund model therefore stands a fair chance of having a better energy dependence.

Is the accuracy of the Lund parametrization all that impressive? If the s/u and qg/q suppression factors are taken as input, the suppression of spin 1 diquarks seems to have been reasonably well predicted to be $(1/3) u_1/d_0 \approx 0.05$, but experimental errors are still very large. The expected suppression of strange diquarks, over and above the ordinary s/u one, was predicted to be $(us/ud)/(s/d) \approx 0.2$, but here data favour a value closer to 0.7, i.e. a very significant deviation, which is not easily explained away. Thus the tunneling explanation for baryon production is today resting on a rather shaky ground.

One suggested solution is to abandon the tunneling mechanism mass suppression and fall back on symmetric fragmentation only [74,75]. In the Lund model, the symmetric fragmentation function $f(z)$ in eq. (9) is interpreted as the unnormalized probability to select a given z , once the particle mass and P_T are known. It is also mathematically possible, however, to interpret the integral of $f(z)$ over z and P_T as giving the relative weight for the production of a given hadron. Thus there is no suppression because a heavy

flavour is produced, but only because heavy hadrons are produced ($K\bar{K}$ for an s quark, $B\bar{B}$ for a diquark). Like in cluster decay models, the only mass dependence would therefore be related to the physical hadron masses, rather than to the unphysical parton ones. When the usual spin counting is included, the agreement with data is impressive [75]. Only two parameters are free to be tuned, a and b , and these are rather constrained as it is by the necessity to reproduce longitudinal momentum spectra. (An extra factor $\exp(c P_T^2)$, with c an arbitrary parameter, can be introduced without affecting the consistency properties of the model, but this is not needed.) Also the transverse momentum distributions implied by the P_T^2 dependence of $f(z)$ come out in close agreement with data, but here the problem of global P_T conservation remains to be solved: since P_T 's are not defined for quarks but only for hadrons, no local P_T compensation mechanism enters naturally. While it is quite possible that some fundamental flavour "phase space" type of effect is correctly modelled in this avenue of approach, judgement must be reserved until all consequences are understood.

7.2. Event Shapes

The information content in an average event is huge. In order to get a feeling for the event-to-event fluctuations, it is useful to condense this information into simple numbers. Thus several different global event shape variables have been proposed, such as sphericity S and aplanarity A [76], thrust T [77], major M_a , minor M_b and oblateness O_b [78], scaled broad and slim jet mass [79], etc. Simple one-particle distributions in P , P_T , P_{min} , P_{out} and y (w.r.t. an event axis or plane) fill a similar function. Distributions of the type above are also convenient for tuning model parameters and testing the general validity of a model. The most detailed study to date of this kind was recently presented by Mark II [80], with comprehensive data tables and comparisons with the Lund (both with showers, Lund+PS, and with second order matrix elements, Lund-ME), Webber and Caltech-II programs. These results will be summarized and commented on in the following.

In all three (four) programs, the main QCD and fragmentation parameters were tuned to the Mark II data. The final comparisons contain 18 experimental distributions, with a total of 450 data points. The summed χ^2 for 50000 model events is used as a simple overall measure for the goodness of the description. Two warnings are here in place. First, the 18 distributions are in no sense orthogonal, but contain a large amount of overlap, such that the

number of degrees of freedom is not well defined, nor the relative impact of different model errors. Second, the χ^2 measure per degree of freedom is only supposed to approach unity if statistical fluctuations is the only source of error. However small a deviation is in an absolute sense, it will lead to a χ^2 growing indefinitely when statistics is increased.

A few examples of distributions are shown in Fig. 20. This is not an unbiased sample, but rather emphasizes those where differences between models are most pronounced. The trend, that Lund fares best and Caltech-II worst, is no coincidence, however: the summed χ^2 is 960 for Lund+PS, 1230 for Lund+ME, 2870 for Webber and 6830 for Caltech-II.

To start with the matrix element program, the main problem is in reproducing properties out of the event plane, such as aplanarity, minor or P_{out} . This will be discussed further in section 7.3. The Lund shower program gives a good account of most event shape variables, and the major problem is actually in the $x = 2p_t/s^{1/2}$ distribution, where the model is above the data at intermediate x and below at large x . (A statement by Gottschalk [81] that significant problems exist with the Energy-Energy Correlation [82] in the Lund program should be disregarded as erroneous [83]; one possibility is that Gottschalk did not correct for the non-default charm branching ratios used in the Mark II analysis.)

If a general theme is to be given for the Webber model deviations, it is that the two-jetlike tails of distributions are overestimated. This is most clearly seen in the minor distribution, but is also visible at thrust close to 1, at small broad and slim jet masses, and at low multiplicity. The problem seems to be more with the cluster fragmentation scheme than with the parton shower: if Lund strings are attached to the Webber shower partons, without any forced $g \rightarrow q\bar{q}$ branchings, the summed χ^2 is quite comparable to the Lund shower value. It is therefore tempting to assume, but by no means proven, that the soft gluon emission problems mentioned in section 6.1 are at play here: the $g \rightarrow q\bar{q}$ branching of an occasional central soft gluon splits the event into two back-to-back, low-mass clusters (or collections of nearby clusters).

In the Caltech-II model, distributions tend to be too broad, i.e. both the two-jetlike tail and the multi-jetlike one are overestimated. This is visible in almost all distributions: sphericity, aplanarity, thrust, minor, broad and slim jet masses, etc. If the Caltech-II parton shower is combined with Lund string fragmentation, the summed χ^2 is roughly halved. The fact that the

multi-jetlike events remain overrepresented probably indicates that some of the problems observed originate with the Caltech-II shower algorithm. If instead the Lund shower is combined with Caltech-II fragmentation, agreement is slightly better than in the other hybrid mixture. The multi-jetlike tails now look reasonable, whereas two-jetlike events still are overrepresented. It has been suggested that some fragmentation P_T should be introduced in the cluster formation process [36]; this would broaden jets and probably lead to better agreement with data.

The Mark II comparisons did not include any independent fragmentation models. Other groups, like TASSO [59], have in the past compared SF and IF models. For these general event measures IF has then done roughly as well as SF. The general event shape is thus not the place where IF can be disproven.

7.3. Perturbative QCD Aspects

Most of the event shape measures in the previous section are also probes of the jet activity of events, and as such may be used in α_s or Λ determinations. The effects of fragmentation are large, however, and can not trivially be corrected for. One particular aspect, the effect of imposing momentum conservation on IF events, is described in section 5.2. The result is an α_s hierarchy, $\alpha_s(\text{Hoyer}) < \alpha_s(\text{Ali}) < \alpha_s(\text{Lund})$, where the relative splitting may vary somewhat from measure to measure, according to reasonably well understood rules [65]. A pessimist would conclude that it is impossible to determine an α_s value at all, an optimist that fragmentation studies can help constrain the range of acceptable models and hence of α_s values. The results of some recent α_s studies may be found in [68, 69, 84]. The Λ value obtained in parton showers is further affected by the details of the shower algorithm used, so that the Λ values in different Monte Carlos can not at all be compared.

With an α_s determined to describe three-jet aspects well, the number of four-jets is severely underestimated with second order matrix elements [65]. Inclusion of third order corrections may remedy this situation, just as large corrections were obtained to the three-jet rate in second order. One obvious difference compared to parton showers is that the Q^2 argument in α_s is W^2 rather than the P_T^2 of a parton branching. Indeed, parton shower models seem to fare much better than matrix element based ones in describing the rate of events with many jets [44, 70, 85], Fig. 21. Furthermore, showers correctly reproduce the variation with CM energy and with resolution in the cluster

algorithm. This success is not trivial, in the sense that leading log approximations are not guaranteed to be good for non-collinear emission. Thus the original Marchesini-Webber program had to be modified in order to give better agreement with the experimental three-jet rate (section 3.2).

The JADE algorithm used for several of these studies is based on successively joining the two particles or clusters with smallest invariant mass to form a new cluster, until all invariant masses are bigger than some m_{cut} . The three-jet rate above some fixed $y_{\text{cut}} = m_{\text{cut}}^2/W^2$ should be energy-independent, apart from fragmentation corrections, if α_s is constant. Data instead favour a running α_s [86], in accordance with expectations, Fig. 22. The results are not conclusive, however, and so far no reliable method has been developed to distinguish between $Q^2 = m^2$ and $Q^2 = P_T^2$ in a parton shower picture. Within the framework of the Lund program, the shape of the sphericity distribution at low values does seem to favour the latter choice [46], Fig. 23.

The cutoff of matrix elements or parton showers, y_{min} or m_{min} , is not a fundamental parameter of the theory. Rather it denotes an arbitrary point, where the nonperturbative fragmentation description is supposed to take over from the perturbative partonic one. There is now an overwhelming body of evidence from various studies that this cutoff has to be chosen rather low, $m_{\text{min}} \approx 1$ GeV for parton showers, ≈ 4 GeV for matrix elements, in order to provide a good description of data [87, 44, 80, 88]. This is certainly not a fragmentation model independent statement, but does seem to hold true for all models in use today. It is also not a priori obvious that a parton shower approach should work well when the evolution is carried down to a region where $\alpha_s \approx 1$, or the matrix element one when the three- plus four-jet rate is close to unity.

A common theme is that the cutoff has to be chosen so small that the fraction of remaining two-parton events is negligible (< 5%) at PETRA/PEP energies. These events, if present in large numbers, give rise to back-to-back jet configurations, which overpopulate the region of very low sphericity etc. The phenomenon is particularly well visible in the energy-energy correlation asymmetry [82], where a large cutoff value gives rise to a visible separation between two- and multijet events [87], Fig. 24. Even rather soft gluon emission is enough to destroy the back-to-back character of the two main jets, and give much better agreement with data. The need for a low cutoff is therefore probably common to all fragmentation models in which transverse momentum is compensated locally in a two-jet event. The appearance of a

Sudakov form factor in the parton shower approach means that, for a common cutoff mass, the two-jet rate is higher with parton showers than with matrix elements (all other things being equal). For a common m_{min} , this means that parton showers actually give worse agreement with data in distributions affected by soft gluon emission. Agreement is restored when the shower cutoff is lowered, so that the two-jet rate again is negligible.

7.4. String Effects

The "string effect" derives its name from first being devised as a way of showing that particles in three-jet events are distributed along strings, and not along the jet directions, as expected in independent fragmentation models [14]. The principle involved is illustrated in Fig. 6. In a $q\bar{q}g$ event, the string is spanned from the q via the g to the \bar{q} . Each of the two string pieces, $q\text{-}g$ and $g\text{-}\bar{q}$, has a transverse motion in a direction intermediate to the endpoint directions. The particles produced along these strings are therefore boosted away from the origin, such that the number of particles in the $q\text{-}g$ and $g\text{-}\bar{q}$ angular regions is increased, whereas the $q\text{-}\bar{q}$ angular region is depleted from particles. In an IF framework, particles are produced along the three jet directions, and there is therefore no depletion in the $q\text{-}\bar{q}$ region. For a soft gluon fragmentation, like in the Ali model, some enhancement in the $q\text{-}g$ and $g\text{-}\bar{q}$ regions is obtained. On the other hand, if gluon jets are assumed to fragment about as quark ones, like in the Hoyer model, also this enhancement is absent.

In order to maximize differences, and minimize the number of IF parameters involved, it is therefore customary to compare the Lund and Hoyer programs, Fig. 25, but the qualitative behaviour is the same for the Ali one. The data here strongly support the Lund string picture, and deals a serious blow to the IF concept [16-19]. The interpretation in terms of a boost effect is strengthened by the fact that the difference between the $q\text{-}g$ ($\bar{q}\text{-}g$) and $q\text{-}\bar{q}$ regions is enhanced for heavier particles (K, p), for particles with large P_T out of the event plane, and in energy flow as compared to particle flow, Fig. 26. It should be emphasized that the small effects observed experimentally, typically 30% - 60% difference between "q-g" and "q- \bar{q} " region, would have been much larger (typically a factor 2 - 3) had it been possible to identify the gluon jet unambiguously. The normal procedure is to assume the lowest-energy jet to be the gluon one, which typically is correct in only 50% - 60% of the events.

In the string picture, high-momentum particles follow the parton directions, whereas lower-momentum ones in the q (\bar{q}) jet are systematically shifted towards the g jet direction. This gives a systematic bias in q jet axis determinations, such that high-momentum particles in a q jet have a tendency to appear on the side of the q jet axis away from the gluon, whereas the medium low momentum ones still tend towards the g direction. Again, no corresponding phenomenon is expected in IF, and again data support the string picture, Fig. 27 [16,17,89].

The TASSO string effect analysis [19] includes a variation on the energy flow theme, where the ratio of particle flow in the central parts of the q - g and q - \bar{q} angular regions is studied as a function of the particle momentum in the event plane. Here neither model agrees well with the data; in the Lund+ME program the main problem is with fairly high-momentum particles ($P_{\text{in}} > 1 \text{ GeV}$). There are some indications that the problem is related to the lack of four-jet events in the Lund+ME program. A comparison with parton shower based models could help enlighten the situation.

The Leningrad group has shown that the string effect appears as a natural consequence of coherence phenomena in the parton shower evolution, i.e. angular ordering [47]. In lowest order, this may be viewed as follows. Start out with a quark, an antiquark and a gluon, all three with approximately the same energy, and let the three partons act as antennae that emit soft gluons in a semiclassical pattern. Due to interference effects, there is then a surplus of radiation in the q - g and g - \bar{q} regions, and a depletion in the q - \bar{q} region. If a term proportional to $1/N_C$ is dropped, the two remaining terms may be interpreted as simple qg and $\bar{q}g$ dipole radiation, boosted from the qg and $\bar{q}g$ rest frames into the overall $q\bar{q}g$ CM frame. The depletion of the q - \bar{q} region is a direct consequence of these boosts. This scenario literally repeats the explanation given in SF, so that the picture of perturbative semiclassical gluon bremsstrahlung and non-perturbative string fragmentation here approach each other.

One specific suggestion of the Leningrad group is to compare $q\bar{q}g$ events with $q\bar{q}\gamma$ ones. In the latter, the colour antenna (string) is spanned directly between the q and \bar{q} , and is thus boosted in the very direction that is avoided in $q\bar{q}g$ events. For symmetric events there is a firm prediction that the amount of soft gluon emission in between the q and \bar{q} directions should appear in the ratio $7 : 16$ for $q\bar{q}\gamma : q\bar{q}g$ events. If local parton hadron duality [90] is

assumed, i.e. that the energy flow of hadrons is a close copy of that of original partons, this prediction should be experimentally verifiable. The effect is reduced by misidentifications of the gluon jet, but is still visible enough [91], Fig. 28. As a test of Monte Carlo programs, the $q\bar{q}\gamma : q\bar{q}g$ ratio does not contain any information not present in the $q\bar{q}g$ energy flow itself, since all models agree on the treatment of $q\bar{q}\gamma$ events.

It is maybe not surprising that the Webber program, based on a coherent parton shower picture, is able to reproduce all the string effects [18,89], see e.g. Figs. 26 and 27. The belief that this agreement is a direct consequence of coherence in the shower was strengthened by the observation that a precursor to the present Caltech-II model [30], which did not contain a coherent parton shower, did not reproduce the data [18,89] (while the present Caltech-II does [35]). Unfortunately, the picture is probably more complicated than that: switching off the intermediate stage where large clusters are broken into smaller along a string direction, the string effect in the Webber program disappears [80,83]. This is not yet fully understood, but the likely explanation is the following. If large clusters are allowed to form and decay isotropically, in what is otherwise essentially a two-jet event, the decaying cluster may easily add two extra "jets". The more energetic of these is identified with the gluon jet of a three-jet event, whereas the less energetic one is to be found opposite in azimuth around the main event axis, i.e. between the " q " and " \bar{q} " jet directions. This gives an "anti-string" effect, which cancels the true string effect. The morale is that the appearance of a string effect or not depends not only on the shower model, but also on the details of the fragmentation model used.

The situation is even more extreme in SF models. Not only is a string effect obtained for three-parton events, where angular ordering constraints do not enter at all, but also if an incoherent shower algorithm is used [46,35]. The reason for this apparent paradox is to be found in the rules of string dynamics, as follows. If a soft gluon is emitted from the q into the q - \bar{q} region, but in colour space is connected to the g , then this gluon can not stretch the string very far before it stops, and starts to be "dragged away" from the q - \bar{q} region. As a consequence, no significant contribution is to be expected to particle production in between q and \bar{q} . The string fragmentation model therefore does not fully respect the assumption of local parton hadron duality. The scenario in the coherent case may be viewed as an attempt to form a string from soft partons, partons which are predominantly emitted in the directions where the string would already have been if only the three hard

partons ($q\bar{q}g$) were used for the string drawing.

7.5. Momentum and Rapidity Distributions

The shape of the particle momentum distribution in SF and IF models is strongly dependent on the choice of fragmentation function $f(z)$, while the parton shower is mainly responsible for results with CF. Since decay products tend to end up at small momenta, the region of large $x = 2p/W$ is particularly interesting for extracting information on primary particle production. Here the HRS group has made the most detailed study [92], with the conclusion that the Lund+ME model agrees well, while cluster models fall far below data, Fig. 29. This is a consequence of the exclusively two- (or multi-) body decay of clusters in use at that time, and prompted the development of scenarios where a low-mass cluster may collapse into a single particle (sections 6.1 and 6.2). With the collapse of roughly 10% of all clusters, reasonable agreement is obtained. The introduction of showers in the Lund program led to a degradation of agreement at large x [80]: the softening due to extra soft gluons is imperfectly balanced by a retuning of the a and b parameters in the symmetric fragmentation function. This is therefore an area where present-day CF models are doing better than the present Lund program, Fig. 20e. The use of an a value smaller than the standard $a = 0.5$ does here give better agreement [85].

At the other end of the momentum spectrum, coherence effects are expected to inhibit particle production at small x values. In the parton $d\sigma/d(\ln x)$ distribution, an approximate Gaussian peak is expected at $x \sim (Q_0/Q)^{1/2}$ for a parton shower cutoff at Q_0 [93]. The concept of local parton hadron duality implies that the same spectrum should be expected for hadrons if Q_0 is replaced by the hadron mass m_h . Indeed, data show good agreement with the predicted shape, including the motion of the peak as $Q = W$ is changed [94,95]. Models based on coherent parton showers successfully describe the data, but so does Lund+ME, and even IF models. This implies that the distributions are dominated by trivial phase space effects at present energies.

With the inclusive momentum distribution accounted for, the momentum spectra for individual particle species de facto contain little information, beyond what is given by the relative particle production rates in section 7.1. This does not mean that all x spectra look the same, but only that differences are mostly due to kinematical effects of different particle masses and to the systematics of resonance decays, which cooperate to give harder spectra for

heavier particles. Recent TPC/2 γ data [70] indicates that the proton fraction among charged particles is slightly lower at large x values than expected in the Lund model. This would be understandable in terms of a slightly larger a in eq. (8) for diquark pair creation, corresponding to a larger effective production time (cf. eq. (10)) than for simple $q\bar{q}$ pairs. Although not physically unreasonable, such a scenario would introduce yet another flavour-related parameter into the program.

In simple two-jet events, a flat central rapidity plateau dn/dy is expected. The experimental distribution instead displays a dip around $y=0$ [88,94,95], Fig. 20d. There are several trivial reasons for this. When charged particles are not identified, the use of m_η also for kaons and protons gives a systematic overestimation of the true y . The determination of a jet axis introduces a bias which depends on the definition used; for thrust the effect is a clear dip at very small y . Charm (and bottom) decays tend to give a small bump around the rapidity of the charm (bottom) hadron, such that a very broad dip results at small y values. Also ordinary light quark jets may have a weak bump at the edge of the rapidity plateau if, as is the case e.g. with the Lund symmetric fragmentation function, $f(z)$ dips down at $z = 0$. Even with these sources corrected for, there still remains a significant dip.

The inclusion of three-jet events makes no difference in IF models, whereas a dip does appear in SF ones. The former is easily understood. In IF, the normal criterion is to require $P_L > 0$ for the generation of particles in a jet. For a jet exactly along the event axis this corresponds to an abrupt cut at $y = 0$. If the jet forms not too large an angle w.r.t. the event axis, then some particles migrate to $y < 0$, but at the same time particles are lost at small positive y , in such a way that the falloff is symmetric around $y=0$. When averaged over positive and negative y , each jet by itself is therefore expected to give a flat plateau. In SF, the angles between are to be found close to each other and to the event axis, the particles produced from the connecting string piece are boosted away from small rapidities. In a typical three-jet event, there is thus one long string piece, from q to g , say, which spans the second piece, from g to \bar{q} , which is boosted and gives a dip at small y .

In a shower description, a rapidity dip is expected already on the parton level, in close parallel with the suppression of small \times gluon emission noted above [93,96]. Angular ordering effects also play a more direct rôle for the

hadron level results, by suppressing the emission of gluons with $y < 0$ from a parton with $y > 0$, and vice versa, such that only one string piece or cluster will bridge the $y = 0$ region. Indeed, CF models also show a dip at $y = 0$, Fig. 20d.

Since the size of the expected dip in an event depends on the underlying parton configuration, it is interesting to study how the size of the rapidity dip depends on shape variables, such as sphericity. This has been done by TPC/2 γ [88], Fig. 30. At small sphericities, two-jet events dominate and no dip is visible. At large S , on the other hand, the events contain extra hard gluons, which then kinematically are constrained to be close to $y = 0$ and leave no room for a dip. It is therefore at intermediate S values that the dip is most pronounced. This is the region of "2 1/2 jet events", i.e. events where it is not possible to distinguish three separate jets on an event-by-event basis, but where the event sample as a whole would not be explainable in terms of simple two-jets. Since the gluon production cross-section is roughly flat in y for a fixed p_T , it is here that the (main) extra gluon of the event may appear over a wide rapidity range. This often gives the scenario described above, with one string piece, or cluster, boosted away from the central region.

As a simple measure for the variation with S , the ratio

$$R_{\pi}(S) = \frac{dn_{\pi}/dy(0.0 < y < 1.0, S)}{dn_{\pi}/dy(1.5 < |y| < 2.5, S)} \quad (16)$$

is shown in Fig. 31. The measure is not precise enough to give the details of the rapidity dip, but is experimentally roughly constant up to $S \approx 0.1$, after which it increases rapidly. With IF, there is an increasing trend for all S values, such that the disagreement with data is quite significant for intermediate S values. The Lund+PS alternative gives a good description, but if the shower cutoff scale Q_0 is increased from 1 to 2 GeV, or if matrix elements are used, R_{π} is consistently too high for $S < 0.1$. This should be seen as an indication that the rapidity dip is indeed a consequence of rather soft/collinear emission. In the Webber CF scheme, the rapidity dip at low S is more marked than in the data. Again, the forced $g \rightarrow q\bar{q}$ splitting of soft gluons may, but need not, be the cause of this discrepancy.

The HRS group has studied charged multiplicity distributions in different rapidity bins [97]. It is here observed that, whereas the total multiplicity is close to Poissonian, the distribution in small, central bins is

significantly broader than Poisson, and can be well described by negative binomial distributions. The Lund model, and probably other fragmentation models as well, seem to reproduce the data fairly well. The basic one-dimensional fragmentation model is here actually rather narrower than Poissonian, but the effects of resonance decays and gluon emission tend to broaden the distribution. In particular, whether a given rapidity range contains a gluon jet or not makes a large difference in the multiplicity.

7.6. Particle Correlations

The concept of short range correlations is well established: charge and flavours have a tendency to be locally compensated [98, 99]. This does not exclude the possibility of some longer range effects, e.g. the correlations due to the initial $q\bar{q}$ pair. Short range correlations are built into the IF, SF and CF frameworks from the onset. In CF most correlations take place inside clusters, and less at the boundary between clusters, whereas the picture is more uniform in IF and SF. In principle, this difference should be visible in p_T correlations, but is almost completely drowned by effects of resonance decays etc. Also a TPC/2 γ study of π and K charge compensation [99] gave very similar results for the Lund and Webber programs.

A more promising possibility is to consider baryon correlations [100]. Baryons are rare enough that usually only one $B\bar{B}$ pair is present in an event, and baryons are also less affected by resonance decays. Therefore they are more direct probes of the underlying production mechanism – the drawback being that this mechanism may well be more complicated for baryons than for mesons. One example is the TPC/2 γ study of the distribution in opening angle θ between the event jet axis and the axis of $p\bar{p}$ pairs, the latter axis defined by boosting to the rest frame of the $p\bar{p}$ pair [101, 70]. If clusters are assumed not to have net baryon number, such that baryons are always pair produced in the isotropic cluster decays, a flat distribution is expected in $\cos\theta$, slightly modified by events with several $B\bar{B}$ pairs. Instead the data show a strong peaking at $|\cos\theta| = 1$, as predicted in the Lund model, where the baryon and antibaryon are pulled apart along the string direction, Fig. 32. Similar results can be obtained in CF models if e.g. $g \rightarrow q\bar{q} + \bar{q}\bar{q}$ branchings are allowed, section 6.1. Needless to say, this is a step removed from a purist's view of CF, where flavour production is an entirely local process, determined by phase space effects inside the individual cluster.

In the Lund popcorn baryon production scenario, the relative mixture of $B\bar{B}$ and $B\bar{M}\bar{B}$ configurations is a free parameter; by default the two are assumed equally probable. One way of measuring this is to consider the transverse momentum correlation between baryons and antibaryons. The variable $\alpha = \langle \bar{P}_T(p)\bar{P}_T(p') \rangle / \langle p_T^2(p) \rangle$ is, unfortunately, rather sensitive to gluon emission effects. Better precision is obtained with α_{out} , where only the transverse momentum component out of the event plane is used. The more negative α_{out} is, the larger the dominance of the more strongly anticorrelated $B\bar{B}$ configurations. As it turns out, an admixture of at least 50% $B\bar{B}$ chains is required, and it seems possible to do entirely without $B\bar{B}$ ones [10]. (In other words, there are not any real signs at all of an anticorrelation in \bar{P}_T between the p and \bar{p} , as also previously noted by TASSO [100].) It is therefore doubtful whether the neglect of $B\bar{M}\bar{B}$ configurations is really justified.

Another interesting TPC/2Y observation is a strong anticorrelation in $p\bar{p}$ and $\bar{p}\Lambda$ pairs: if an event contains two antibaryons, these are unlikely to be found close to each other in rapidity [102], Fig. 33. In an IF or SF model, the two antibaryons can not be nearest neighbours in rank, but must be separated by a baryon, at least. Depending on how strong the correlation is between ordering in rank and ordering in rapidity, two \bar{p} may still end up close in rapidity. The data may then be interpreted as disfavouring fragmentation functions $f(z)$ which do not vanish in the limit $z \rightarrow 0$, i.e. which give weak rank-rapidity correlations. The Lund symmetric fragmentation function, eq. (9), with its stronger correlation, gives agreement with the data.

Strong Bose-Einstein correlations have been seen in the π data, i.e. identical pions have a tendency to cluster [103,71]. This is not an integral part of any fragmentation model, but explanations have been proposed within the framework of fragmenting strings, of the Artru-Mennissier [104] or Lund [105] type. One may e.g. see the exponential decay area law, $\exp(-ka)$, where k is the ordinary string tension. The introduction of a phase into the amplitude gives interference effects between different event topologies, which correspond to different string areas. If the effects of intermediate resonances are neglected, good agreement is obtained with data. This is probably a reasonable attitude for short-lived resonances like ρ , but more troublesome for η and η' [104].

7. Gluon versus Quark Jets

Whereas IF models have little predictive power for differences between gluon and ordinary (u , d or s) quark jets, SF and CF models agree that gluon jets should have higher multiplicity and a more spread out energy and particle flow. In one case this prediction is based on gluons being attached to two string pieces rather than one, in the other on a more profuse gluon shower evolution than quark one. The common denominator is the larger colour charge of gluons, the famous $N_C/C_F = 9/4$ factor.

The asymptotic prediction of a factor $9/4$ larger multiplicity in gluon than in quark jets is adjusted downwards by higher order corrections in the perturbation theory [106]. At present energies, further effects are at play in reducing expected differences: c and b jets have higher multiplicities than u , d or s ones; a large fraction of the energy is used just for giving masses to the particles produced, so that a doubling of multiplicity would often be kinematically impossible; the extra multiplicity in gluon jets appear at low x values, where jet assignment is uncertain; and so forth. It is therefore not surprising that differences have been hard to find.

A study by JADE [17] showed that g and q multiplicities are comparable, but that a model with a softer gluon than quark fragmentation is still needed to explain this condition, because of the effects noted above. HRS has also failed to find a significant difference, but some signs of a softer gluon fragmentation show up if symmetric three-jet events are considered [107].

It is somewhat more rewarding to look for differences related to momentum distributions. The JADE study above [17] found signs of a softer \times spectrum and a higher $\langle p_T \rangle$ in gluon jets. The largest signal was found in particle flow as a function of angle away from the jet axis, since this measure combines the two aspects noted above. The softer gluon \times spectrum was more conclusively established by a Mark II study of symmetric 3-jet events at 29 GeV, in comparison to two-jet events at 19.3 GeV [108], Fig. 34. Note that the Lund+ME model, with a demonstrably soft gluon jet, still fails to predict enough of an effect. This is mainly due to the use of fixed order perturbation theory, which does not give enough additional jet softening (scaling violations) by gluon emission between 19 and 29 GeV. The shortfall is in q and g jets alike, but is pushed into the reconstructed g fragmentation function by the extraction procedure, which is based on the equality of quark jets at 19.3 and at 29 GeV. The Webber shower model here agrees well with data. Finally,

evidence for softer gluon than quark jets have been obtained by CLEO, in a comparison of Γ and continuum events [109].

The CELLO group has also studied transverse momentum properties, and found gluon jets to have a larger $\langle p_T \rangle$ than quark ones [70]. In the event plane, the effect is smaller than what is expected from the string boost of low-momentum particles away from the g jet axis, such that $\langle p_{T\text{in}} \rangle$ is only slightly larger than $\langle p_{T\text{out}} \rangle$. The result is therefore gluon jets that are "rounder" than Lund predictions. The effects are small, however.

Attempts at identifying flavour content differences between gluon and light (u, d, s) quark jets at PETRA/PEP have been inconclusive. Rather more interesting are comparisons between Γ decays into three gluons and the adjacent continuum $q\bar{q}$ events, mainly performed by CLEO and ARGUS, Fig. 35 [70]. For mesons, the most crucial issue is whether particles with a large isoscalar content, such as η and η' , are enhanced on resonance. This is predicted in the gluon jet model by Peterson and Waiss [110], where the fragmentation process is supposed to produce gg bound states. Such glueball states would then mix with isoscalar mesons. The data does not show any η enhancement, however.

More firmly established is the enhancement of baryon production on resonance, by a factor of 2-3. A large amount of this difference can be understood in terms of purely kinematical effects, such as a longer effective string length or a larger number of clusters in ggg than in $q\bar{q}$ events, and the smaller number of primary hadrons in $c\bar{c}$ continuum events. A trivial, but very important, effect is that a $q\bar{q}$ string has two endpoints that are constrained to be quarks rather than diquarks, whereas a ggg string (or collection of clusters) has no ends and therefore no place where diquark production is forbidden. As a consequence, the Lund model predicts almost a factor of two difference in proton production, and slightly smaller factors for heavier baryons (probably due to phase space effects) [53]. In the Webber cluster model, on the other hand, differences between resonance and continuum increase for heavier baryons, as a consequence of a larger average cluster mass on resonance than in the continuum [111]. The trend of the data here is favouring the Webber approach.

7.8. Heavy Flavour Jets

7.8. Heavy Flavour Jets

Experimentally, it is well established that heavy flavour jets deposit a major fraction of their energy in the leading charm or bottom hadron [60], and that the effect is more pronounced the heavier the quark is. This is most succinctly expressed by the Bjorken (Suzuki) [112,113] formula

$$\langle z \rangle \approx 1 - \frac{1}{m_Q} \text{ GeV} \quad (17)$$

for a heavy flavour mass m_Q . The formula may be understood as follows.

Because of its large mass, the heavy quark is not expected to decelerate very much during the fragmentation process, so the rapidity of the heavy hadron should be close to that of the initial heavy quark. The subsequent ordinary hadrons should normally have a rapidity smaller than this, as is easily visualized by boosting to a frame where the heavy quark initially is at rest: if the recoiling jet then is moving out in the $-z$ direction, no sensible fragmentation mechanism would be expected to spew out particles in the $+z$ direction, even if it in principle would be kinematically possible. If therefore the typical rapidity separation between adjacent rank ordinary hadrons is taken to be $0.7 \approx \ln 2$, the same difference should also be expected to hold between the first rank heavy flavour hadron and the second rank ordinary hadron, Fig. 36a. With an average primary hadron transverse mass of 1 GeV, this gives for the light-cone fraction z taken by the heavy hadron

$$\langle z \rangle \approx \frac{m_H}{m_H + (1 \text{ GeV}) \{ e^{-\ln 2} + e^{-2\ln 2} + e^{-3\ln 2} + \dots \}} = \frac{m_H}{m_H + 1 \text{ GeV}}. \quad (18)$$

This formula is asymptotically equivalent to the Bjorken one, but is more useful for not quite so heavy quarks, like charm.

Several different fragmentation functions $f(z)$ have been proposed which obey this relation. The most well-known one is the Peterson formula, eq. (14), which is based on arguments in old-fashioned perturbation theory for the process $Q + H (= Q\bar{q}) + q$ [61]. It is also possible to use the area decay law, in the spirit of the Arttu-Mennissier model, to derive an $f(z)$ which conforms with eq. (17) [114]. Important for this derivation is that the invariant string area spanned during a period of an oscillating $Q\bar{Q}$ system is smaller than that of a massless $q\bar{q}$ pair of the same energy, Fig. 37.

The Lund symmetric fragmentation function, eq. (9), is the only publicly propounded function which breaks the Bjorken relation. Instead the asymptotic behaviour is here given by

$$\langle z \rangle \approx 1 - \frac{1+a}{b m_H^2}, \quad (19)$$

where a and b are the parameters of the symmetric fragmentation function. In terms of the rapidity picture above, the difference is that the average separation is no longer expected to be the same for all hadrons, but rather that heavier particles will appear with larger rapidity separation than lighter one. This is because left-right symmetry requires that a heavier particle should take a larger average z than a lighter one, and thereby leave less energy for subsequent particles. In some sense, a heavier particle will "eat a larger piece of the string", and so there can be fewer of them. It could be argued that this reasoning should only apply when comparing the production of protons and pions, say, inside the string, and not for the two endpoint hadrons. If applied for a leading heavy hadron, however, the argument is that this hadron will become more and more isolated in rapidity as m_Q is increased, Fig. 36b, leading to an (asymptotically) larger $\langle z \rangle$ than in eq. (17). This also means that the area decay law is deemed irrelevant (cf. the discussion in section 4.3) or, put another way, that the relevant area is not reduced when going from a massless to a massive quark, Fig. 37.

Unfortunately, the mass range and experimental precision of current charm and bottom data is not enough to distinguish between the possibilities. Comparisons with data are also complicated by the use of different z definitions (energy fraction, momentum fraction or lightcone fraction), and by the effects of gluon and photon emission, which are explicitly accounted for in Monte Carlo simulations but not in most fits to the charm spectrum shape [60]. The Lund symmetric fragmentation function, with a and b determined mainly by ordinary hadron fragmentation properties, gives good agreement with charm and bottom data, but so does the Peterson formula, or formulae based on the area decay law, or cluster decay models [35,50]. It is therefore for top that differences will become interesting. In this case the peak at $z = 1$ is extremely narrow in the Lund approach, with rather broader peaks in other models. Some distance above the top threshold, gluon emission effects will start to broaden also the Lund distribution, however.

7.9. Energy Dependence

A good model should be able to describe data over a wide range of energies, without the necessity to retune any of the basic parameters. In models based on matrix elements, the impossibility of using a fixed m_{\min} cut is likely to cause troubles. One example is given in [86], where it is shown that the running of α_s is inconsistent with perturbative QCD expectations in the Lund+ME program.

For parton shower based programs, no corresponding inconsistencies are known to date. The Mark II comparison of the Lund, Caltech-II and Webber programs [80] did not reveal any significant differences over the energy range so far probed. If extrapolated to the Z^0 pole, the models do deviate somewhat, however, Figs. 38 and 39. The Caltech-II average charged multiplicity is higher than the Webber one by 3 units, with Lund somewhere in between. Much of the extra multiplicity in Caltech-II seems to be due to a significant tail out to very large multiplicities ($n_{ch} > 50$), absent in the other programs. Many of the differences present at lower energies persist, e.g. in aplanarity or rapidity distributions. The largest differences are still in comparison with the Lund+ME program, which gives significantly less multiplicity and activity out of the event plane.

In the Z^0 studies at SLC and LEP I, the multijet structure will be readily visible. It will be very difficult to observe directly coherence effects, such as angular ordering. At somewhat higher energies, accessible by LEP II, tests could be devised [46] which would significantly constrain the coherence properties of parton showers, and thus give a better handle on the stage that precedes the fragmentation. Once the top threshold is passed, however, the multijet signal from ordinary events will have to be found against an imposing background.

8. Leptoproduction and Hadron Collisions

Compared to the field of e^+e^- annihilation, fragmentation models are less developed for interactions between a lepton and a hadron, or between two hadrons. Furthermore, experimental studies are usually much more difficult, and results therefore less conclusive. What is given in this section is therefore only a very brief overview of models and a few examples of results. Further areas of high energy physics, such as $\gamma\gamma$ -physics, photoproduction,

hadron-nucleus and nucleus-nucleus interactions, are not covered at all.

8.1. Leptoproduction Models

In leptoproduction, only one Monte Carlo program has been extensively used to compare with data. That is the LEBTO program, version 4.3 [115], which belongs to the Lund family. Indeed, exactly the same fragmentation routines are used as for e^+e^- annihilation events [54], once the partonic configuration has been chosen. In version 4.3, first order QCD matrix elements [116,117] are used. The more recent version 5.2 also has an option with parton showers [118,119]. In leptoproduction, this involves not only the final state timelike showers, but also initial state spacelike ones, Fig. 40. Technically, spacelike showers are much more difficult to generate efficiently with Monte Carlo methods. Here, a "backward evolution" formalism is used [120,121,42], in which the parton shower evolution is traced backwards in time, from the hard interaction to the shower initiator.

It is necessary to supplement the standard fragmentation model with a recipe for the fragmentation of the diquark target remnant, formed when a valence quark is kicked out of the original proton [122,123]. A flavour chain is then formed in much the same vein as in the popcorn $\bar{B}B$ production model (once the \bar{B} has been selected), but with the difference that the baryon in a diquark jet may be formed not only as the first or second rank particle (i.e. analogous to $B\bar{B}$ and $B\bar{B}$ configurations in the popcorn model) but also as a higher rank one. This is achieved by defining, once and for all, a fraction x_J for the energy-momentum position of one of the two diquark partons, with the other sitting at the endpoint, $x_L = 1$. The colour field then changes direction at the J-quark, Fig. 41. A varying number of mesons may be produced in the string piece between the L- and J-quarks; the baryon is produced in the fragmentation step which bridges x_J . Actually, with the default $f(x_J) = 6x_J(1-x_J)$ distribution, the diquark sticks together in roughly 65 % of all events, and the probability for the baryon to have rank 3 or higher is rather small. The baryon momentum fraction is larger than it would have been in a popcorn scenario, however, since the baryon is preferentially produced in a fragmentation step where a large z is selected. The diquark fragmentation model precedes, historically, the popcorn and symmetric fragmentation ideas in the Lund framework, and is therefore conceptually separate from them.

When a gluon is kicked out, the remnant colour octet is subdivided into one quark and one (colour antitriplet) diquark, each attached by a string to the forward moving parton system. If instead a sea quark or antiquark is hit, the remaining $qq\bar{q}$ or $q\bar{q}q\bar{q}$ system is split into a meson plus a remnant diquark or a baryon plus a remnant quark. In all these three cases, the energy sharing between the two objects represents a further degree of freedom. Usually some counting rule based formulae are used, such that all valence quarks on the average take 1/3 of the remnant energy.

As noted, no real alternative exists to the Lund program(s). An early model was based on IF and matrix elements [117], but never seems to have caught on.

In the upcoming HERWIG version 1.5, Marchesini and Webber also include an option for leptoproduction events [45]. The program is based on initial and final state parton showers formulated in terms of angular variables, followed by cluster fragmentation as used in e^+e^- annihilation. It will offer a most interesting alternative but, while existing, not even the authors have yet had time to do any comparisons with data. Many interesting problems of principle remain to be studied, like whether the mass spectrum (and hence the flavour composition) of clusters formed in the target remnant region is any different from that in the standard timelike parton shower region.

8.2. Leptoproduction Data

A recent detailed review of experience accumulated in leptoproduction experiments may be found in [124]. While some areas of discrepancy do exist, to a larger extent than in e^+e^- annihilation, there is no doubt that the Lund fragmentation model provides a good description of the data. In particular, parameter values determined in e^+e^- annihilation are close to optimal also in leptoproduction, thus supporting the hypothesis of jet universality [125]. New degrees of freedom are added in the baryon target fragmentation description, but here data is difficult to obtain.

One area of special interest is that of p_T properties. For known incoming and scattered lepton momenta, the jet axis is known in absolute terms, without the need for a sphericity or thrust axis search. Fig. 42 shows the resulting $\langle p_T^2(x_F) \rangle$ determined by EMC [126,127], with its characteristic "seagull" shape. This shape, in particular the large $\langle p_T^2 \rangle$ value at large positive x_F , can not be explained by first order QCD plus string fragmentation alone. It would be possible to force agreement in the forward direction if the assumed primordial

k_T of the struck quark is increased from $\langle k_T \rangle^2 = (0.44 \text{ GeV})^2$ to $(0.88 \text{ GeV})^2$, but then one would overshoot data at negative x_F . In the older Lund programs, agreement was obtained by the invocation of a simple soft gluon resummation procedure [128], wherein extra p_T was given to central hadrons, with the recoil taken by the leading endpoint quark. This has given good agreement with the data. In the more recent parton shower approach, an explicit simulation of (hard and) soft gluon emission does not give equally good a description of data [129], Fig. 42. Since the latter approach in principle should be the more reliable one, with a more detailed simulation of both transverse and longitudinal momentum effects of gluon emission, the issue remains a mystery.

It should be noted that the parton shower approach in other respects is doing very well. Thus the EMC data on the p_T compensation of a leading particle in the forward or backward jet is well described by the parton shower, Fig. 43, as it was with the soft gluon resummation technique, while models without soft gluons fail.

8.3. Hadron Collision Models

The profusion of programs for collisions between two hadrons is almost comparable to that in e^+e^- annihilation. The most frequently used program is ISAJET by Paige and Protopescu [8]. This is an independent fragmentation based model, where hard $2 \rightarrow 2$ interactions are supplemented by initial and final state showers. Beam jets are described in a cut Pomerons language, the end result of which is a varying number of back-to-back pairs of jets along the beam axis. Special allowance is made for leading baryons stemming from the incoming projectiles.

Among other IF programs, COJETS by Odorico has found some amount of use [130]. Again hard interactions are included with initial and final state radiation, whereas beam jets are described by longitudinal phase space, with multiplicities selected according to a parametrization of data. A third IF program, by Field and collaborators [131], has been used in theoretical studies, but has never been made publicly available. For a while, an attempt was made to adapt it to cluster fragmentation, but that did not work out and IF was reinstated. The EUROJET program [132], constructed to study heavy flavour physics, also belongs to the IF family.

Within the Lund group, no fewer than three different approaches have been proposed. While the way strings connect partons in the event may vary, all three base the subsequent fragmentation on the standard routines familiar from e^+e^- annihilation. In the oldest approach, which is only intended to describe low- p_T interactions, one single string is assumed to be stretched from the beam to the target side, with the quarks placed along this string [122], in an extension of what is described in section 8.1 for diquark fragmentation. While phenomenologically successful in the fragmentation regions, this model fails to account for the central region of events, and is no longer actively pursued.

The PYTHIA program [133] is, together with ISAJET, the only program on the market to cover a wide range of physics processes, in addition to the standard QCD $2 \rightarrow 2$ ones. Initial and final state radiation is included, using the same shower algorithms as in e^+e^- annihilation and leptoproduction. The possibility of multiple pairwise parton-parton interactions is included, and this mechanism plays a significant rôle in building up the "beam jet" background [134]. Special emphasis is put on the colour flow in hard interactions, which for one and the same partonic process may lead to several different ways of connecting the scattered partons and the beam remnants [135], Fig. 44.

FRTIOF is the newest member of the Lund family [136]. It is based on a picture where the two incoming hadrons may exchange momentum by repeated soft interactions, but the net colour exchange is vanishing. After the interactions, two longitudinal strings are stretched, each inheriting the flavours of one original hadron. Hard interactions may be included, and then give more complicated string topologies, but still without any colour mixing between the two hadrons. Initial and final state radiation is included in the dipole formulation described in section 3.2.

No cluster fragmentation model is in use in hadron physics but, as in leptoproduction, HERWIG is intended to change that [45]. Initial and final state radiation is described in angular variable terms, with constraints on maximum angles set by the hard interaction [137]. This requires the same division into different colour flows as is used in PYTHIA. The description of beam jets is based on the UAS cluster algorithm [138], of longitudinal phase space type.

Within the framework of dual topological unitarization, several closely related models have been proposed for low- P_T events [139]. A cut Pomerons formalism is used to predict a varying number of chains stretched between q , \bar{q} , qq and $\bar{q}\bar{q}$ ends. Since no dynamical gluons appear, whether these chains are thought of as strings or as pairs of back-to-back jets is not particularly important. Work in extending the DTU scenario to also include hard interactions is under way.

8.4. Hadron Collision Data

The amount of data collected on hadron-hadron collisions is very large. This has given many constraints on models but, since the underlying partonic processes are more or less unknown, in particular for low- P_T events, it is very difficult to untangle implications for fragmentation models and for parton level models. Thus it has been possible for IF and SF models to coexist.

As in e^+e^- annihilation, one would like to look for string effects: some angular regions between jets are expected to be more populated than others, depending on how the strings are stretched between the scattered partons and the beam jets. Explicit proposals have been given for the case of prompt photoproduction, more specifically the process $gg \rightarrow Yg$ [140]. Corresponding strategies could maybe be worked out for W/Z production. It has even been suggested to exploit the differences in colour flow in Higgs production, $gg \rightarrow H$ vs. $WW \rightarrow H$ [141], although that is almost certainly beyond the edge of the possible. A more realistic task might be to try to determine the direction of the colour flow in a string piece [142].

In contrast to these speculative proposals, one piece of experimental data exists that can be interpreted as a strong support for the string picture: the shape of the charm x_F spectra. With charm quark x_F spectra given by perturbative QCD, the IF concept would include folding the quark spectrum with a $c \rightarrow D$ fragmentation function, such that the final D spectrum is more strongly peaked at $x_F = 0$ than the c one. In SF, on the other hand, a charm quark is connected with a string to a beam remnant parton, and the D meson produced out of this field may be "dragged along" to a larger x_F than the original c quark [143]. Indeed, detailed calculations give quite good agreement with data for different charmed particles [144], although with a few half failures that remain to be understood.

High- P_T jets show many similarities with e^+e^- jets [145,146]. The UAI group comparison of quark and gluon fragmentation functions, Fig. 45, shows good agreement with expectations in the Lund string model [147]. Despite the methodological problems involved, this is probably the most direct test of q/q differences we have (a proposal for a somewhat safer method is found in [148]).

If longitudinal and transverse fragmentation properties agree with expectations, the same can not be said of flavour properties, as observed at ISR and fixed target energies. The K^-/π^- ratio at high P_T , which should reflect the s/u production ratio, is measured to be ≈ 0.46 [149], whereas the standard s/u ratio of 0.3 from e^+e^- annihilation would give a K^-/π^- ratio of at most 0.40 [150]. The problems do not end there; also p and \bar{p} production disagrees with expectations [149]. For high- P_T jets this could be explained by a larger baryon a value in the symmetric fragmentation function [150] (cf. section 7.5). One specific problem is the large p rate in the forward region at transverse momenta of a few GeV [151], which has been interpreted as evidence for diquark scattering [152].

Finally, among the developments in recent years, the exploration of diffractive states deserves mentioning. Not only has a clear longitudinal structure been found [153], but studies of exclusive states like $\Lambda\bar{\Lambda}K$ show good agreement with expectations from fragmentation models [154]. Thus it seems that also diffractive states fit nicely into standard fragmentation phenomenology.

9. Summary and Outlook

In the paper of Field and Feynman, which came to provide the ideological basis for independent fragmentation models, the emphasis was on the need for a convenient parametrization of jet properties, rather than on the need for a physics model. Indeed, the IF concept allows a large flexibility, in particular in leaving the relation between quark and gluon jets completely open. In e^+e^- annihilation, the study of string effects has given strong evidence against IF. As a consequence, IF is not actively pursued any more in e^+e^- . It is still going strong in other areas, however, specifically hadron-hadron collisions. The continued evolution of ISAJET along IF lines is the prime example. In the messy hadronic events, the extreme ease of programming

in the IF framework seems to weigh heavier than the well-known conceptual problems: lack of Lorentz covariance and the absence of explicit energy, momentum and flavour conservation. It is maybe symptomatic that a way of making a respectable model out of IF does exist – the Montvay scheme – but has never actively been pursued: the evolution of a consistent program code would require a larger effort than for any fragmentation model developed to date (and may in the end have little to show for it that is not already present in SF).

The string fragmentation model, as developed by the Lund group, is today unquestionably dominating the stage in e^+e^- annihilation and lepto-production. One may, of course, ask [70] whether this is due to having the best phenomenology, to having the largest number of tunable parameters (second to IF models), or to the Lund group having spent more time and effort on model development than anybody else. To its credit should be said that the Lund group has presented a line of correct predictions, most notably for the string effect. It should also be remembered that the momentum space picture only contains a handful of parameters: Λ and m_{\min} of the parton shower, a and b of the symmetric fragmentation function, and σ of the transverse momentum distribution. The description of flavour properties is more messy, since the results obtained with the tunnelling formalism depend on unknown quark and diquark masses. In e^+e^- annihilation, some of the resulting flavour parameters may not have the originally expected values (in particular, strange diquarks are less suppressed than predicted), but the picture is consistent. Results on the flavour composition in high- P_T jets may then be more difficult to explain. Despite the age of the SF concept, SF models are still actively being developed today. With a few exceptions (Bose-Einstein correlations, the UCLA flavour ansatz [75]), the emphasis is no longer on the SF concept as such, but on its application to different physical processes. In particular, there is a (friendly) civil war being fought between PYTHIA and FRITIOF in the area of hadron collisions.

In terms of simplicity and predictive power, the cluster fragmentation concept originally offered more than any of its predecessors. Today, the situation is more complex: simple cluster models fail to describe the data, whereas more realistic ones are no longer quite as simple, as follows. If large invariant mass clusters are left after the shower evolution, it is necessary to split them into smaller ones, anisotropically along the "string" direction. Further, in order to explain the momentum spectrum at large x , it is necessary to introduce special rules for the occasional collapse of a cluster to a single

particle. Finally, baryon production can not be understood simply by isotropic cluster decays, but it is necessary to require diquark-antidiquark production already in the cluster formation stage. Potentially even more important than the need for these modifications is the problems encountered in describing the systematics of baryon flavour production: the phase space ansatz of the Webber program gives too little suppression of the heavier baryons, the low-energy based parametrization of Caltech-II too much. Also the description of general event shape distributions is significantly worse than in the string approach.

At present, the evolution of CF models diverges. The new Marchesini-Webber program will offer a unified description of e^+e^- , ep and pp ($p\bar{p}$) interactions, in terms of angular ordered parton showers and cluster fragmentation. The emphasis is here definitely on the perturbative aspects and no major improvement of the cluster decay algorithms is planned in the near future. The Caltech-II program has followed an evolutionary line that has brought the program closer and closer to the Lund string model, e.g. by abolishing forced $g \rightarrow q\bar{q}$ splittings. It is maybe then symptomatic that proposed further modifications include introducing transverse momenta at string breaks and making cluster masses smaller, so that a cluster more often corresponds to a single particle [36]. Whereas the Marchesini-Webber program can live on the competence in perturbative QCD issues, the Caltech-II model is today badly squeezed between a hostile reality, on the one side, and the necessity to keep an identity separate from the Lund model, on the other. In the future, it may well be that Lund and Marchesini-Webber are the only survivors.

One should maybe note that the measure of success is different to different people. In the eyes of Gottschalk [81], the good results obtained with the Lund shower program is due to a cancellation of errors between an incorrect shower algorithm and a false fragmentation model. In particular, it is claimed that a good leading log shower program should not be required to reproduce correctly the four-jet rate, but that this should be obtained by explicit inclusion of four-jet matrix elements (an attitude opposite to the one in [38]). These errors in the Caltech-II shower algorithm are purportedly left uncompensated by any errors in the fragmentation description. The bad agreement with data is therefore seen as a success for Caltech-II [81].

There is no indication of a decreasing need for good fragmentation models in the future. It may be that interest in QCD as such is steadily declining within the high energy physics community, but a lack of understanding of standard processes may often prove fatal in the search for new physics

(remember the monojet débâcle at CERN). Many vital questions also remain to be answered, like that of jet universality. With a large admixture of c and b jets in e^+e^- annihilation, a quark dominance in leptoproduction and gluon one (at not too high P_T) in hadron physics, how could one ever hope to make headway without realistic models to normalize deviations to?

The models present today seem to have reached some stable plateau, with the possible exception of CF ones, which may (or may not) continue to evolve in the string direction. It is quite clear that something very close to the string picture is needed to describe the overall event properties, i.e. a highly correlated particle production along directions given by the colour flow of the event. This production certainly contains some fraction of higher resonances, clusters, that is not included in the present Lund program, but it seems unlikely that this fraction is close to unity, as in current CF models. Where new ideas really are needed is in the field of flavour production: no full-fledged model proposed so far has succeeded in correctly reproducing the known pattern of particle production rates.

In the perturbative description, we have witnessed the emergence of coherent parton showers as the main alternative. This certainly makes sense, in view of an increasing need to account for multijet states at TRISTAN/SLC/LEP. Experimentally, there are two reasons why matrix elements are in trouble: (i) the four-jet rate is incorrectly predicted, and (ii) reasonable agreement with the "internal" structure of jets necessitates so low a cutoff that higher order effects are not expected to be negligible. The success of the shower models is not just due to internal virtues, however, but also to the larger flexibility in playing with the hard emission rate (for (i)) and to a use of a perturbative description in a regime where this is not guaranteed to make sense (for (ii)). Thus the need for a better understanding also of perturbative QCD remains, despite the progress made.

Acknowledgements

Contacts over the years with a number of theorists and experimentalists have been very helpful. Special thanks go to B. Andersson, H.-U. Bengtsson, M. Bengtsson, S. Bethke, C. D. Buchanan, T. D. Gottschalk, G. Gustafson, W. Hofmann, G. Ingelman, F. E. Paige, A. Petersen, T. Takahashi, M. van Zijl and B. R. Webber. The opinions expressed in this paper, as well as any factual errors, have to be blamed entirely on the author, however.

1. Particle Data Group, M. Aguilar-Benitez et al., Phys. Lett. 170B (1986) 1
2. L. Van Hove, Phys. Rep. 1 (1971) 347
3. A. Krzywicki, B. Petersson, Phys. Rev. D6 (1972) 924
4. J. Finkelstein, R. D. Peccei, Phys. Rev. D6 (1972) 2606
5. F. Niedermayer, Nucl. Phys. B79 (1974) 355
6. A. Casher, J. Kogut, L. Susskind, Phys. Rev. D10 (1974) 732
7. R.D. Field, R.P. Feynman, Nucl. Phys. B136 (1978) 1
8. X. Artru, G. Mennessier, Nucl. Phys. B70 (1974) 93
9. P. Hoyer, P. Osiand, H.G. Sander, T.F. Walsh, P.M. Zerwas, Nucl. Phys. B161 (1979) 349
10. A. Ali, J.G. Körner, G. Kramer, J. Willrodt, Nucl. Phys. B168 (1980) 409
11. A. Ali, E. Pietarinen, G. Kramer, J. Willrodt, Phys. Lett. 93B (1980) 155
12. B. Andersson, G. Gustafson, C. Peterson, Z. Physik C1 (1979) 105
13. B. Andersson, G. Gustafson, Z. Physik C3 (1980) 223
14. B. Andersson, G. Gustafson, T. Sjöstrand, Phys. Lett. 94B (1980) 211
15. A. Petersen, in Elementary Constituents and Hadronic Structure, ed. J. Tran Thanh Van (Editions Frontières, Dreux, 1980), p. 505
16. JADE Collaboration, W. Bartel et al., Phys. Lett. 101B (1981) 129, 134B (1984) 275
17. JADE Collaboration, W. Bartel et al., Z. Physik C21 (1983) 37
18. TPC/2 γ Collaboration, H. Ahara et al., Z. Physik C28 (1985) 31
19. TASSO Collaboration, M. Althoff et al., Z. Physik C29 (1985) 29
20. J. Ellis, M.K. Gaillard, G.G. Ross, Nucl. Phys. B11 (1976) 253
21. A. Ali, J.G. Körner, Z. Kunszt, E. Pietarinen, G. Kramer, G. Schierholz, J. Willrodt, Nucl. Phys. B167 (1980) 454
22. R.K. Ellis, D.A. Ross, A.E. Terrano, Nucl. Phys. B178 (1981) 421
23. J.A.M. Vermaasen, K.J.F. Gaemers, S.J. Oldham, Nucl. Phys. B187 (1981) 301
- K. Fabricius, G. Kramer, G. Schierholz, I. Schmitt, Z. Physik C11 (1982)

- 315
24. Z. Kunszt, Phys. Lett. 99B (1981) 429, 107B (1981) 123
 - T.D. Gottschalk, Phys. Lett. 109B (1982) 331
 - R.-Y. Zhu, MIT Ph.D. thesis (1983)
 - A. Ali, F. Barreiro, Nucl. Phys. B236 (1984) 269
 - F. Gutbrod, G. Kramer, G. Schierholz, Z. Physik C21 (1984) 235
 - T.D. Gottschalk, M.P. Shatz, Phys. Lett. 150B (1985) 451, CALT-68-1172 (1984)
 - G. Kramer, B. Lampe, DESY 86-119 (1986)
 - F. Gutbrod, G. Kramer, G. Rudolph, G. Schierholz, Z. Physik C35 (1987) 543
 25. Yu.L. Dokshitzer, D.I. Dyankonov, S.I. Troyan, Phys. Rep. 58 (1980) 269
 - E. Reya, Phys. Rep. 69 (1981) 195
 - G. Altarelli, Phys. Rep. 81 (1982) 1
 26. G. Altarelli, G. Parisi, Nucl. Phys. B126 (1977) 298
 27. K. Konishi, A. Ukawa, G. Veneziano, Nucl. Phys. B157 (1979) 45
 28. R. Rajantie, E. Pietarinen, Phys. Lett. 93B (1980) 269
 - R. Odorico, Nucl. Phys. B172 (1980) 157
 - C.-H. Lai, J.L. Petersen, T.F. Walsh, Nucl. Phys. B173 (1980) 244
 - R. Kirschner, S. Ritter, Physica Scripta 23 (1981) 763
 29. G.C. Fox, S. Wolfram, Nucl. Phys. B168 (1980) 285
 - R.D. Field, S. Wolfram, Nucl. Phys. B213 (1983) 65
 30. T.D. Gottschalk, Nucl. Phys. B239 (1984) 325, B239 (1984) 349
 31. B.R. Webber, Nucl. Phys. B238 (1984) 492
 32. G. Marchesini, B.R. Webber, Nucl. Phys. B238 (1984) 1
 33. A.H. Mueller, Phys. Lett. 104B (1981) 161
 - B.I. Ermolaev, V.S. Fadin, JETP Lett. 33 (1981) 269
 34. L.A. Gribov, E.M. Levin, M.G. Ryskin, Phys. Rep. 100 (1983) 1
 - A. Bassetto, M. Ciafaloni, G. Marchesini, Phys. Rep. 100 (1983) 201
 35. T.D. Gottschalk, D.A. Morris, Nucl. Phys. B288 (1987) 729
 36. D.A. Morris, Caltech Ph.D. thesis, CALT-68-1440 (1987)
 37. T. Sjöstrand, in Proceedings of the XXIII International Conference on High Energy Physics, ed. S.C. Loken (World Scientific, Singapore, 1987), p. 1157
 38. M. Bengtsson, T. Sjöstrand, Phys. Lett. 185B (1987) 435
 39. V. Černý, P. Lichard, J. Pišť, Phys. Rev. D16 (1977) 2822, D18 (1978) 2409
 - W. Ochs, Z. Physik C23 (1984) 131
 40. L. Angelini, L. Nitti, M. Pellicoro, G. Preparata, G. Valentini, Riv. Nuovo Cimento 6 (1983) 1, Computer Phys. Comm. 34 (1985) 371
 41. G. Gustafson, Z. Physik C15 (1982) 155
 42. B.R. Webber, Ann. Rev. Nucl. Part. Sci. 36 (1986) 253
 43. B.R. Webber, Phys. Lett. 193B (1987) 91
 44. JADE Collaboration, W. Bartel et al., Z. Physik C33 (1986) 23
 45. B.R. Webber, private communication
 46. M. Bengtsson, T. Sjöstrand, Nucl. Phys. B289 (1987) 810
 47. Ya.I. Azimov, Yu.L. Dokshitzer, V.A. Khoze, S.I. Troyan, Phys. Lett. 165B (1985) 147, Leningrad preprint 1051 (1985)
 48. G. Gustafson, Phys. Lett. 175B (1985) 453
 - G. Gustafson, U. Pettersson, LU TP 87-9 (1987)
 49. J. Kalinowski, K. Konishi, T.R. Taylor, Nucl. Phys. B181 (1981) 221
 - J.F. Gunion, J. Kalinowski, L. Szymanowski, Phys. Rev. D32 (1985) 2303
 - K. Kato, T. Munehisa, Phys. Rev. D36 (1987) 61
 50. B. Andersson, G. Gustafson, G. Ingelman, T. Sjöstrand, Phys. Rep. 97 (1983) 31
 51. B. Andersson, G. Gustafson, B. Söderberg, Z. Physik C20 (1983) 317
 52. T. Sjöstrand, Phys. Lett. 142B (1984) 420, Nucl. Phys. B248 (1984) 469
 53. B. Andersson, G. Gustafson, T. Sjöstrand, Physica Scripta 32 (1985) 574
 54. T. Sjöstrand, Computer Phys. Comm. 39 (1986) 347
 - T. Sjöstrand, M. Bengtsson, Computer Phys. Comm. 43 (1987) 367
 55. X. Artru, Phys. Rep. 97 (1983) 147
 56. G. t Hooft, Nucl. Phys. B72 (1974) 461
 57. B. Andersson, G. Gustafson, T. Sjöstrand, Nucl. Phys. B197 (1982) 45
 58. B. Andersson, G. Gustafson, LU TP 82-5 (1982)
 59. TASSO Collaboration, M. Althoff et al., Z. Physik C26 (1984) 157
 60. S. Bethke, Z. Physik C29 (1985) 175
 - J. Chrin, Z. Physik C36 (1987) 163
 - and references therein
 61. C. Peterson, D. Schlatter, I. Schmitt, P. Zerwas, Phys. Rev. D27 (1983) 105
 62. E.M. Ilgenfritz, J. Kripfganz, A. Schiller, Acta Phys. Pol. B9 (1978) 881
 - J. Ranft, S. Ritter, Acta Phys. Pol. B1 (1980) 259
 - A. Bartl, H. Fraas, W. Majerotto, Phys. Rev. D26 (1982) 1061
 - S. Ekelin, S. Fredriksson, M. Jändel, T.I. Larsson, Phys. Rev. D30 (1984) 2310
 63. T. Meyer, Z. Physik C12 (1982) 77
 64. CELLO Collaboration, H.-J. Behrend et al., Nucl. Phys. B218 (1983) 269,
 - Phys. Lett. 138B (1984) 311
 65. T. Sjöstrand, Z. Physik C26 (1984) 93
 66. I. Montvay, Phys. Lett. 84B (1979) 331

67. D. Amati, G. Veneziano, Phys. Lett. 83B (1979) 87
68. G. Marchesini, L. Trentadue, G. Veneziano, Nucl. Phys. B181 (1981) 335
69. H. Yamamoto, in Proceedings of the 1985 International Symposium on Lepton and Photon Interactions at High Energies, eds. M. Konuma, K. Takahashi (Kyoto, 1986), p. 50.
70. S. Bethke, in Proceedings of the XXIII International Conference on High Energy Physics, ed. S.C. Loken (World Scientific, Singapore, 1987), p. 1079
71. P. Kooijman, ibid., p. 1173
72. W. Hofmann, LBL-23922 (talk at the 1987 International Symposium on Lepton and Photon Interactions at High Energies, Hamburg, July 27-31, 1987) and private communication
73. D.H. Saxon, Rutherford preprint RAL-86-057 (1986)
74. R. Sugano, Argonne preprint ANL-HEP-CP-86-133 (1986)
75. P. Mättig, DESY 86-161 (1986)
76. S.L. Wu, Phys. Rep. 107 (1984) 59
77. MARK J Collaboration, B. Adeva et al., Phys. Rep. 109 (1984) 131
78. MARK J Collaboration, B. Adeva et al., Phys. Rep. 148 (1987) 67
79. B. Naroska, Phys. Rep. 148 (1987) 67
80. M.G. Bowler, Z. Physik C22 (1984) 155
81. C.D. Buchanan, S.B. Chun, UCLA-87-005 (1987)
82. J.D. Bjorken, S.J. Brodsky, Phys. Rev. D1 (1970) 1416
83. S. Brandt, Ch. Peyrou, R. Sosnowski, A. Wroblewski, Phys. Lett. 12 (1964) 57
84. S.L. Wu, talk at the 1987 International Symposium on Lepton and Photon Interactions : High Energies, Hamburg, July 27-31, 1987
85. P.N. Burrows, private communication
86. S. Petersen, private communication
87. JADE Collaboration, W. Bartel et al., Z. Physik C35 (1984) 231
88. T. Takahashi, University of Tokyo Ph.D. thesis, UT-HE-87/2 (1987)
89. JADE Collaboration, W. Bartel et al., Phys. Lett. 157B (1985) 340
90. Ya.I. Azimov, Yu.L. Dokshitzer, V.A. Khoze, S.I. Troyan, Z. Physik C27 (1985) 65
91. TPC/2 γ Collaboration, H. Aihara et al., Phys. Rev. Lett. 57 (1986) 945
92. MARK II Collaboration, P.D. Sheldon et al., Phys. Rev. Lett. 164B (1985) 199
93. Yu.L. Dokshitzer, V.S. Fadin, V.A. Khoze, Phys. Lett. 115B (1982) 242
94. A.H. Mueller, Nucl. Phys. B213 (1983) 85
95. TASSO Collaboration, D. Bender et al., Phys. Rev. D31 (1985) 1
96. Ya.I. Azimov, Yu.L. Dokshitzer, V.A. Khoze, S.I. Troyan, Z. Physik C31 (1986) 213
97. HRS Collaboration, M. Derrick et al., Phys. Rev. Lett. 168B (1986) 299, Phys. Rev. D34 (1986) 3304
98. TASSO Collaboration, R. Brandelik et al., Phys. Lett. 100B (1981) 357
99. TPC/2 γ Collaboration, H. Aihara et al., Phys. Rev. Lett. 53 (1984) 2199
100. TASSO Collaboration, M. Althoff et al., Z. Physik C17 (1983) 5
101. TPC/2 γ Collaboration, H. Aihara et al., Phys. Rev. Lett. 55 (1985) 1047
102. TPC/2 γ Collaboration, H. Aihara et al., Phys. Rev. Lett. 57 (1986) 3140
103. TPC/2 γ Collaboration, H. Aihara et al., Phys. Rev. D31 (1985) 996
104. TASSO Collaboration, M. Althoff et al., Z. Physik C29 (1985) 347, C30 (1986) 355
105. CLEO Collaboration, P. Avery et al., Phys. Rev. D32 (1985) 2294
106. M.G. Bowler, Z. Physik C29 (1985) 617, Phys. Lett. 180B (1986) 299, 185B (1987) 205
107. B. Andersson, W. Hofmann, Phys. Lett. 160B (1986) 364
108. J.B. Gaffney, A.H. Mueller, Nucl. Phys. B250 (1985) 109
109. CLEO Collaboration, S. Behrends et al., Phys. Rev. D31 (1985) 2161
110. C. Peterson, T.F. Walsh, Phys. Lett. 91B (1980) 455
111. C.-K. Ng, Phys. Rev. D33 (1986) 3246
112. M. Suzuki, Phys. Lett. 71B (1977) 139
113. J.D. Bjorken, Phys. Rev. D17 (1978) 171
114. M.G. Bowler, Z. Physik C11 (1981) 169
115. G. Ingelman, T. Sjöstrand, LUTP 80-12 (1980)
116. G. Altarelli, G. Martinelli, Phys. Lett. 76B (1978) 89
- A. Méndez, Nucl. Phys. B145 (1978) 199

- R. Peccei, R. Rückl, Nucl. Phys. B162 (1980) 125
117. Ch. Rumpf, G. Kramer, J. Willrodt, Z. Physik C7 (1981) 337
118. M. Bengtsson, T. Sjöstrand, LU TP 87-10 (1987)
119. G. Ingelman, private communication
120. T. Sjöstrand, Phys. Lett. 157B (1985) 321
- M. Bengtsson, T. Sjöstrand, M. van Zijl, Z. Physik C32 (1986) 67
121. T.D. Gottschalk, Nucl. Phys. B277 (1986) 700
122. B. Andersson, G. Gustafson, I. Holgersson, O. Måansson, Nucl. Phys. B178 (1981) 242
123. B. Andersson, G. Gustafson, G. Ingelman, T. Sjöstrand, Z. Physik C13 (1982) 361
124. N. Schmitz, MPI-PAE/Exp.EI.180 (1987)
125. EMC Collaboration, M. Arneodo et al., Z. Physik C35 (1987) 417
126. EMC Collaboration, J.J. Aubert et al., Phys. Lett. 119B (1982) 233
- EMC Collaboration, M. Arneodo et al., Phys. Lett. 149B (1984) 415
127. EMC Collaboration, M. Arneodo et al., CERN-EP/87-112 (1987)
128. G. Ingelman, B. Andersson, G. Gustafson, T. Sjöstrand, Nucl. Phys. B206 (1982) 239
129. M. Bengtsson, G. Ingelman, T. Sjöstrand, DESY 87-097/LU TP 87-11 (1987)
130. R. Odorico, Nucl. Phys. B228 (1983) 381, Computer Phys. Comm. 32 (1984) 139
131. R.D. Field, G.C. Fox, R.L. Kelly, Phys. Lett. 119B (1982) 439
132. A. Ali, B. van Eijk, T. ten Hove, Nucl. Phys. B292 (1987) 1 and references therein
133. H.-U. Bengtsson, T. Sjöstrand, Computer Phys. Comm. 46 (1987) 43
134. T. Sjöstrand, M. van Zijl, LU TP 87-5 (1987)
135. H.-U. Bengtsson, Computer Phys. Comm. 31 (1984) 323
136. B. Andersson, G. Gustafson, B. Nilsson-Almqvist, Nucl. Phys. B281 (1987) 289, LU TP 87-6 (1987)
- B. Nilsson-Almqvist, E. Stenlund, Computer Phys. Comm. 43 (1987) 387
137. R.K. Ellis, G. Marchesini, B.R. Webber, Nucl. Phys. B286 (1987) 643
138. UAS Collaboration, G.J. Alner et al., Nucl. Phys. B291 (1987) 445
139. A. Capella, J. Tran Thanh Van, Phys. Lett. 114B (1982) 450, Z. Physik C18 (1983) 85, C23 (1984) 165
- P. Aurenche, F.W. Bopp, J. Ranft, Z. Physik C23 (1984) 67, C26 (1984) 279, Phys. Lett. 147B (1984) 212
140. B. Andersson, H.-U. Bengtsson, G. Gustafson, LU TP 82-10 (1982)
141. Yu.L. Dokshitzer, V.A. Khoze, S.I. Troyan, Leningrad preprint 1218 (1986)
142. B. Andersson, H.-U. Bengtsson, LU TP 87-8/UCLA-87-002 (1987)
143. B. Andersson, H.-U. Bengtsson, G. Gustafson, LU TP 83-4 (1983)
144. NA27 LEBC-EHS Collaboration, M. Aguilar-Benitez et al., Phys. Lett. 161B (1985) 400, 164B (1985) 404
145. UA2 Collaboration, P. Bagnaia et al., Phys. Lett. 144B (1984) 291
- AFS Collaboration, T. Åkesson et al., Z. Physik C30 (1986) 27
- UA2 Collaboration, R. Ansari et al., Z. Physik C36 (1987) 175
146. UA1 Collaboration, G. Arnison et al., Nucl. Phys. B276 (1986) 253
147. P. Ghez, G. Ingelman, Z. Physik C33 (1987) 465
148. T. Sjöstrand, in Proceedings of the 1984 Snowmass SSC Summer Study, eds. R. Donaldson, J.G. Morfin, p. 84
149. W.M. Geist, CERN-EP/87-127 (1987) and references therein
150. B. Andersson, H.-U. Bengtsson, private communication
151. A. Breakstone et al., Phys. Lett. 147B (1984) 237
152. A. Breakstone et al., Z. Physik C28 (1985) 335
- S. Fredriksson, M. Jändel, Z. Physik C14 (1982) 41
153. UA4 Collaboration, D. Bernard et al., Phys. Lett. 166B (1986) 459
154. R608 Collaboration, A.M. Smith et al., Phys. Lett. 163B (1986) 267

Table 1

Particle production rates in the Lund and Webber programs (default values) at 29 GeV [70]. Particle rates also includes antiparticles, and different baryon charge states, where applicable. Feeddown from decays is included in all figures.

Particle	Lund	Webber
π^\pm	10.5	11.3
π^0	6.1	6.5
K^\pm	1.48	1.24
K_S^0, K_L^0	1.40	1.21
η	0.73	0.72
η'	0.39	0.12
ρ^\pm	1.71	1.37
ρ^0	0.91	0.66
ω	0.81	0.53
$K^{*\pm}$	0.76	0.52
K^{*0}	0.71	0.48
ϕ	0.12	0.07
p	0.64	0.45
n	0.57	0.40
Λ	0.22	0.23
Σ	0.12	0.094
Ξ	0.028	0.069
Δ	0.34	0.37
Ξ^*	0.06	0.09
Ξ^*	0.006	0.035
Ω^-	0.0003	0.005

Figure Captions

Fig. 1. Schematic illustration of an e^+e^- annihilation event: (i) perturbative phase, (ii) fragmentation, (iii) particle decays and (iv) experimental observation.

Fig. 2. The iterative ansatz for flavour, transverse momentum and lightcone energy-momentum ($W_+ = E + p_T$) fraction.

Fig. 3. Breaking of a string à la Artru-Mennessier [5], into clusters with a continuous mass spectrum, where the clusters in their turn may break further. Hatched areas indicate nonvanishing field.

Fig. 4. Breaking of a string in the Lund approach [9], into particles with discrete masses, with any subsequent decays decoupled from the string picture. Hatched areas indicate nonvanishing field.

Fig. 5. Snapshot of string drawing in e^+e^- three-jet events, from q via g to \bar{q} , full line. Motion of partons is indicated by dashed lines and arrows. The velocity of a string piece is $v = \cos(\theta/2)$.

Fig. 6. The momentum distribution of final state particles in a $q\bar{q}g$ event. The size of the strokes indicates the approximate extent of transverse momentum fluctuations.

a) In string fragmentation the particles appear along two hyperbolae (dashed).
b) In independent fragmentation the particles appear along the three jet directions.

Fig. 7. Schematic picture of parton shower evolution in e^+e^- events.

Fig. 8. The cluster fragmentation scenario: (i) shower evolution, (ii) forced $g \rightarrow q\bar{q}$ branchings, (iii) cluster formation and (iv) cluster decay. Occasionally, a cluster is associated with a single particle.

Fig. 9. The two different ways of stretching a string in a $q\bar{q}gg$ event.

Fig. 10. A uniform colour flux tube stretched between a q and a \bar{q} endpoint – one possibility of visualizing the linear confinement property.

Fig. 11. A closed gluon string is obtained e.g. in $T \rightarrow ggg$ decays.

Fig. 12. The flavour chain of primary hadrons in a fragmenting string, with rank assignment.

Fig. 13. A colour field is stretched between a quark q and an antiquark \bar{q} . If virtual $q'|\bar{q}'$ pairs are produced, the colour field can be changed from red-antired to green-antigreen or blue-antiblue. The direction of the field (going from triplet to antitriplet) is also changed. If a second pair is produced inside such a region, the colour field can break and a $B\bar{B}$ pair can be produced (to the right). If two pairs are produced inside the region, the B and the \bar{B} are separated in rank by a meson (to the left).

Fig. 14. The string drawing for

- a) an ordinary three-jet event,
 - b) a three-jet event with a soft gluon, and
 - c) a three-jet event with a collinear gluon.
- Dashed lines give the momenta (and hence trajectories) of the partons; in (c) dots indicate the construction of $\bar{p}_q + \bar{p}_{\bar{q}}$. Full lines give the string shape at different times, with numbers representing time in some suitable scale.

Fig. 15. A slightly exaggerated picture of momentum conservation effects. In (a) the momenta of initial partons are full arrows and of jets after fragmentation dashed, with dotted indicating final momentum imbalance. In (b) – (d) the momenta before conservation are dashed, as in (a), and after full. Hoyer rescaling in (b), Ali boost in (c), Lund strings (along which particles are sitting) in (d).

Fig. 16. In the Montvay scheme the gluon stretches an octet field which joins the two triplet fields at a junction.

Fig. 17. The cluster mass spectrum at CM energy 35 GeV (dashed) and 53 GeV (full) in the Webber program [31].

Fig. 18. The Caltech-II approach: (i) shower evolution, (ii) string evolution

and breakup into (iii) clusters, (iv) cluster decay into a varying number of particles.

Fig. 19. Compilation [70] of baryon production ratios at 10–35 GeV, compared with Webber, Lund and Caltech-II predictions at 10 GeV, with varying

- a) strangeness content,
- b) angular momentum.

Fig. 20. Mark II data at 29 GeV compared with Lund+PS (here denoted Lund Shower), Webber, Caltech-II and Lund+ME (Lund MA) results [80].

- a) Thrust distribution.
- b) Minor distribution.
- c) Aplanarity distribution.
- d) $x = 2p/W$ distribution of charged particles.
- e) Rapidity distribution $dn/dy|_{\text{thrust axis}}$ of charged particles w.r.t. the thrust axis.

Fig. 21. JADE n-cluster event rates at $W = 34$ GeV, as a function of the y_{cut} of the cluster algorithm. Data are compared with Lund+ME ($O(\alpha_s^2)$ model) and Webber (LLA model) [44].

Fig. 22. JADE 3-cluster event rates at different CM energies, with $y_{\text{cut}}=0.08$. Data are compared with Lund+PS, either with a fixed α_s or with a running $\alpha_s(p_T^2)$, p_T being the transverse momentum in a branching a+b+c [86].

Fig. 23. Sphericity distribution, Mark II data [80] compared with Lund+PS results for running $\alpha_s(p_T^2)$ (full), running $\alpha_s(m^2)$ (dotted) and fixed α_s (dashed) [46].

Fig. 24. Energy-energy correlation asymmetry, JADE data [87] compared with Lund+ME for different Y_{\min} cutoffs on the matrix elements [65].

Fig. 25. Energy and particle flow in three-jet events, with the rightmost valley likely to correspond to the $q\bar{q}$ angular region. JADE data compared with Lund+ME and Hoyer model [17].

Fig. 26. Ratio of particle flow in central part of rightmost and leftmost valley in Fig. 25, JADE data [89] compared with Lund+ME, Hoyer, Ali, Webber, Gottschalk [30] and fire-string [40].

Fig. 27. The average transverse momentum component in the event plane with respect to the jet axis, as a function of the momentum component parallel to the jet axis. The transverse momentum sign convention is shown by insert. JADE data [89] compared with Lund+ME, Ali, Webber, Gottschalk [30] and fire-string [40].

Fig. 28. Ratio of particle flow in (assumed) $q-\bar{q}$ angular region of $q\bar{q}g$ and $q\bar{q}\gamma$ events; TPC/2 γ , Mark II and JADE data [91, 70].

Fig. 29. Momentum spectrum of charged particles close to $z = 2p/W = 1$, HRS data compared with Lund+ME and Webber (here with each cluster decaying into two particles) [92].

Fig. 30. Charged pion rapidity distribution $d\eta/dy$ in different sphericity bins, TPC/2 γ data [88].

Fig. 31. Ratio $R_{\eta}(S)$, eq. (16), which gauges how peaked $d\eta/dy$ is close to $y=0$, TPC/2 γ data compared with Lund+PS (full), Lund+ME (dashed), IF (dotted) and Webber (dash-dotted) [88].

Fig. 32. Distribution in $|\cos\theta|$, with θ angle between event axis and $p\bar{p}$ axis in rest frame of pair, TPC/2 γ data compared with isotropic cluster decay and Lund+ME popcorn baryon production [101, 70].

Fig. 33. Rapidity correlation function $C_{ab}(Y_a, Y_b)$ for $\bar{p}\bar{p}$ and $\bar{p}\bar{\Lambda}$ pairs, as a function of Y_b for Y_a fixed in region marked at rapidity axis. TPC/2 γ data compared with Lund symmetric fragmentation function and with fragmentation function nonvanishing at $z = 0$ (FF, stand. Lund), eq. (13), in string framework.

Fig. 34. Reconstructed ratio $r(x)$ of gluon to quark fragmentation functions, Mark II data compared with Ali, Lund+ME and Webber results [108].

Fig. 35. Ratio of particle production in $T \rightarrow ggg$ (or $gg\gamma$) events to production in background continuum events. ARGUS and CLEO data compared with Lund predictions [70].

Fig. 36. Average rapidity distribution of hadrons, with fluctuations around this average suppressed for clarity.

- a) In the Bjorken picture, the separation between any two next rank hadrons is assumed the same.
- b) In the Lund symmetric fragmentation picture, the separation is larger between heavier particles, wherever they are in the flavour chain.

Fig. 37. The motion of a massive $q\bar{q}$ pair (with fragmentation suppressed), where the hatched area indicates the region of nonvanishing field, while the dashed rectangle shows the corresponding area for a massless $q\bar{q}$ pair with the same energy.

Fig. 38. Energy dependence of some variables, data compared with Lund+PS, Webber, Caltech-II and Lund+ME programs [80].

- a) Average charged multiplicity and reconstructed number of clusters.
- b) Energy-energy correlation, integrated between 57.6° and 122.4° , and the asymmetry, integrated between 28.8° and 90° .

Fig. 39. Model predictions at 93 GeV for Lund+PS, Webber, Caltech-II and Lund+ME [80].

- a) Charged multiplicity distribution.
- b) Aplanarity distribution.
- c) Rapidity distribution.

Fig. 40. Schematic picture of parton shower evolution in leptoproduction: k' incoming lepton, k' outgoing, q virtual $Y/Z/W^\pm$, unprimed p : initial state shower before hard interaction, primed p : final state shower.

Fig. 41. Assumed string drawing in a leptoproduction event. Top: the colour force field changes direction at the green quark, a bit away from the leading endpoint quark. Bottom: it is the particle formed around this green junction quark that inherits the original baryon number.

Fig. 42. Average p_T^2 as a function of $x_F = 2p_L^*/W$ in the hadronic CM frame. Lund+PS with cutoff mass 1 GeV (full line) and 4 GeV (dashed line) [129]; data from EMC [127].

Fig. 43. Rapidity distribution dp_T^{bal}/dy^* of the transverse momentum balancing an (a) forward and (b) backward trigger particle. Notation as in Fig. 42.

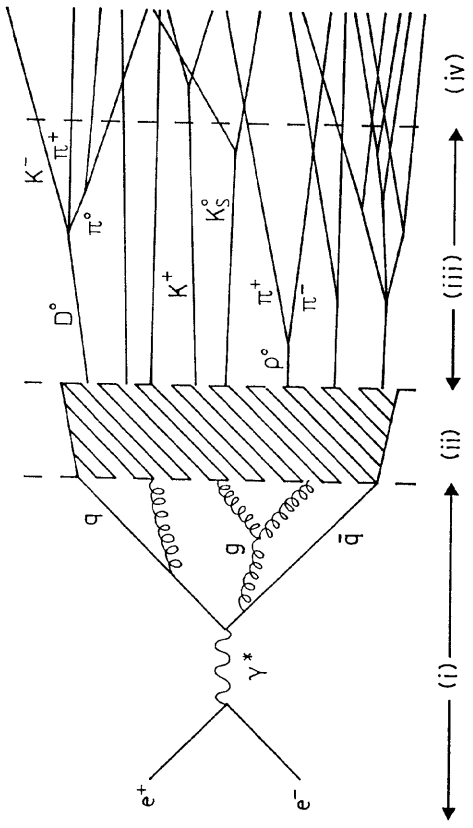


Fig. 44. Gluon-gluon scattering in a high- p_T event. The incoming (outgoing) colour octet gluons are called 1, 2 (3, 4). The hadron remnants $\bar{1}$ and $\bar{2}$ are also octets and continue stretching the field in the same way as gluons. The colour field between the four outgoing octets can be stretched in six different ways.

Fig. 45. Ratio of gluon to quark fragmentation functions, UAI data points [146] compared with a simulation [147] of PYTHIA [133] expectations, full line.

Fig. 1

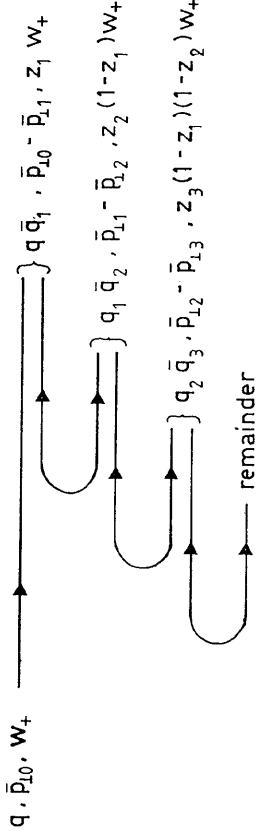


Fig. 2

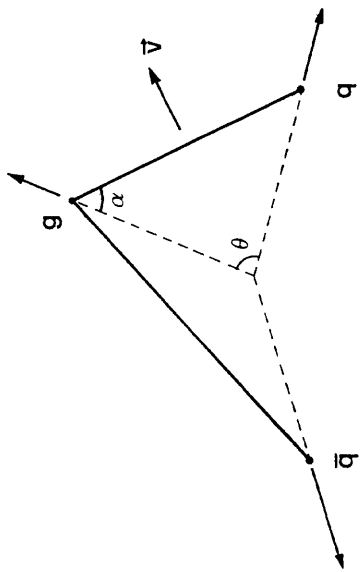


Fig. 5

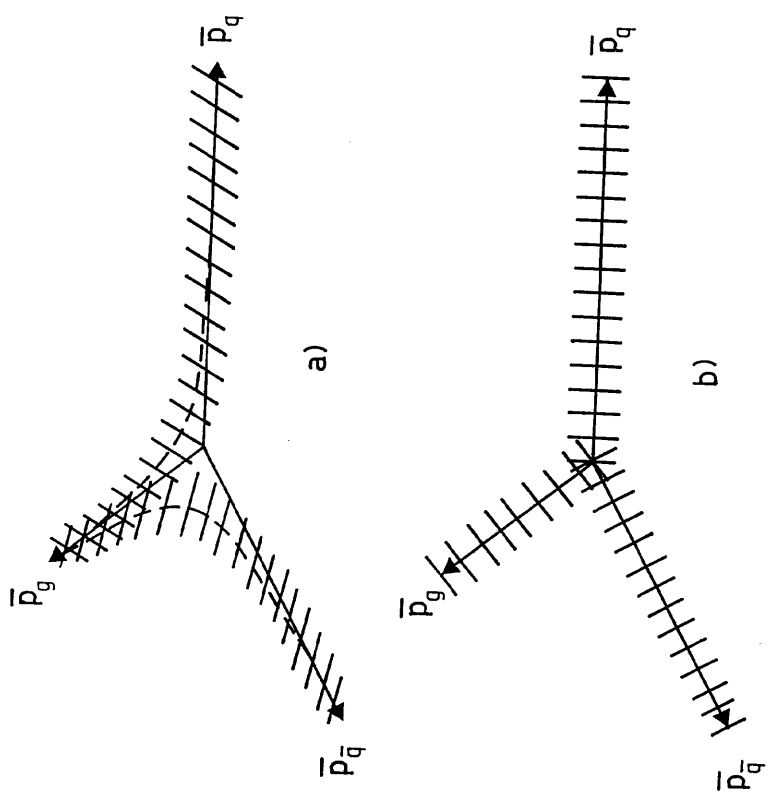


Fig. 6

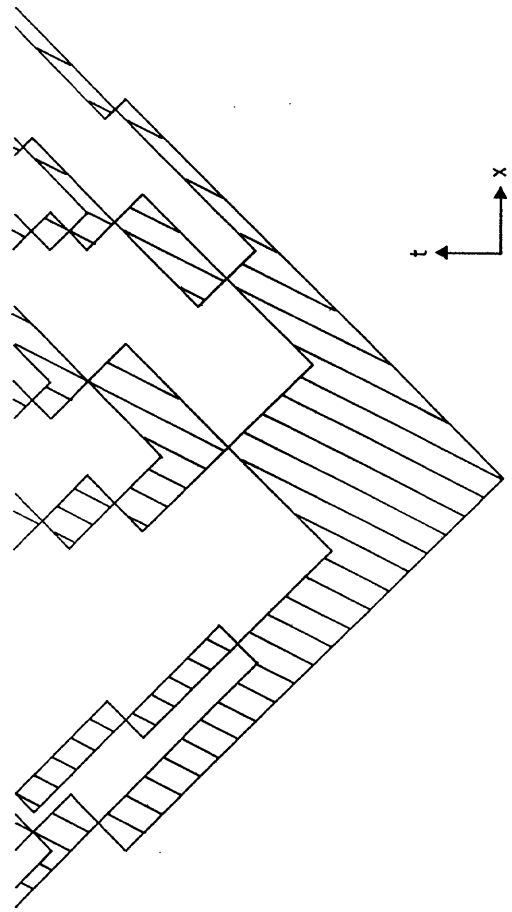


Fig. 3

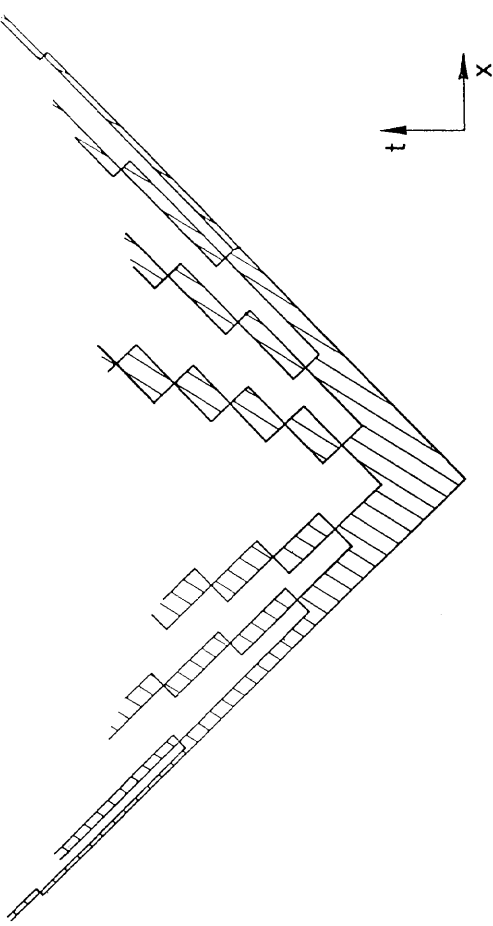


Fig. 4

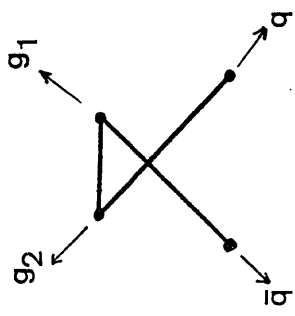


Fig. 9

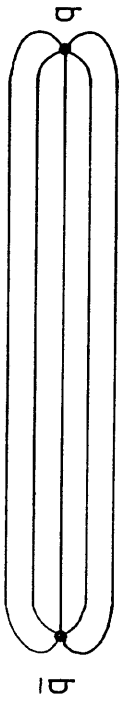
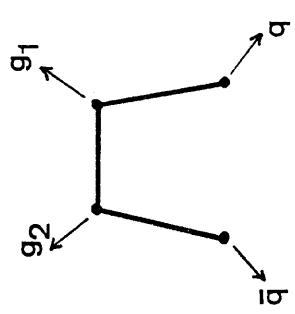


Fig. 9

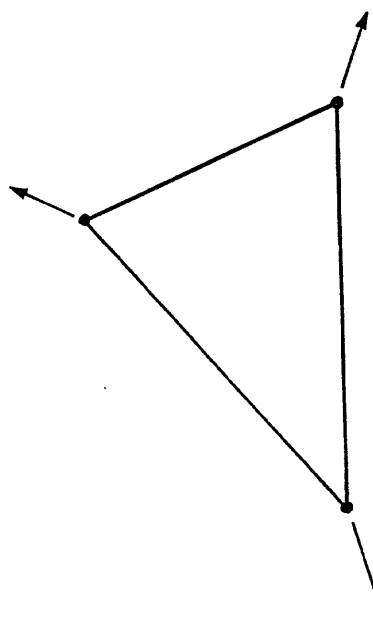


Fig. 10

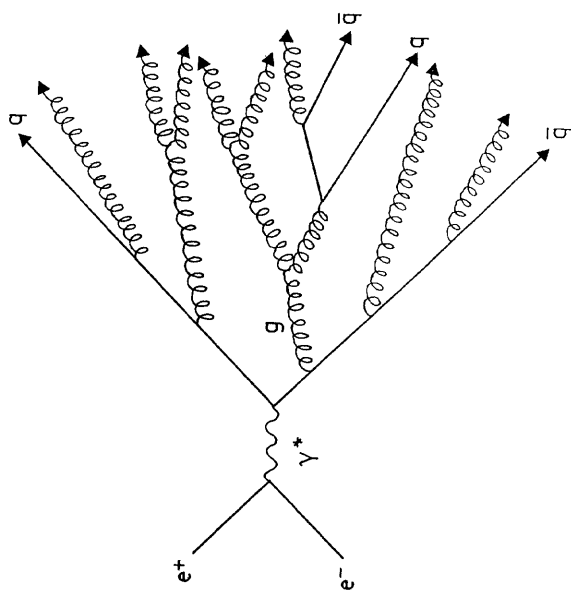
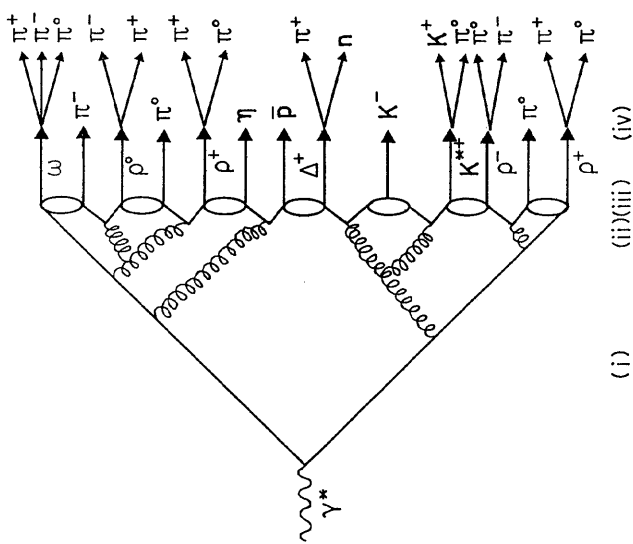


Fig. 7



(i) (ii)(iii) (iv)

Fig. 8

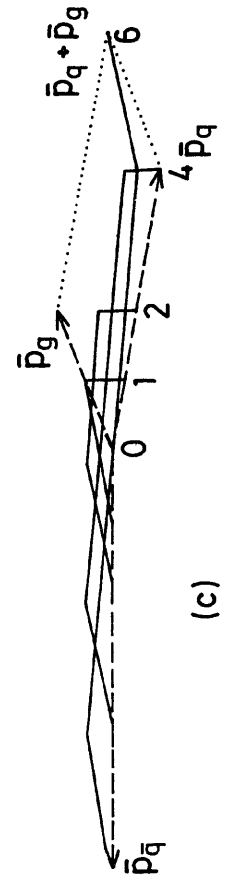
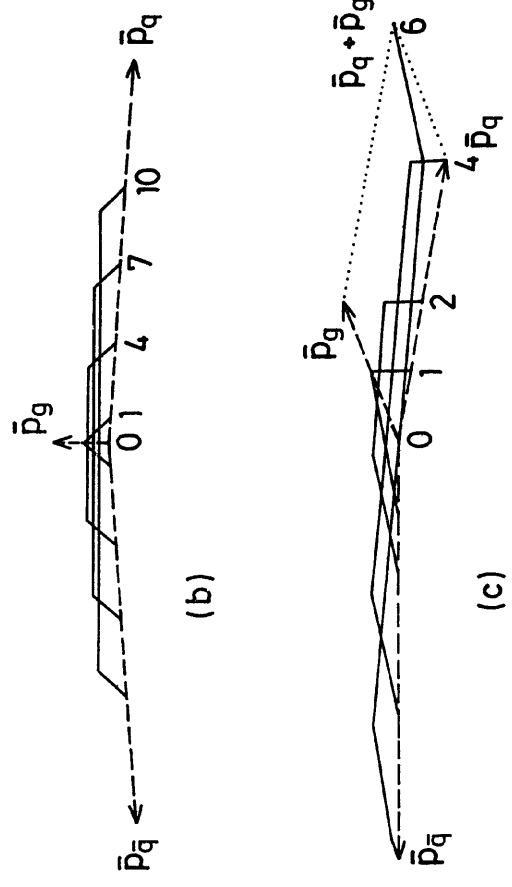
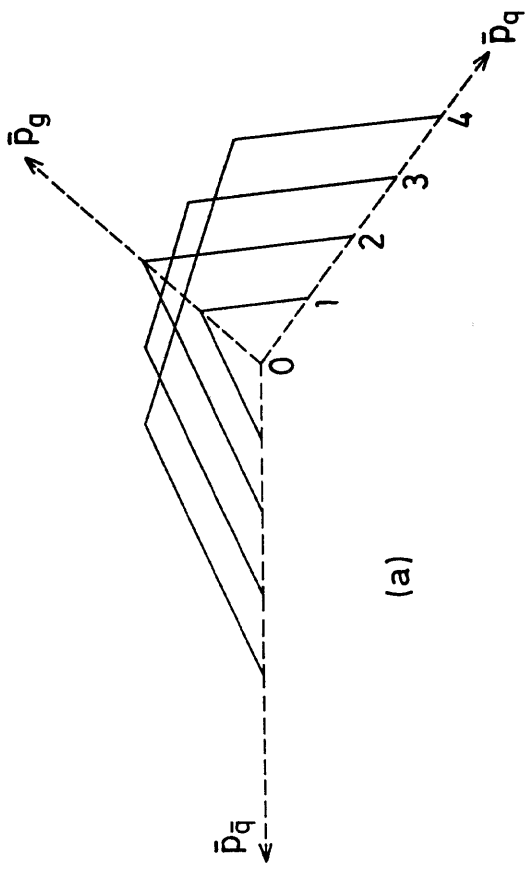
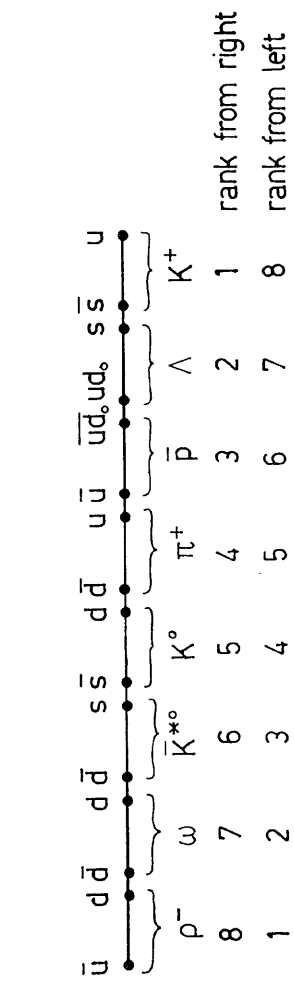
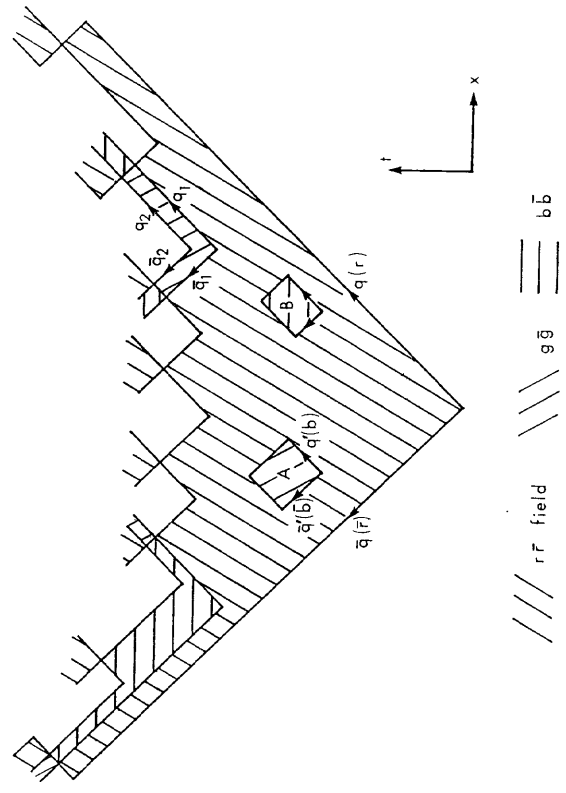


Fig. 14



36901

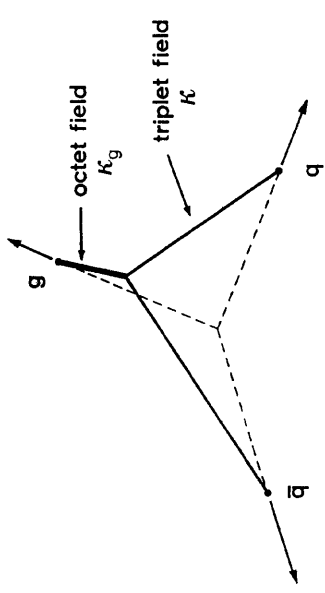


Fig. 16

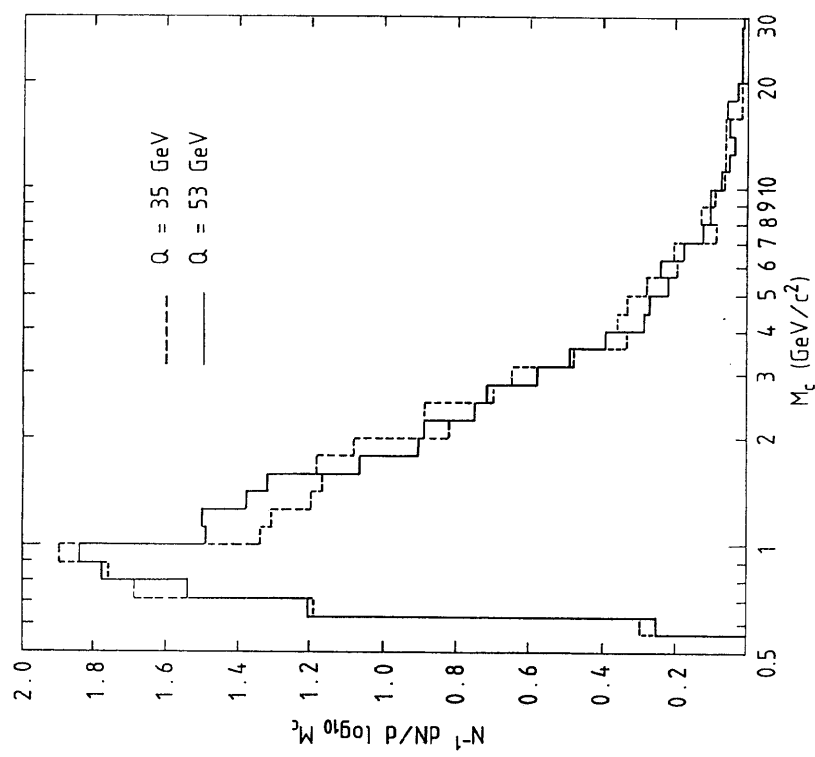


Fig. 17

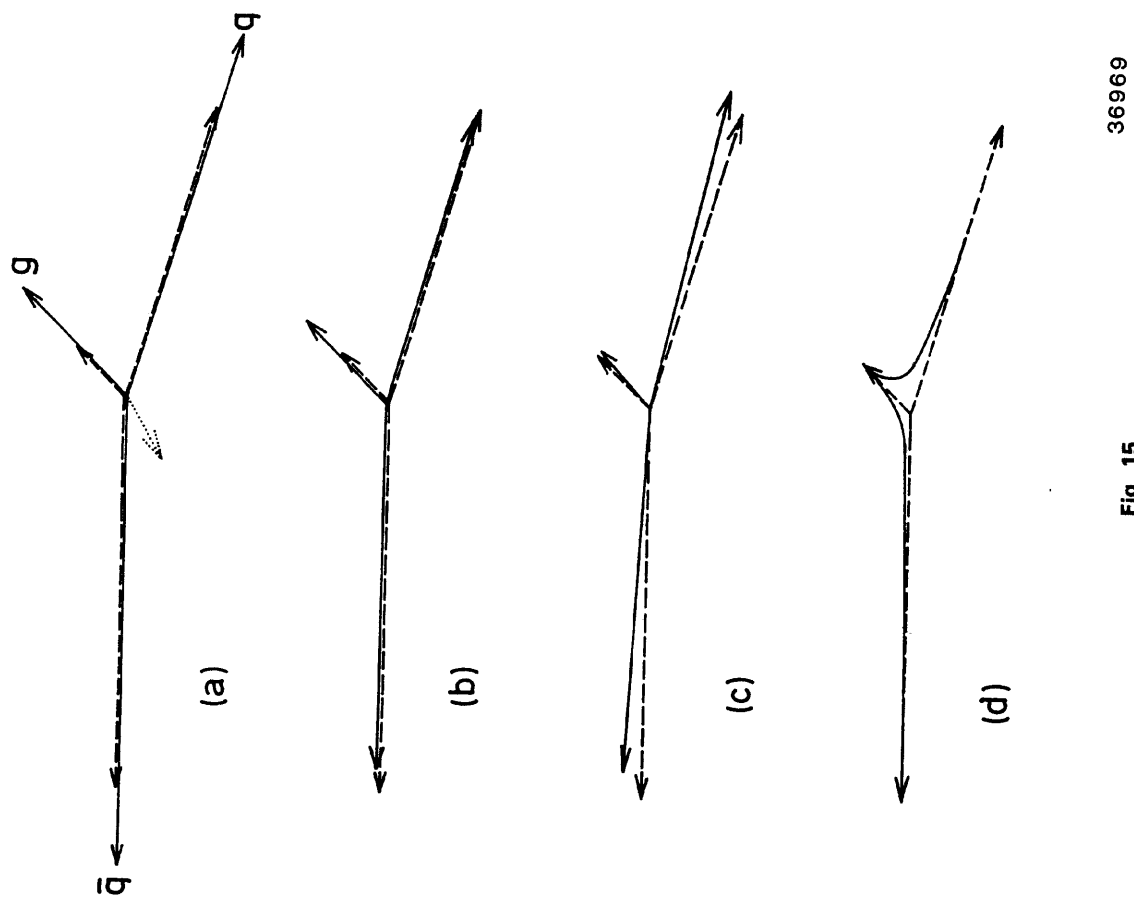


Fig. 15

A) Strangeness (no feeddown corr.)

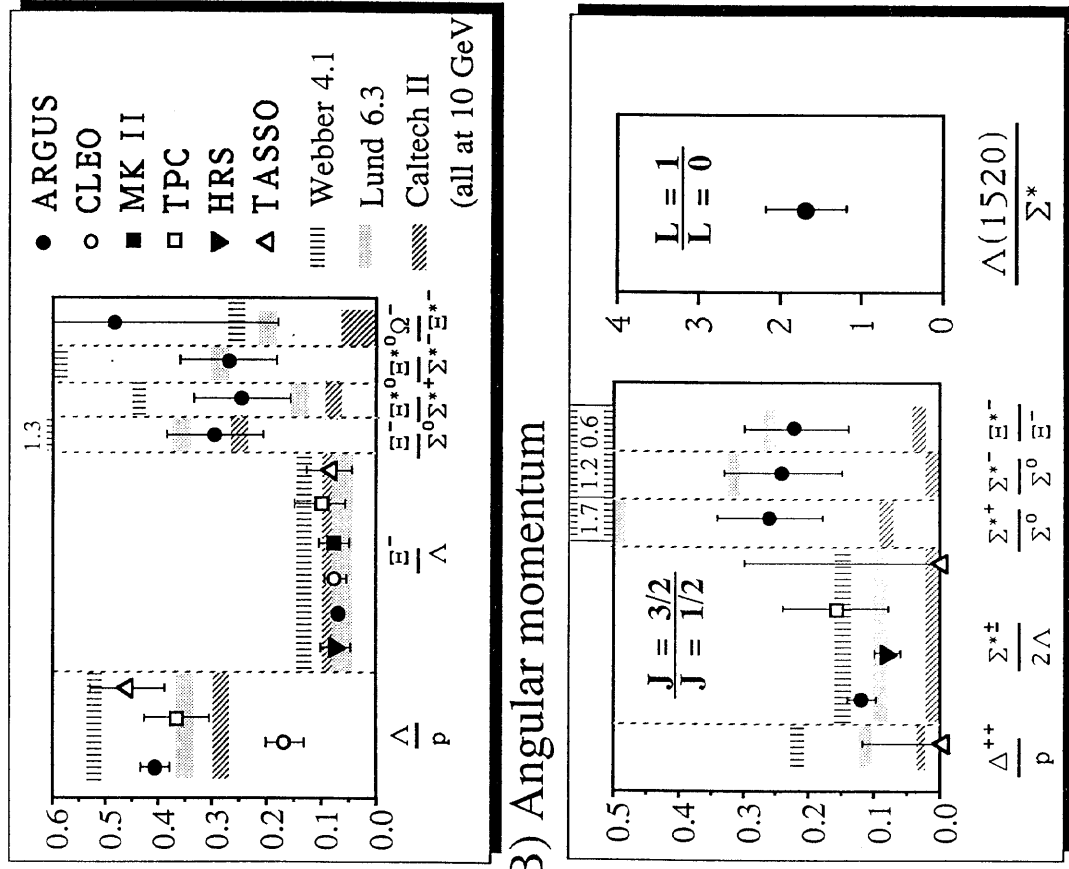


Fig. 19

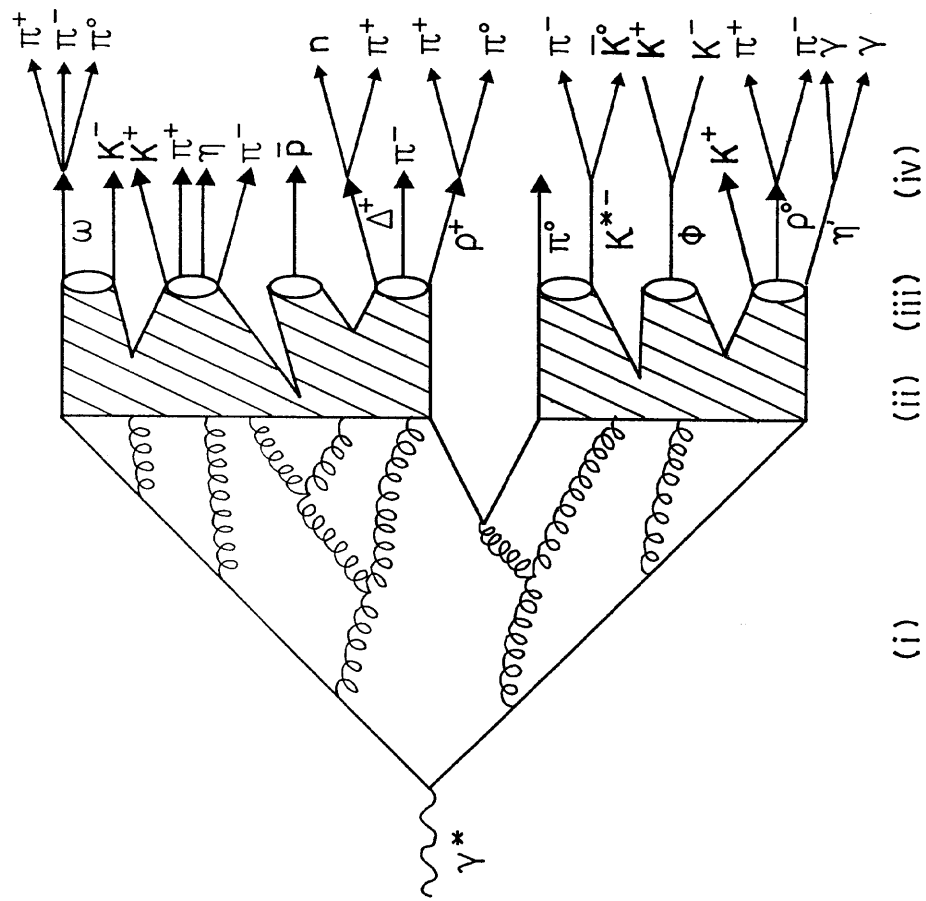
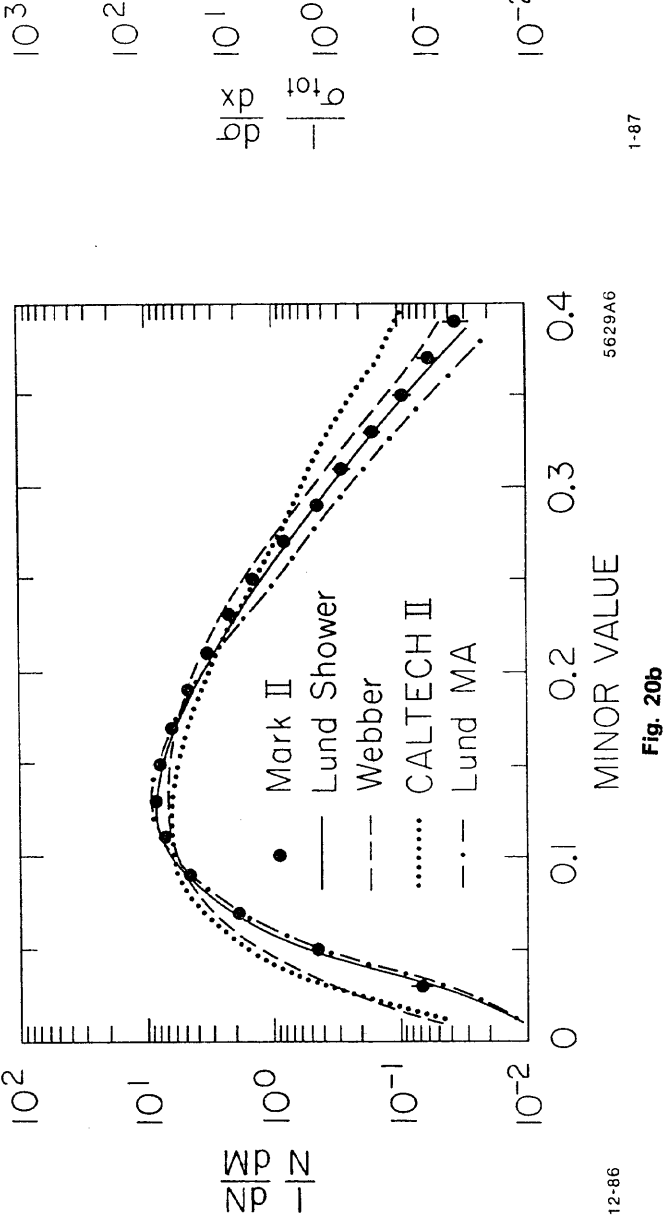
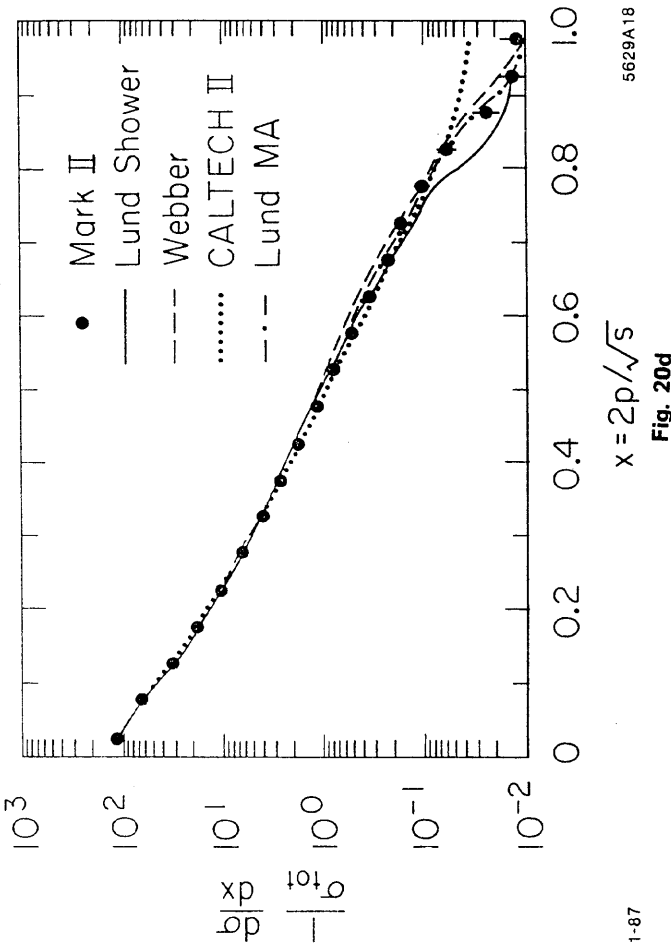
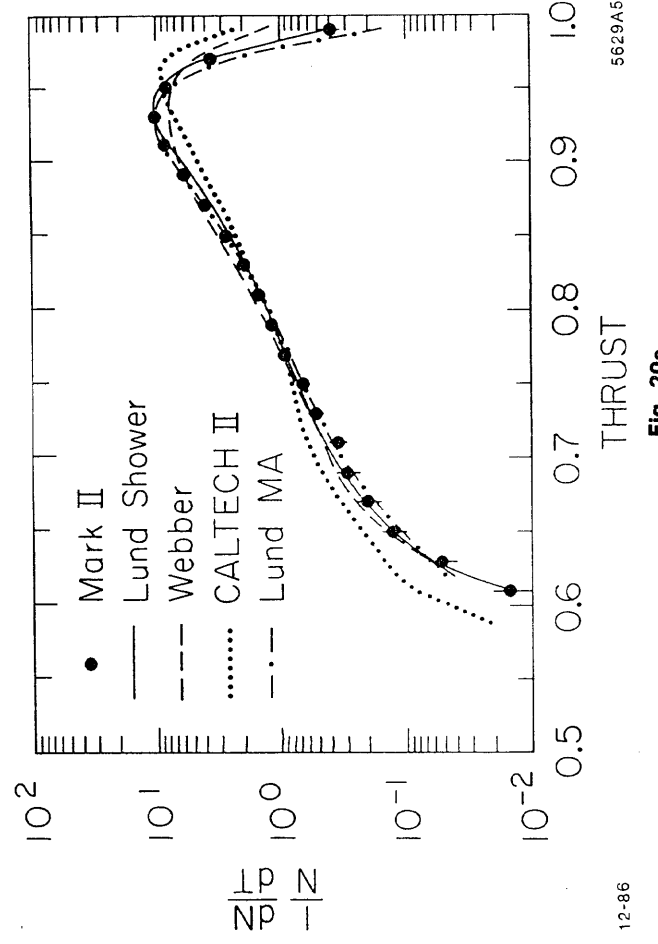
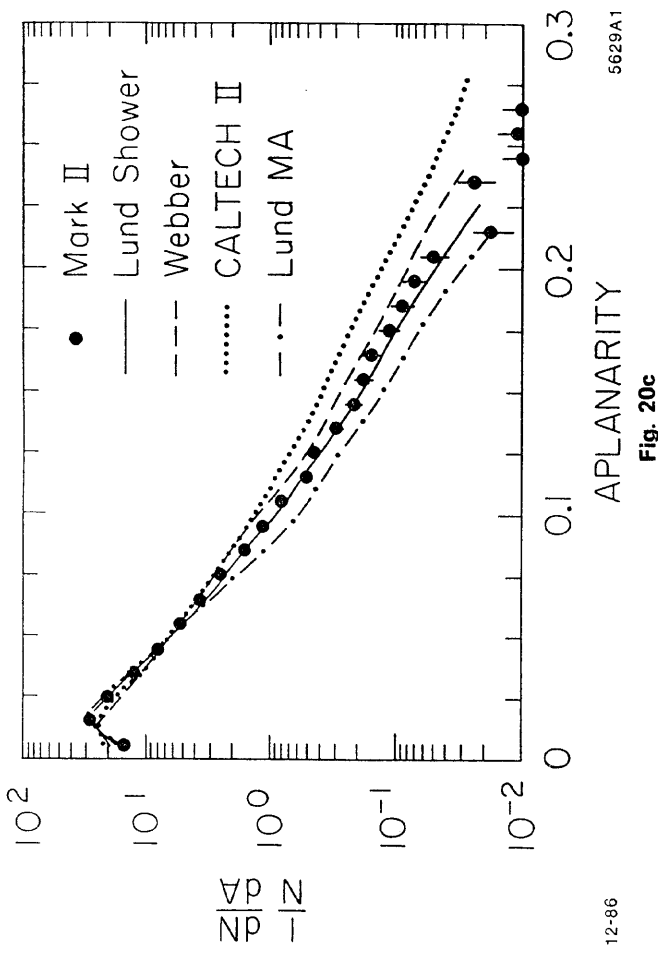


Fig. 18



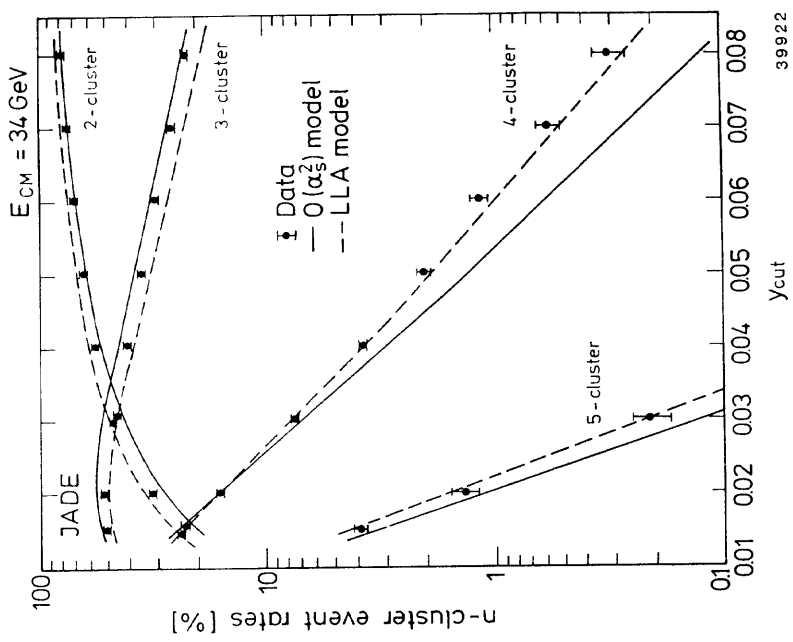
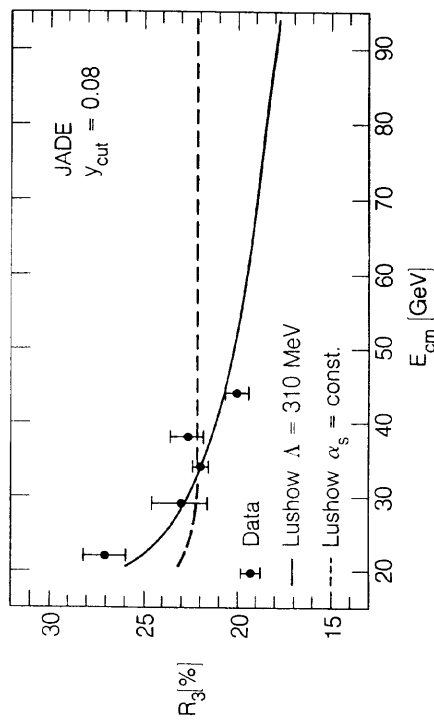


Fig. 21



xBL 873:8823

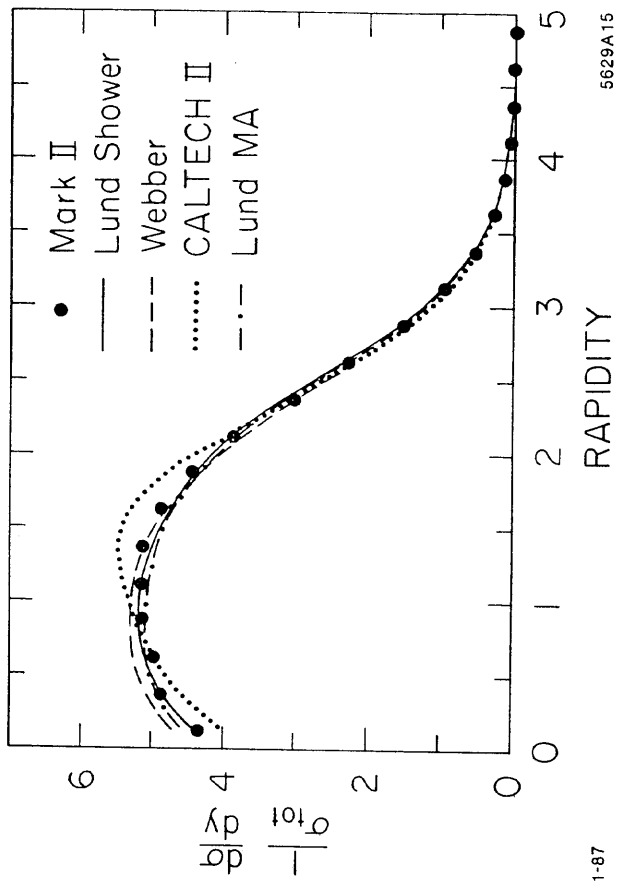


Fig. 20e

Fig. 22

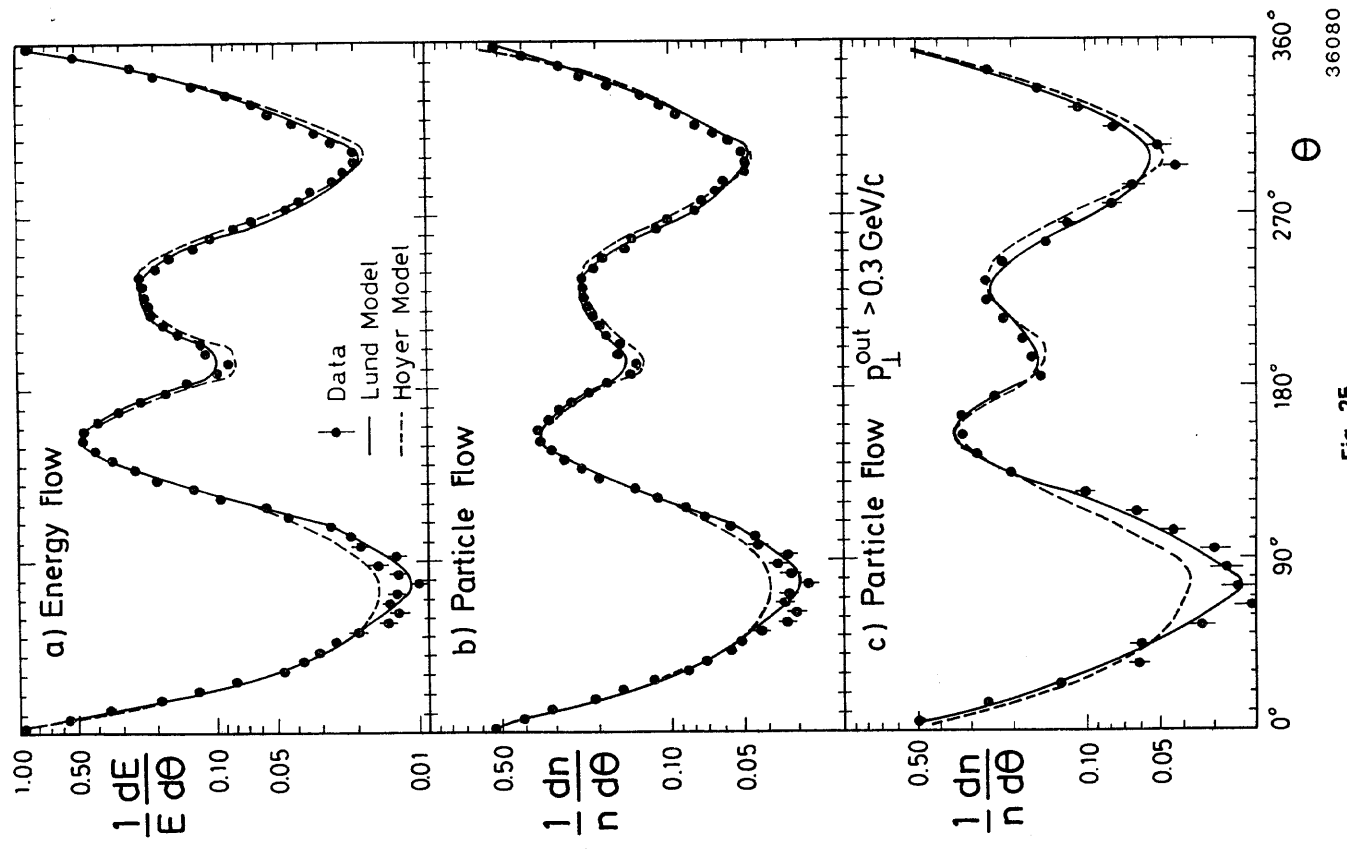


Fig. 25

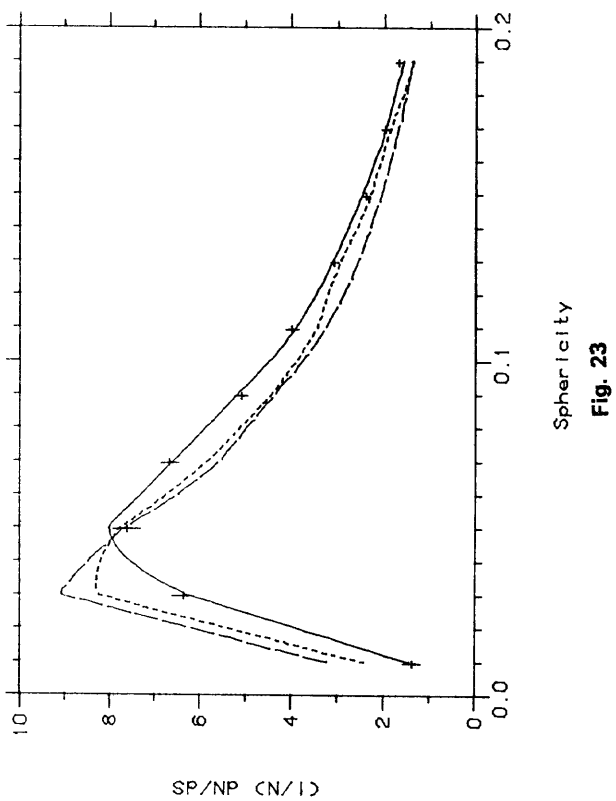
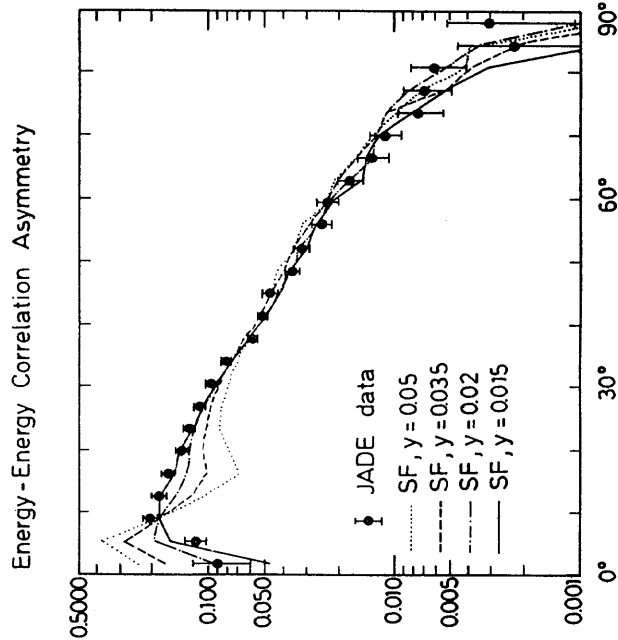


Fig. 23



36970

Fig. 24

36080

Fig. 25

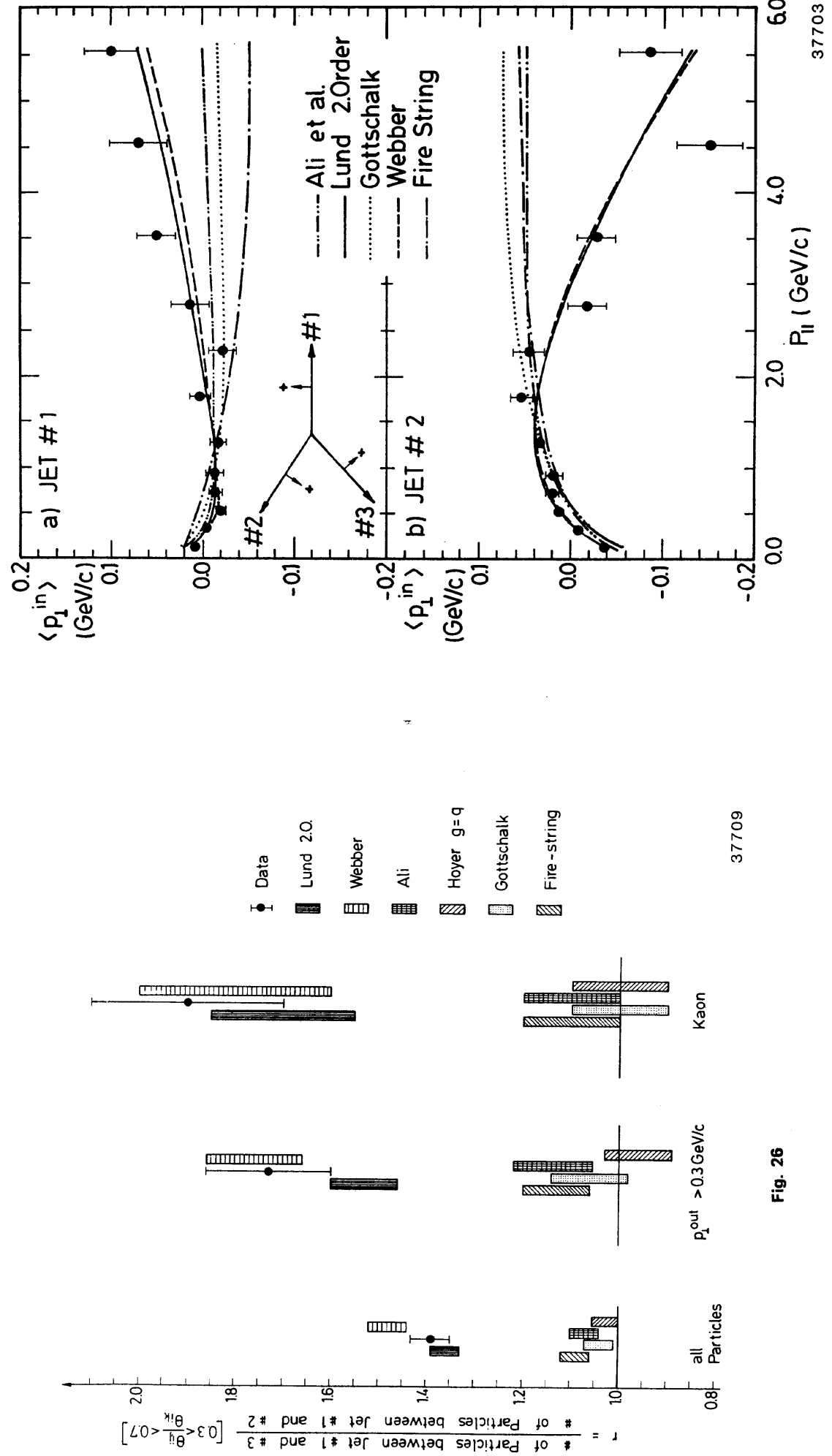


Fig. 27

37703

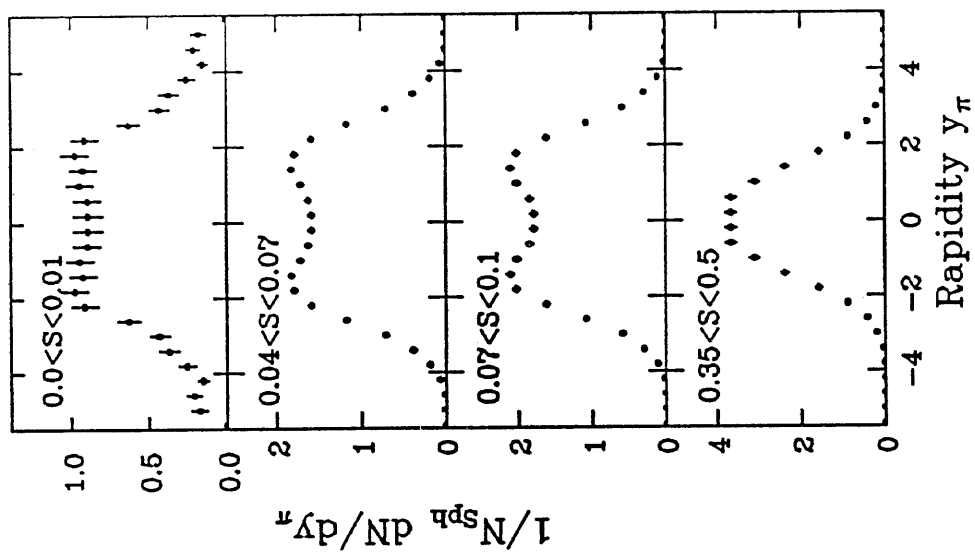


Fig. 30

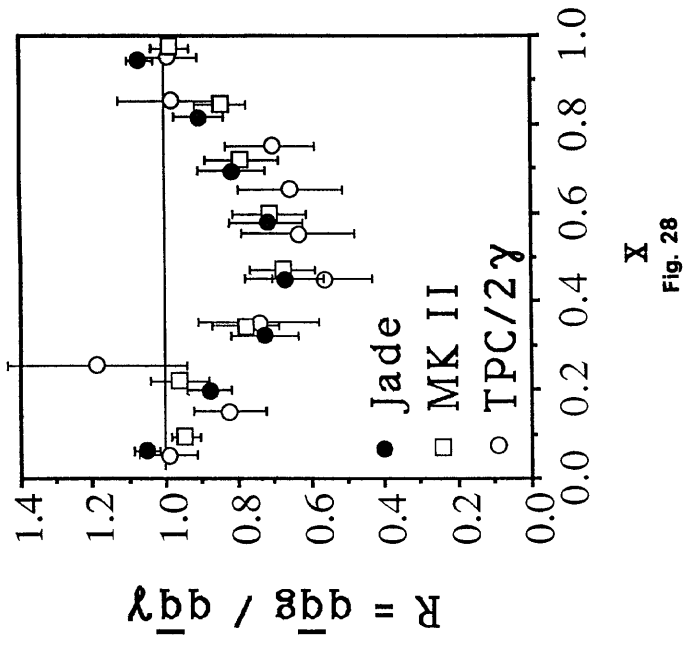


Fig. 28

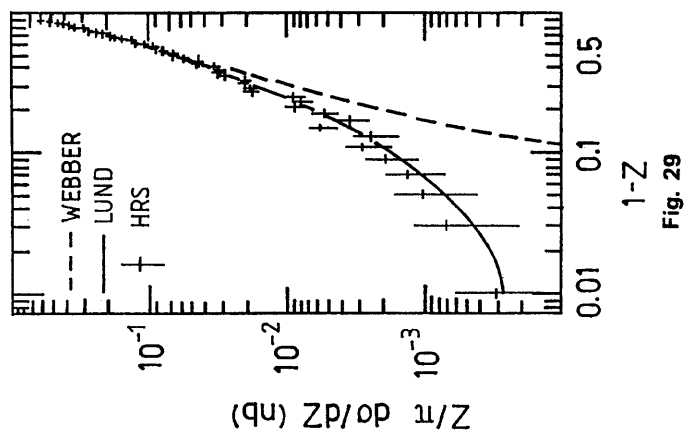


Fig. 29

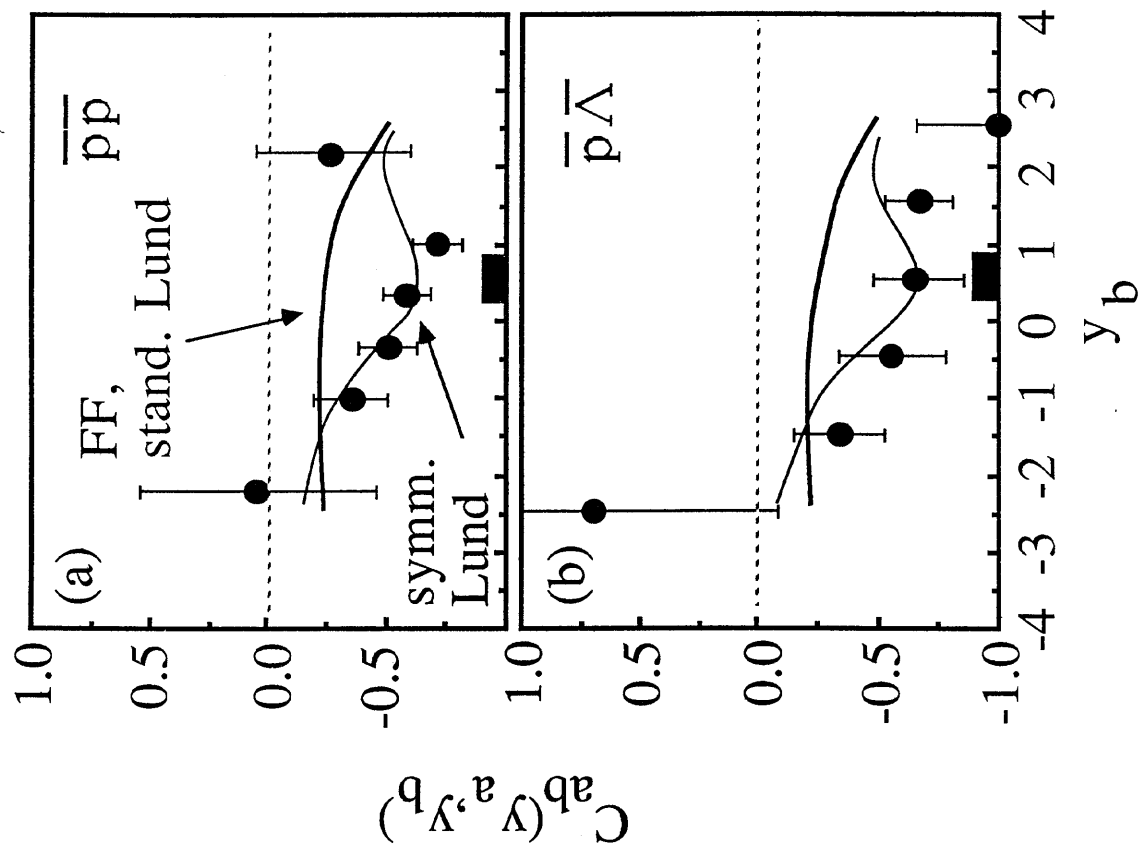


Fig. 33

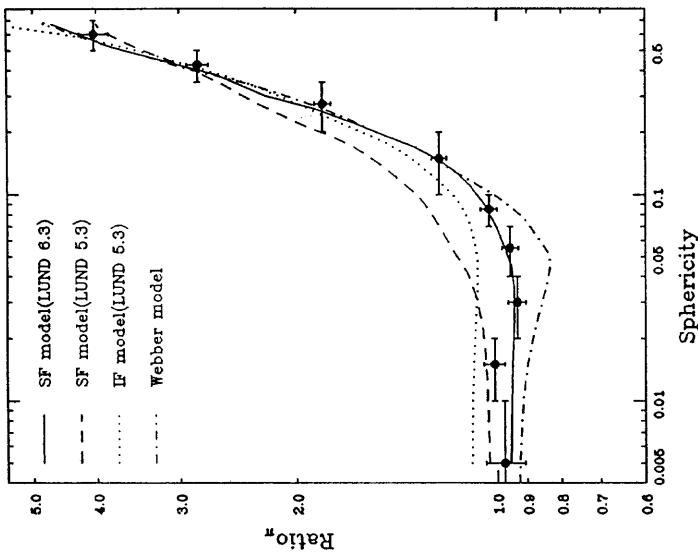


Fig. 31

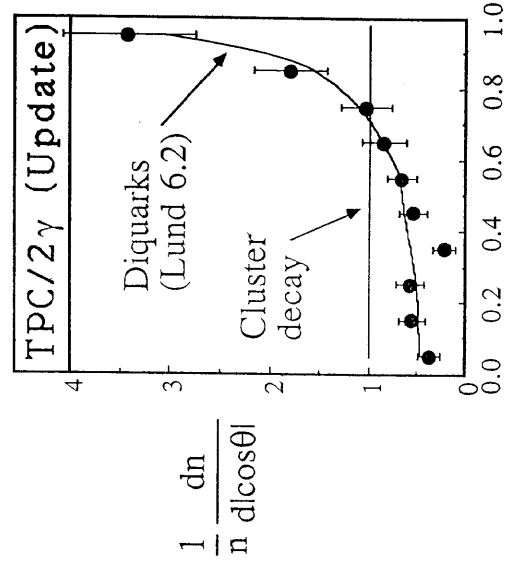


Fig. 32

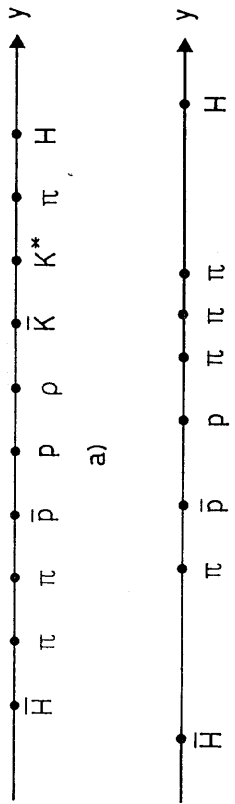


Fig. 36

Fig. 34

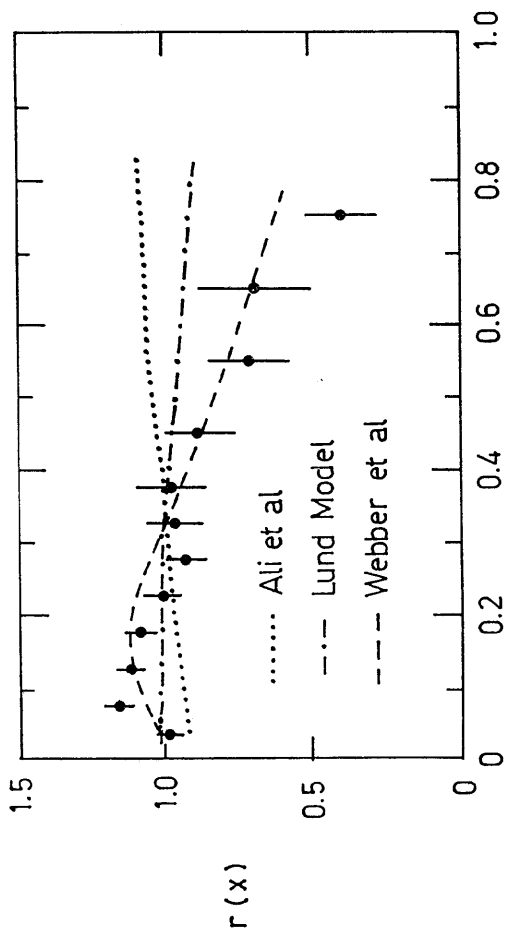


Fig. 34

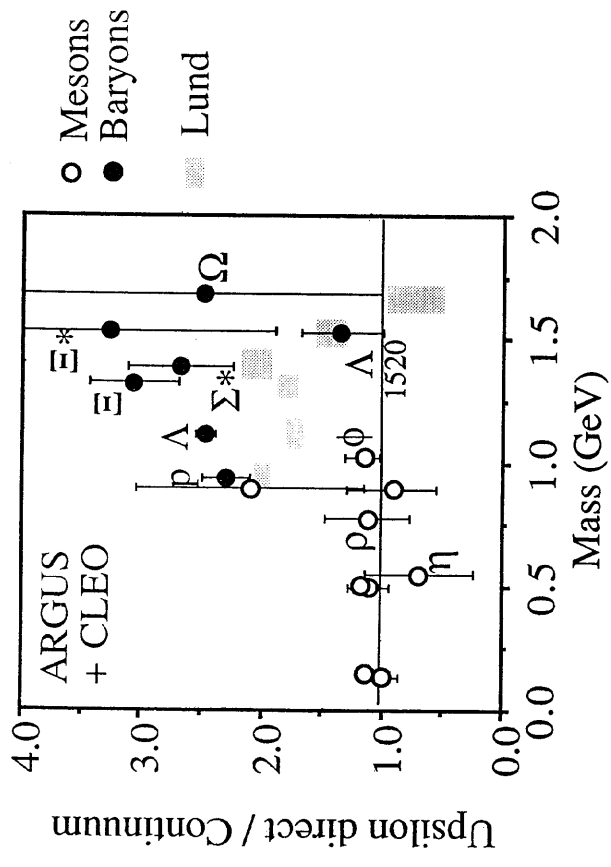


Fig. 35

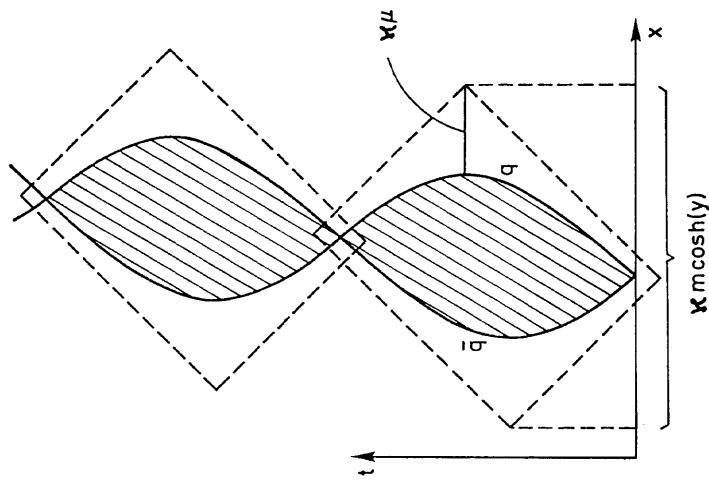


Fig. 37

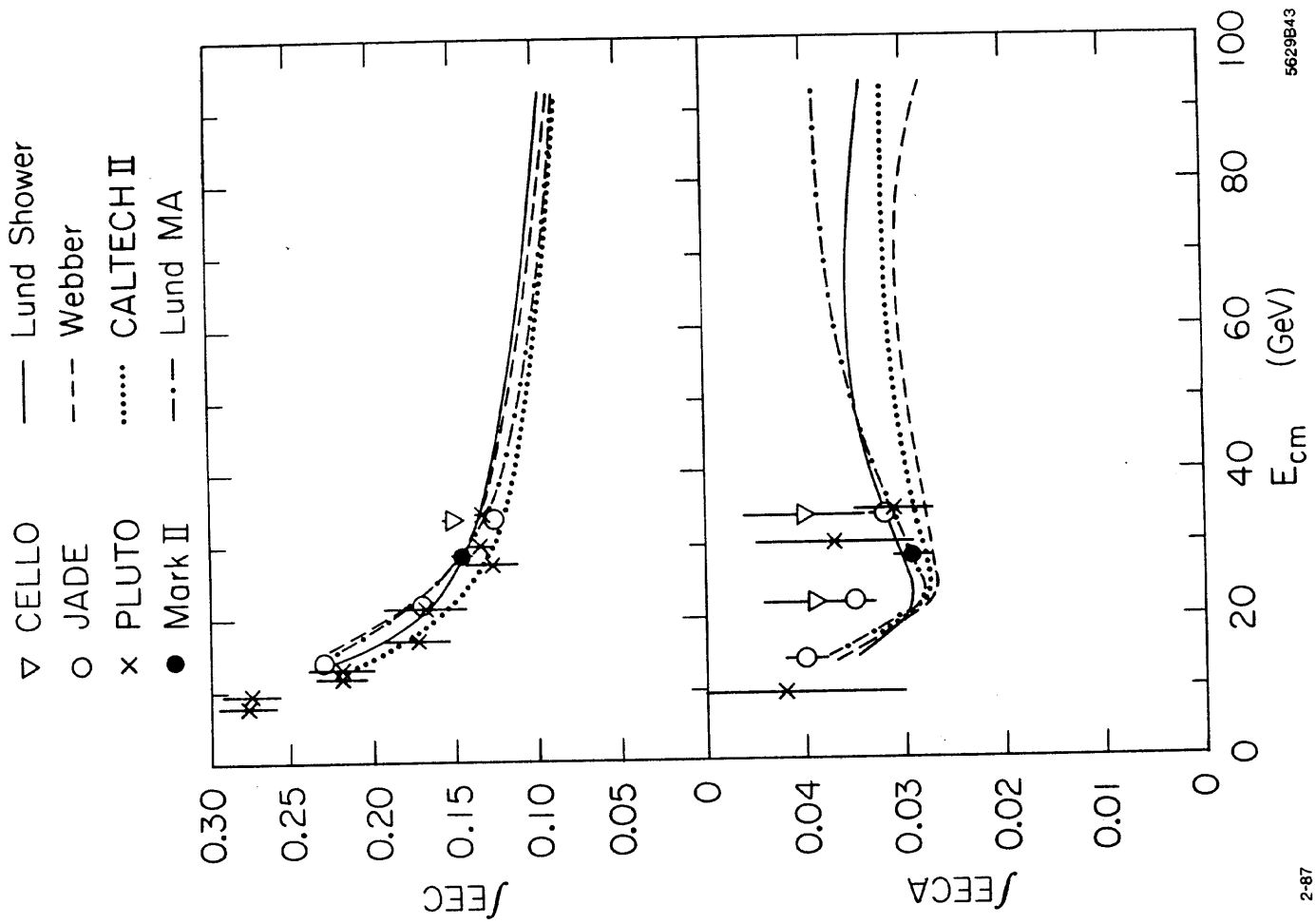


Fig. 38b

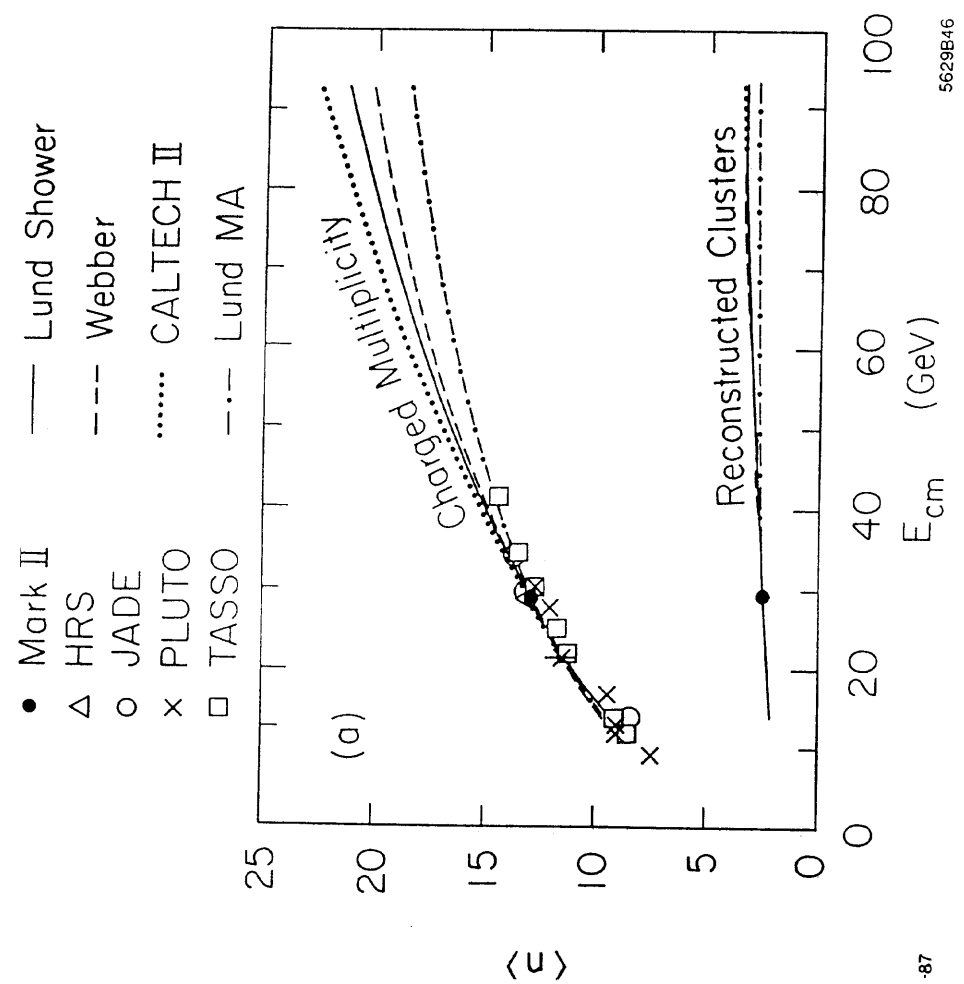
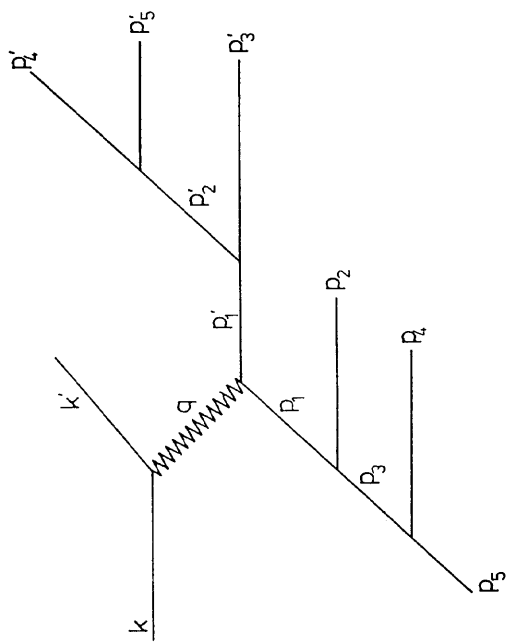
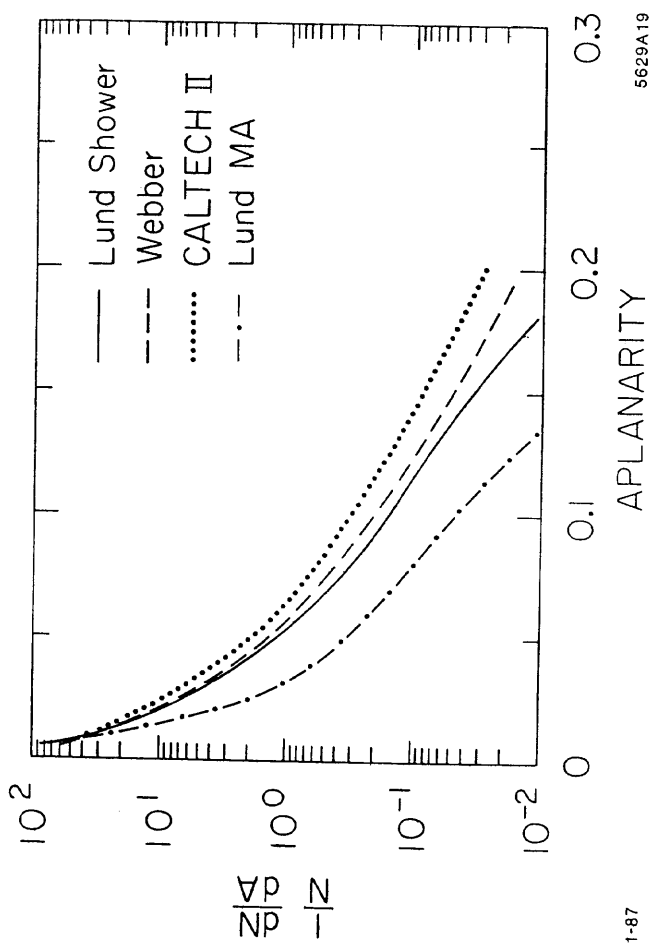
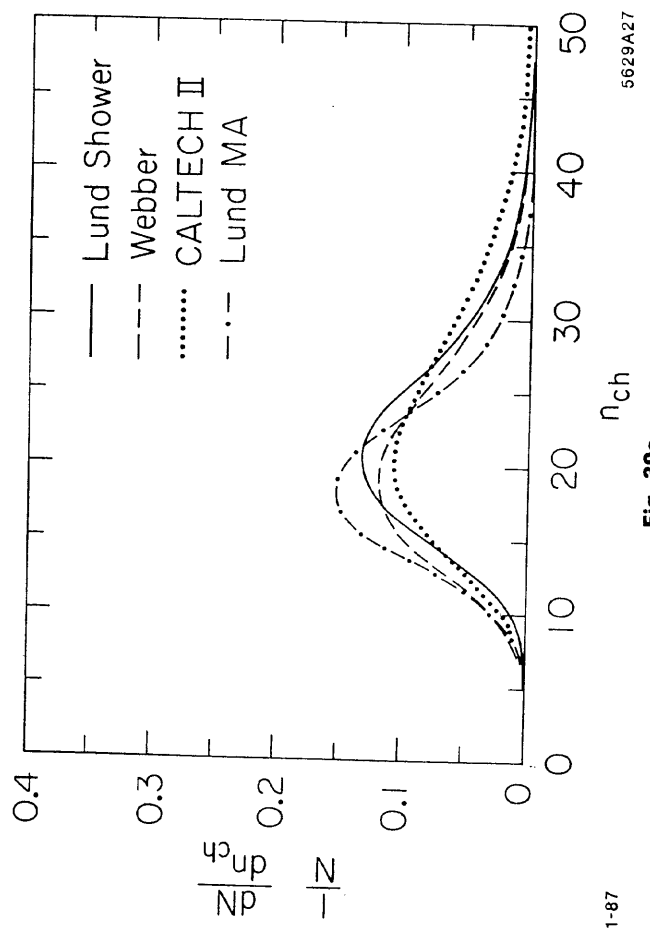
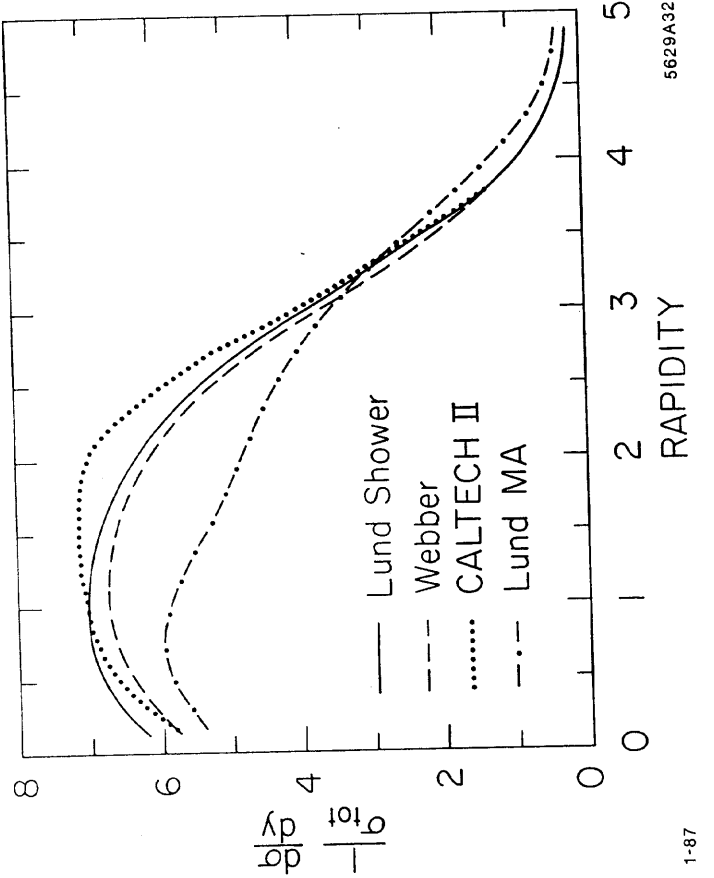


Fig. 38a



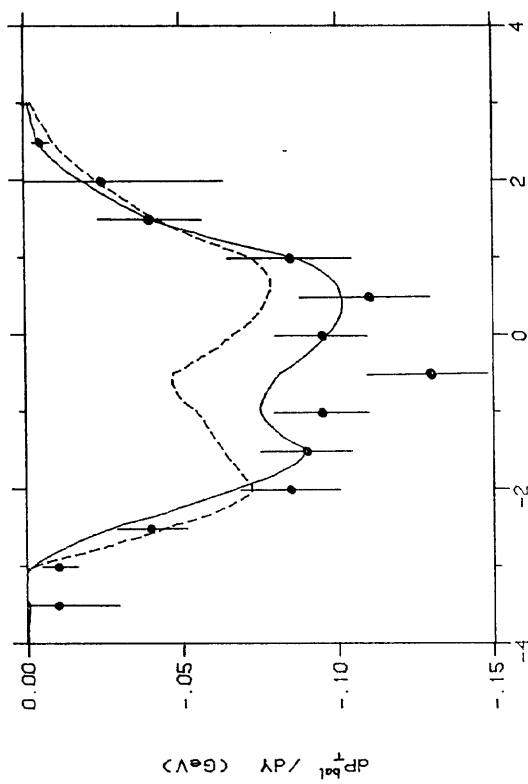


Fig. 41

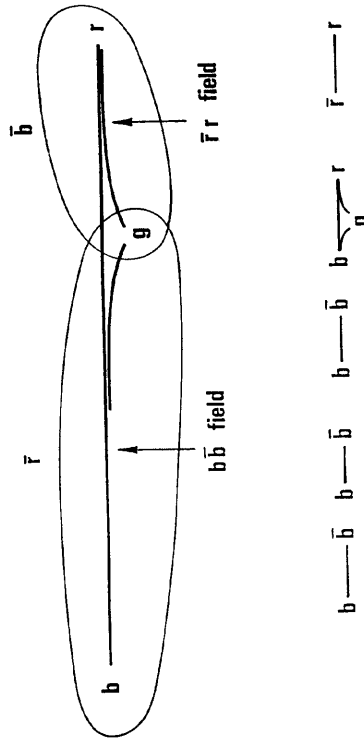


Fig. 41

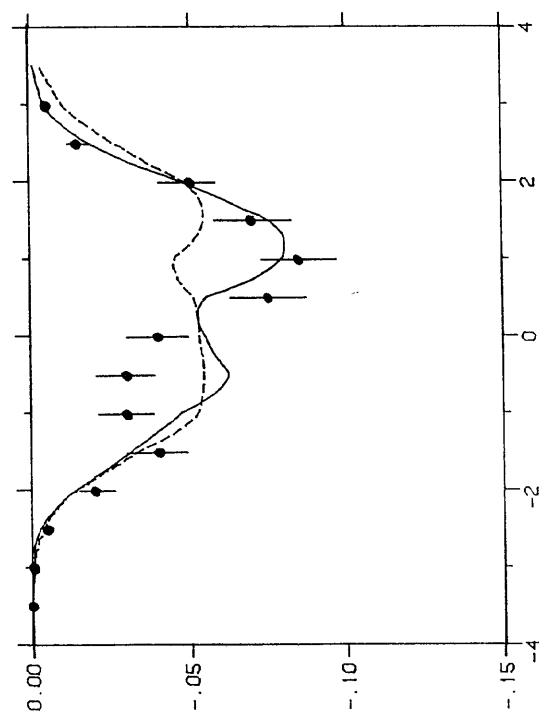


Fig. 43a

Fig. 43b

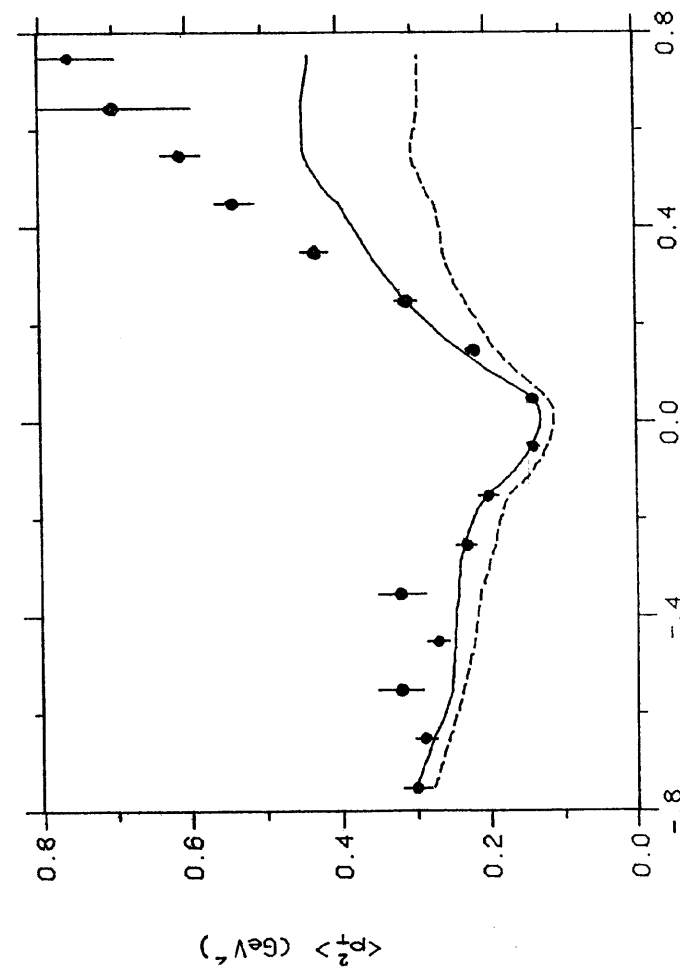


Fig. 42

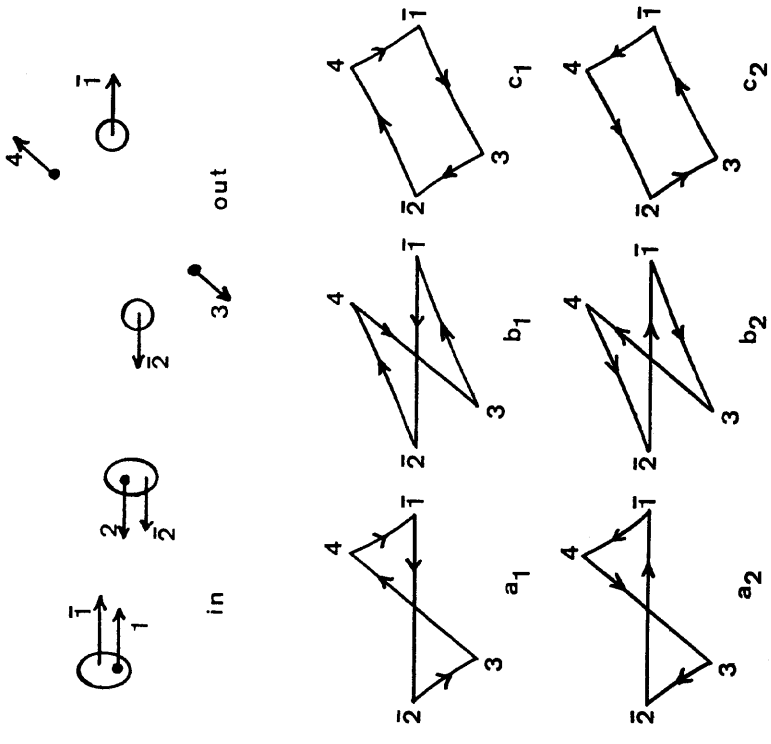


Fig. 44

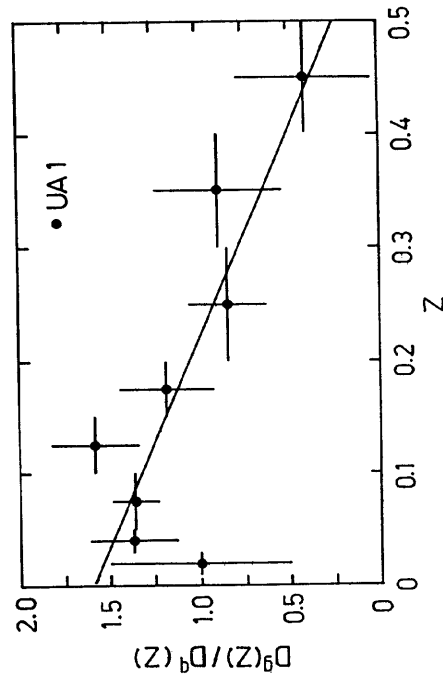


Fig. 45